ISSN. 0377 - 2969
Vol. 48(1), March 2011

PROCEEDINGS

OF THE PAKISTAN ACADEMY OF SCIENCES

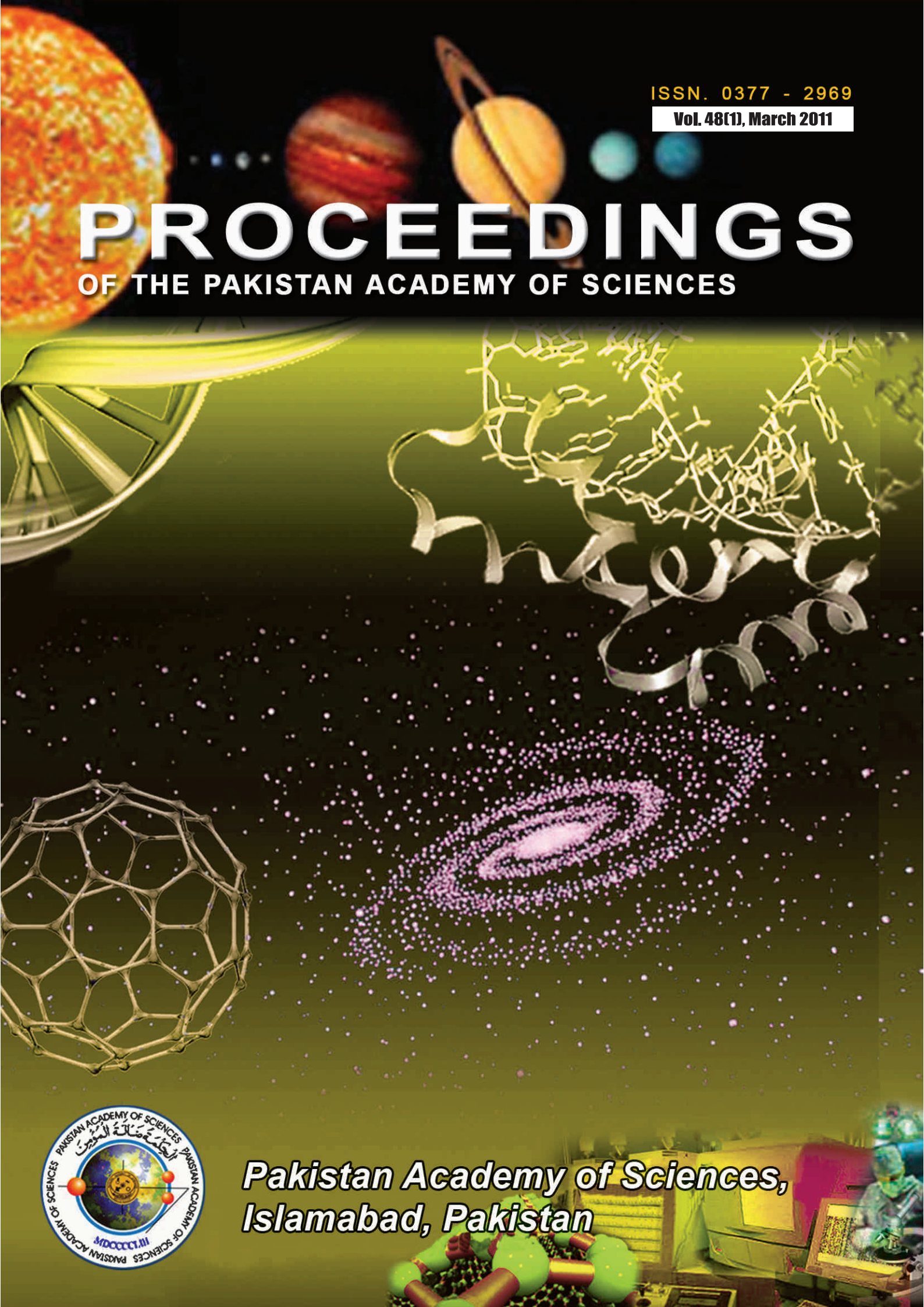

Pakistan Academy of Sciences,
Islamabad, Pakistan

PAKISTAN ACADEMY OF SCIENCES

Founded 1953

Proceedings of the Pakistan Academy of Sciences, published since 1963, is quarterly journal of the Academy. It publishes original research papers and reviews in basic and applied sciences. All papers are refereed externally. Authors are not required to be Fellows or Members of the Academy, or citizens of Pakistan.

Annual Subscription for 2011

Pakistan: Institutions, Rupees 2000/- ; Individuals, Rupees 1000/-
Other countries: US$ 100.00 (Price includes air-lifted overseas delivery)

HEC Recognized, Category X

Published by **Pakistan Academy of Sciences**, 3 Constitution Avenue, G-5/2, Islamabad, Pakistan
Tel: 92-5 1-9207140 & 9215478; **Fax:** 92-51-9206770; **Website: www.paspk.org**

Printed at **PanGraphics (Pvt) Ltd.,** No. 1, I & T Centre, G-7/l, Islamabad, Pakistan
Tel: 92-51-2202272, 2202449 Fax: 92-51-2202450 E-mail: pangraph@isb.comsats.net.pk

CONTENTS

Volume 48, No. 1, March 2011 **Page**

Research Articles

Engineering Sciences & Technology

Life Sciences

Medical Sciences

Physical Sciences

Citations

Proceedings of the Pakistan Academy of Sciences 48 (1): 1–11, 2011

ISSN: 0377 - 2969

Pakistan Academy of Sciences

Probabilistic Analysis of Deep Excavation Design and Construction Practices in Pakistan

A. H. Khan* and M. Irfan

Department of Civil Engineering, University of Engineering and Technology, Lahore, Pakistan

Abstract: Probability analysis provides a sound basis for choosing a course of action against the uncertainties involved in the geotechnical exploration. The modern probabilistic techniques have been successfully applied to classical geotechnical engineering problems such as seepage, settlement, bearing capacity, slope stability in the past throughout the world. This research is more specific towards the application of probabilistic analysis concept in the design and construction of deep excavation, which have emerged as a new trend used in the construction of high-rise buildings in the urban areas of Pakistan specifically. In this research paper, the design and construction data of deep excavation from running construction projects was collected and probabilistic method of analysis was applied for the evaluation of risks, uncertainties, probabilities and cost impacts. From the finding of the results, It is observed that if excessive unplanned risks are taken in design of deep excavations than its cost impact during construction become very high. However if controlled risks are taken in deep excavation construction than that can help in the cost reduction of the project.

Keywords: Probabilistic analysis, risks, geotechnical engineering, deep excavation

INTRODUCTION

Probabilistic analysis is used globally to evaluate the impact of uncertainties and risks taken during the projects execution on its associated activities. Probability theories provide a formal basis for quantifying risks and uncertainties which must not be dealt by engineering judgment (qualitatively).

Soils and rocks are among the most variable of all engineering materials and as such are highly amendable to a probabilistic treatment [1]. Risks and uncertainties in the determination of the in situ geotechnical profiles and material parameters for individual soil layers are one of the most significant problems geotechnical engineering professionals have to cope with. It is important to realize that different sources of uncertainty exist, material parameters varying in a certain but known range may be one of them but simply the lack of knowledge may be the more pronounced one [2].

Risk and reliability analysis is an area of growing importance in geotechnical engineering, where many variables have to be considered. Statistics, reliability modeling and engineering judgment are employed together to develop risk and decision analyses for civil engineering systems. The resulting engineering models are used to make probabilistic predictions, which are applied to geotechnical problems [3]. A formal procedure of geotechnical data evaluation and analysis by mathematical calculations, numeric or computational modeling of all aspects of risks and uncertainties is not a straightforward task. That is why, in common geotechnical engineering practice engineering judgment is pronounced.

Recent theoretical developments and advances [4-16] in probabilistic analysis application techniques and computational modeling allow geotechnical engineers for a more recognized consideration of risks and uncertainties during design and construction. However, it could not replace the role of engineering judgment in the practice of geotechnical engineering.

The horizontal trend of urban development has been the popular expansion mode in Lahore (23rd largest city of world; 2nd largest city of

Received September 2010, Accepted March 2011
*Corresponding author: A.H. Khan; Email: ammadhk@hotmail.com

Pakistan with a population of over 10 millions and an extended area of 2,491 km) until year 2005. After year 2005 with rapid growth in the economy, real estate becomes one of the most prime areas of investment in Lahore. The rapid shoot in the land prices diverts the direction of the government and private developers towards the vertical urban development thus necessitate the deep excavation [17]. Even until recent times the deep excavation and shoring system adaptation in the industry has been facing numerous challenges and uncertainties. As a result of these uncertainties recent design and construction failures have been observed [18]. In this research an attempt was made to address these challenges and uncertainties by developing an analysis of deep excavation design and construction based on the probabilistic techniques. The deep excavation design and construction related technical and financial data in Lahore from the twenty projects (Table 1) year wise was collected and used for our analysis. Table 1 is showing the list of deep excavation projects in Lahore, Pakistan. Tables 1a & 1b are showing the major causes of failure in design and construction of these deep excavation projects.

Table 1. The list of deep excavation projects in Lahore.

Year	Design Failure Projects	Construction Failure Projects		Successful Projects	
2006	Pace	Alfalah Tower	City Tower	MCB Tower	Tricon Corporate Center
2007	Ahad Center	Alamgir Tower	China Center	Liberty Trade Center	IT Tower
2008	Pace Hayat	Boulevard Heights	Warid Office	Mubarak Center	Sherpao Plaza
2009	Haly Tower	DHA Mall 1	DHA Mall 2	Fortress Tower	Lahore City Center

Table 1(a). Major causes of failure in design projects.

Year	Projects	Type of failure	Major causes of failure	Remarks
2006	Alfalah Tower	Design failure	Inadequate interval between bracing beams, inaccurate bonded and unbonded lengths. Inadequate diameter of anchor piles and undersize reinforcement bars in anchor piles.	Project abandoned
2006	Tricon Corporate Center	Design failure	In adequate geotechnical investigation parameters. Insufficient geotechnical profiling of the adjacent high rise building. In accurate alignment of the anchor piles and multi level tier system.	Project under construction
2007	Alamgir Tower	Design failure	Inadequate spacing between piles, bracing beams. Insufficient grouting in the bonded length of the anchorage system. In appropriate exaction and non exaction lengths of the system	Project abandoned

Table 1(b). Major causes of failure in construction project.

Year	Projects	Type of failure	Major causes of failure	Remarks
2007	China Center	Construction failure	The deep excavation carried out with out the installation of anchors and multilevel tier system only top tie up beam provided. Inappropriate implementation of HSE and QA/QC systems.	Project under construction
2007	Liberty Trade Center	Construction failure	The deep excavation carried out with out the installation of anchors, multilevel tiers and top tie up beam. Inappropriate implementation of HSE and QA/QC systems.	Project under construction
2007	Sherpao Plaza	Construction failure	The deep excavation carried out with out the top tie up beam. Inappropriate implementation of HSE and QA/QC systems.	Project abandoned

The geotechnical investigation for the design of deep excavation and shoring in all above projects was based on field testing (SPT - ASTM D1586) and relevant laboratory testing (Natural Moisture Content Deteremination (ASTM D2216), sieve analysis test (ASTM D422), direct shear test (ASTM D3080), unconfined compression test (ASTM D2166), Atterberg limits test (ASTM D4318), etc).

The design and construction failure photographs are shown in Fig. 1(a) & 1(b).

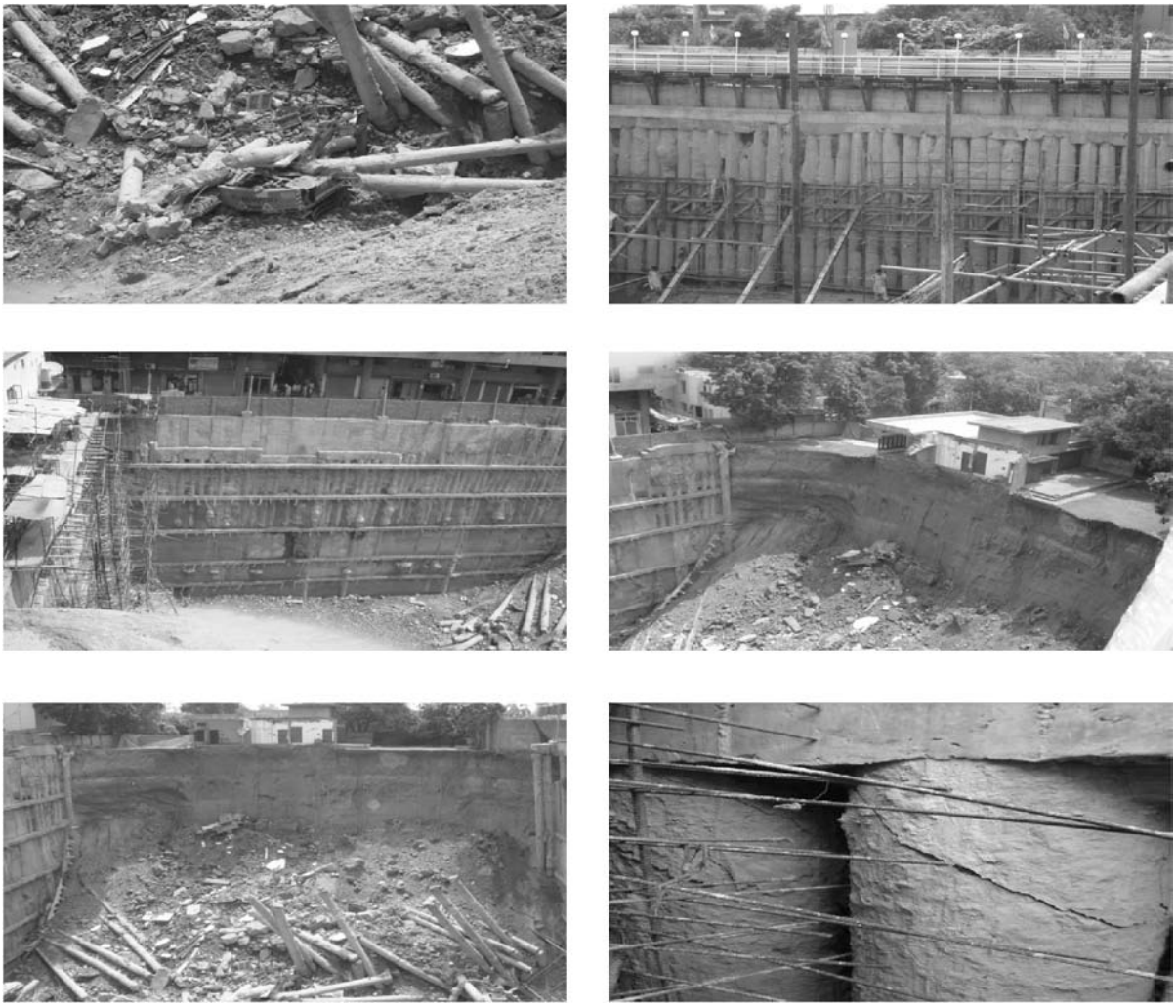

Fig.1(a). Design failure sites.

The major risks taken in the design and construction failure projects are shown in Table 2.

Application of Probability Theory for Deep Excavation

Probability theory is based on engineering mathematics associated with random analysis of variables, processes and events. The human made activities involving quantitative analysis are largely dependent on the concepts of probability theory for its analysis. In geotechnical engineering we mainly encounter such random phenomena for which basic mathematical analysis is not enough to analyze the event or activity; this necessitates the application of probability theory in geotechnical engineering i.e. deep excavations.

The deep excavation comprise of two events i.e. design and construction. The design event comprise of following processes i.e. geotechnical exploration, laboratory testing and report and geotechnical design. The construction event comprise of following processes i.e. anchor piles casting, level 1 excavation, level 1 anchor beam casting and anchor installations, level 2 excavation, level 2 anchor beam casting and anchor installation, level 3 excavation.

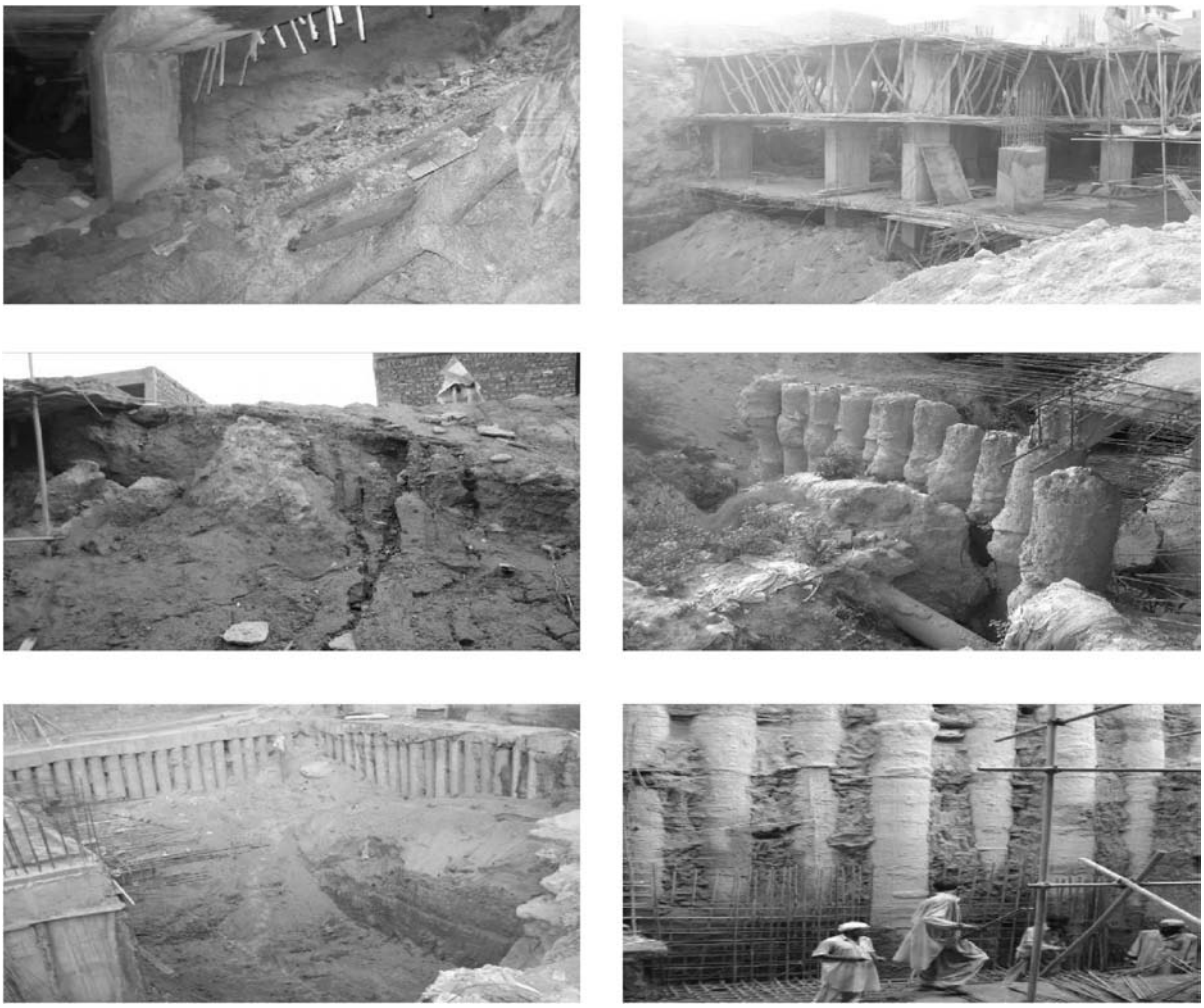

Fig. 1(b). Construction failure sites.

Table 2. Risks identified in the design and construction failure projects.

Phase	Risks Identified
DESIGN	Insufficient geotechnical exploration
	Safety factors in foundation design
	Safety factors in bracing design
	Insufficient technical staff employed
	Bye laws violation
	Credibility & commitment
	Inexperience designer
CONSTRUCTION	Deep excavation with inappropriate or without anchor installation
	Safety
	Health
	Environment
	Loss prevention
	Quality assurance and quality control
	Inexperience contractor
	Financial impacts

The major variables associated in the design process include field testing (SPT), relevant laboratory testing (natural moisture content determination, sieve analysis, Atterberg limits, direct shear test, unconfined compression test etc). The major variables associated in construction process include marking and lay out, excavation manual or mechanical (type of excavator, size of bucket, wheel or chain type, boom length), disposal of excavated material (manual or mechanical (type of truck, capacity of truck, with or without jacking system, need for disposal), drilling for anchor piles (type of machine – straight or reverse rotary, control of caving, steel fixing for reinforcement cage, lowering of cage through crane, concreting – through conventional mixer or batching plant, casting of concrete through conventional trimmy or concrete pump, anchor beams, steel fixing, shuttering and casting, type and size of anchor, bonded and unbonded anchor length, type of chemical for bonding).

The data of success or failure in the projects was collected from client organizations with consent of design consultants purely for research and analysis purpose. The yearly rate of success, design failure and construction failure is represented by figure above. The trend shows that initially the design and construction failure projects rate was high which decreased gradually with the passage of time. The rate of success of design and construction was low initially but it also gradually improved.

The deep excavation as event (E) can happen in "h" (way of success or failure of event) ways out of a total of "n" (possibly equally likely ways of event). In the analysis deep excavation design and construction was taken as two independent events (E* & E^) in each project. The design and construction nomenclature are with superscript of * and ^ respectively.

The probability of occurrence of success and failure in various design events are shown in Table 3(a), 3(b) and 3(c).

Table 3(a). The success and failure probability in geotechnical exploration (SPT, drilling of bore holes, collection of UDS, etc).

Year	E*	h*	n*	p*	q*	p*+q*
2006	5	2	4	0.5	0.5	1
2007	5	2	2.86	0.7	0.3	1
2008	5	2	2.5	0.8	0.2	1
2009	5	2	2	1	0	1

Table 3(b). The success and failure probability in laboratory testing (NMC, UCCT, Sieve Analysis, Atterberg's Limits, Direct Shear Test, etc).

Year	E*	h*	n*	p*	q*	p*+q*
2006	5	2	3.33	0.6	0.4	1
2007	5	2	2.86	0.7	0.3	1
2008	5	2	2.5	0.8	0.2	1
2009	5	2	2	1	0	1

Table 3(c). The success and failure probability in reporting (report writing, geotechnical design, FOS, etc).

Year	E*	h*	n*	p*	q*	p*+q*
2006	5	2	2.86	0.7	0.3	1
2007	5	2	2.5	0.8	0.2	1
2008	5	2	2.5	0.8	0.2	1
2009	5	2	2	1	0	1

The success and failure probability in various construction events are shown in Table 4(a), 4(b) and 4(c).

Table 4(a). The success and failure probability in anchor piles casting.

Year	E^	h^	n^	p^	q^	p^+q^
2006	5	2	4	0.5	0.5	1
2007	5	2	4	0.5	0.5	1
2008	5	2	3.33	0.6	0.4	1
2009	5	2	2.5	0.8	0.2	1

Table 4(b). The success and failure probability in excavation.

Year	E^	h^	n^	p^	q^	p^+q^
2006	5	2	4	0.5	0.5	1
2007	5	2	4	0.5	0.5	1
2008	5	2	3.33	0.6	0.4	1
2009	5	2	2.5	0.8	0.2	1

Table 4(c). The success and failure probability in anchor installation.

Year	E^	h^	n^	p^	q^	p^+q^
2006	5	2	4	0.5	0.5	1
2007	5	2	2.86	0.7	0.3	1
2008	5	2	2.86	0.7	0.3	1
2009	5	2	2.22	0.9	0.1	1

where,

$$p = Pr\{E\} = h/n \quad (1)$$

$$q = 1 - Pr\{E\} \quad (2)$$

p, q are the success and or failure variables of deep excavation design (SPT, various laboratories testing etc) and or construction (drilling, anchoring, shoring, deep excavation etc).

These variables are discrete in nature and are based on various uncertainties and risks discussed above. The deep excavation design and construction events are dependent on each other. Thus using the concept of empirical probability, conditional probability of dependent events and mutually exclusiveness of the events are evaluated as shown in Table 5 and Table 6 below.

Table 5. Conditional probability and mutually exclusiveness of dependent events in the design of deep excavations.

Year	E*	Pr . E*	Pr . F*	Pr . F*/E*	Pr . E*- F*	Pr . E* . Pr . F*/E*	Pr . F* . Pr . F*/E*	Pr . E*+F*
2006	15	0.60	0.40	0.67	0.20	0.400	0.267	1.00
2007	15	0.73	0.27	0.36	0.47	0.267	0.097	1.00
2008	15	0.8	0.2	0.25	0.6	0.200	0.050	1.00
2009	15	1	0	0	1	0	0	1.00

Table 6. Conditional probability and mutually exclusiveness of the dependent events in the construction of deep excavation.

Year	E*	Pr . E*	Pr . F*	Pr . F*/E*	Pr . E*- F*	Pr . E* . Pr . F*/E*	Pr . F* . Pr . F*/E*	Pr . E*+F*
2006	15	0.50	0.50	1.00	0.00	0.500	0.500	1.00
2007	15	0.57	0.43	0.76	0.13	0.433	0.331	1.00
2008	15	0.63	0.37	0.58	0.27	0.367	0.212	1.00
2009	15	0.83	0.17	0.20	0.67	0.167	0.033	1.00

RESULTS

The analysis results reflect that the success in design and construction is showing the invert trend in comparison with failure in design and construction over the passage of time. The trend of the design and construction success of deep excavation is increasingly improved in Lahore. Meanwhile, the trend of the design and construction failure of deep excavation is decreased as shown in Fig. 2(a) and Fig. 2(b).

The analysis results also reflect the improvement trend in the probability of design and construction success of deep excavation practice in Lahore. The increasing difference in the dependency of mutual exclusiveness of the deep excavation events on conditional probability is also recognized as shown in Fig. 3 and Fig. 4.

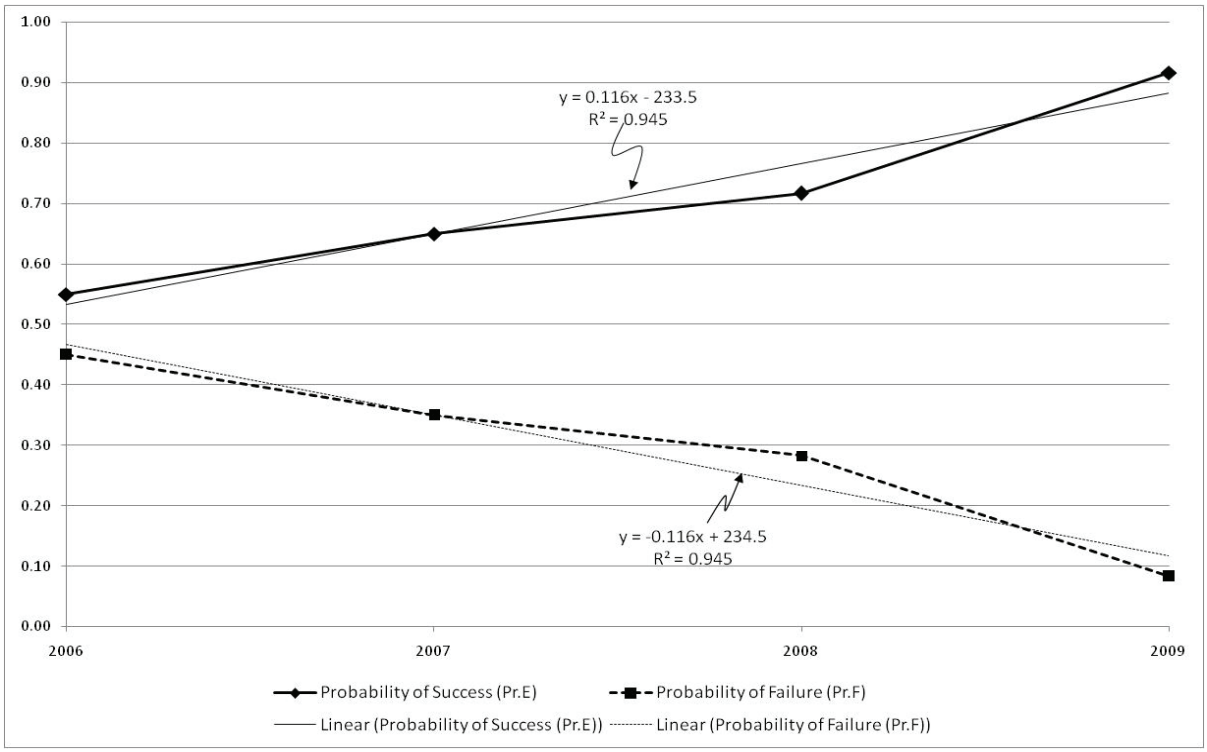

Fig. 2(a). Overall probability of success and failure for projects in Lahore.

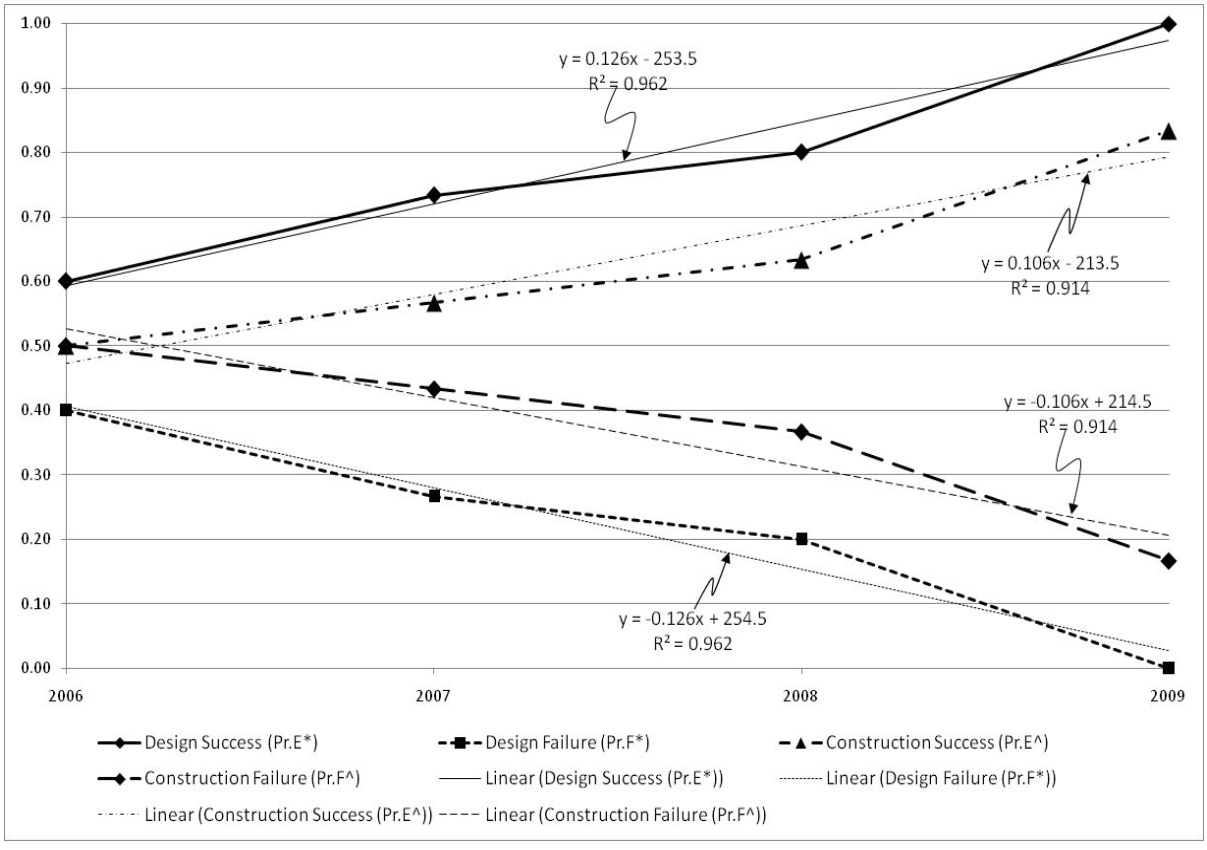

Fig. 2(b). Design/construction success/failure cumulative probability.

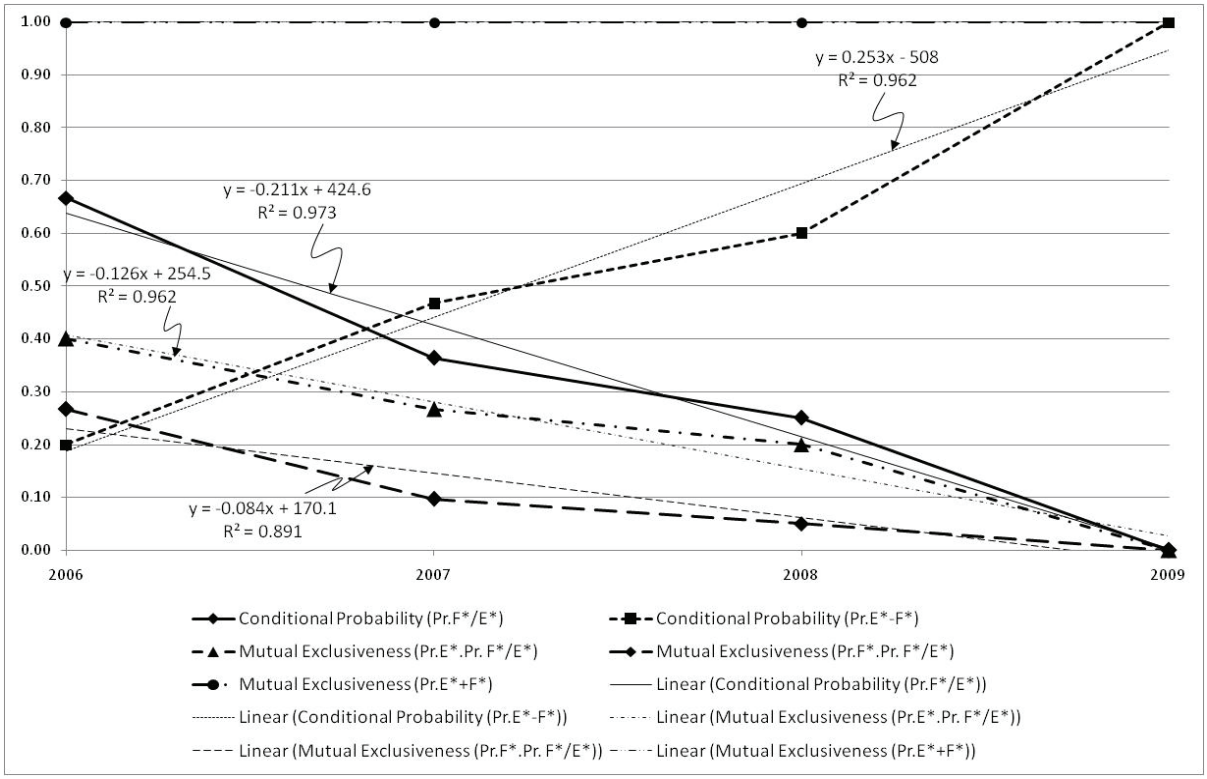

Fig. 3. Design conditional probability along with events mutual exclusiveness.

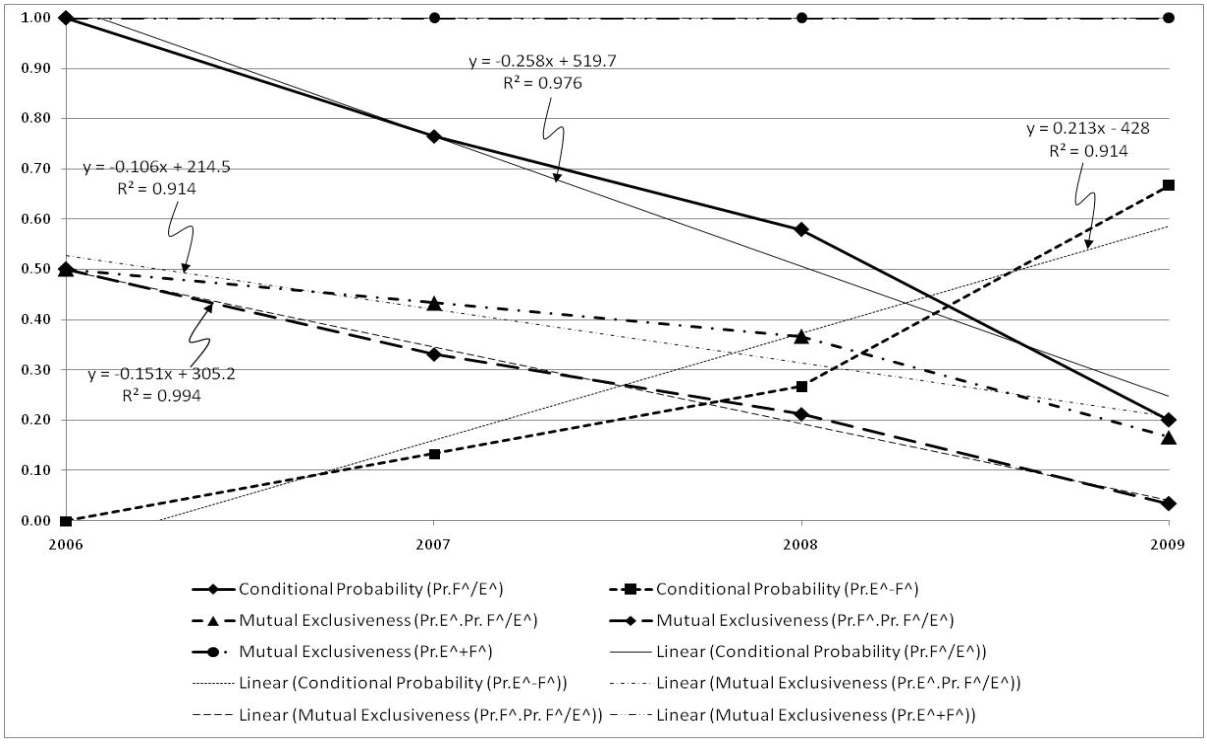

Fig. 4. Construction conditional probability along with events mutual exclusiveness.

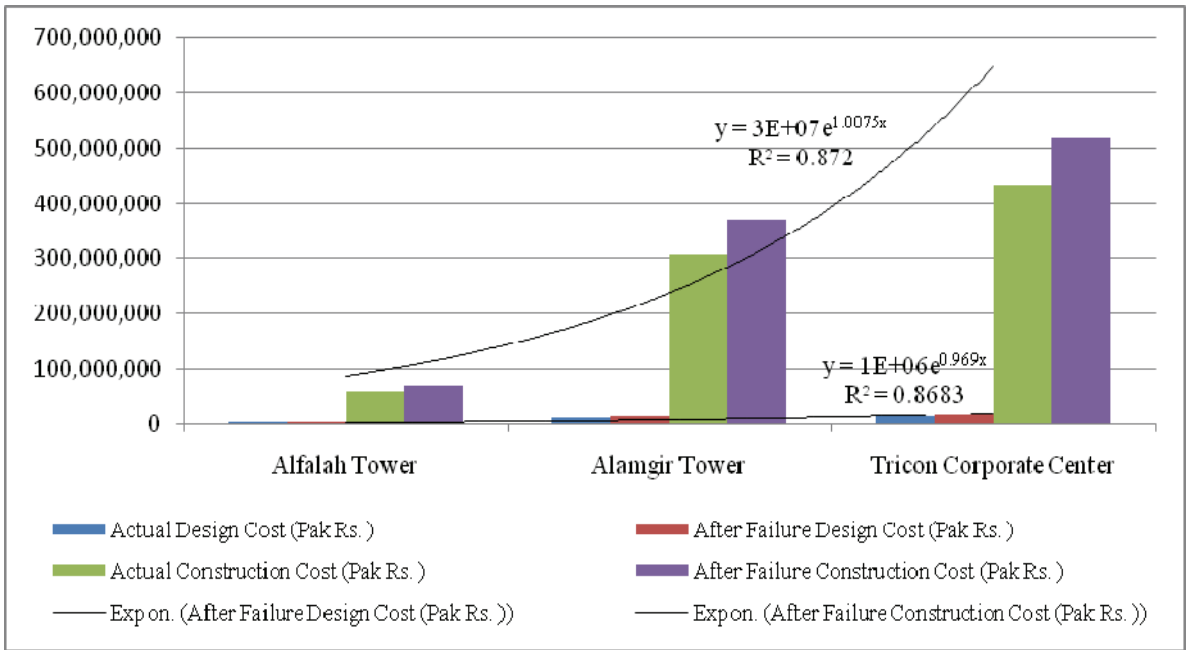

Fig. 5. Comparison of the design and construction cost of the design failure project before and after failure (Source: Project Tender Documents).

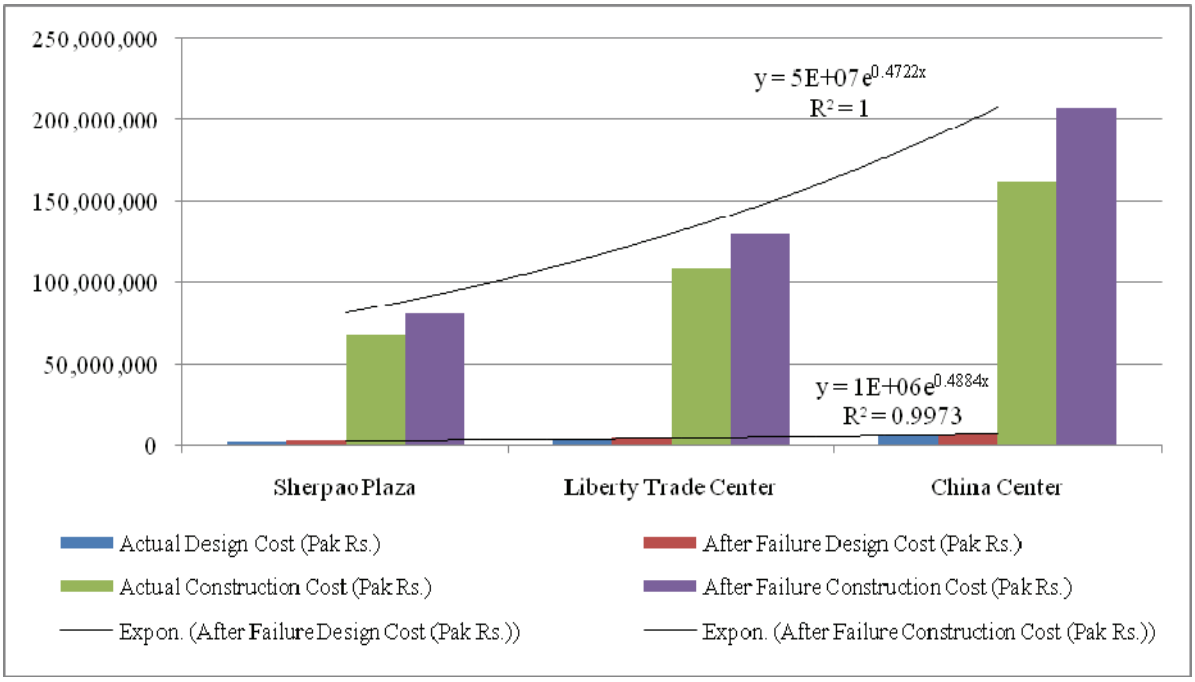

Fig. 6. Comparison of the design and construction cost of the construction failure project before and after failure (Source: Project Tender Documents).

Based on the probability analysis the impact of the uncertainties and risks on the projects are established. This is presented through a cost comparison established between the actual cost of the design and construction project with the cost after failure of the design and construction projects as shown in Fig. 5 & 6.

CONCLUSIONS

The faults observed in huge deep excavation design and construction projects must be carefully analyzed for the benefit of the researchers and engineers, including those responsible for the success/failure so that these

defects are taken care of in all ongoing and future similar design and construction projects. The major conclusions based on this research are:

- The historic or surrounding geotechnical data can only be used as reference during feasibility, however before detailed design independent geotechnical investigation should be carried out for the deep excavation project.
- The projects where the reliability in the performance and implementation of conventional geotechnical field investigation and laboratory testing is inappropriate, in such cases the modern field exploration techniques (curtailing the frequency of laboratory testing) i.e flat rigid piston dilatometer(ANDMT), cone penetration test (CPT) or pressuremeter test may be employed.
- The geotechnical design, construction and supervision enterprises previous work experience of similar deep excavation projects should be carefully considered in its selection.
- The organizational structure and project control during the construction is required to delegate the authority and assess the variation in deep excavation project scope, schedule and budget.
- The presence and importance of professional geotechnical engineer in foundation engineering, anchor system, tieback, lagging, deep excavation, geotechnical investigation should not be over ruled.
- The building approval authority should not allow any deep excavation construction until the design of deep excavation is prepared and vetted by a professional geotechnical engineer.
- Risks in geotechnical design and construction at the cost of economy should be curtailed.
- Economy at the cost of quality should not be the ideology in certain functional disciplines of deep excavation projects, i.e., geotechnical; however, it can be achieved in other allied disciplines e.g., architectural.

REFERENCES

1. Fenton G.A., D.V. Griffiths & W. Cavers. Resistance factors for settlement design. *Canadian Geotechnical Journal* 42: 1422-1436 (2005).
2. Schweiger, H.F. & G.M. Peschl. Reliability analysis in geotechnics with the random set finite element method. *Computers and Geotechnics* 32: 422-435 (2005).
3. Baecher, G.B. & J.T. Christian. *Reliability and statistics in geotechnical engineering.* John Wiley and Sons, USA (2005).
4. Griffiths, D.V. *Finite element analyses of walls, footings and slopes*. Proceedings of Symposium on Computer based Geotechnical Problems, Cambridge, UK. p. 122–146 (1980).
5. Moses, F. & D. Verma. Load capacity evaluation of existing bridges. *National Cooperative Highway Research Program Report 310.* Transportation research board, National Research Council, Washington, DC. (1987).
6. Wolff, T. F. & W. Wang. Engineering reliability of navigation structures research report. *Michigan State University, for U.S. Army Engineer Waterways Experiment Station, Vicksburg, MS. (*1992).
7. Shannon & Wilson, Inc., and T. F. Wolff. Probability Models for geotechnical aspects of navigation structures. *Report to the St. Louis District, U. S. Army Corps of Engineers (*1994).
8. Wolff, T. F. Probabilistic methods in engineering analysis and design. *Notes from short course for the Jacksonville District, U.S. Army Corps of Engineers* (1995).
9. U.S. Army Corps of Engineers. Reliability assessment of pile founded navigation structures. *Extract, Transform and Load* 1110-2-354 (1995).
10. U.S. Army Corps of Engineers. Introduction to probability and reliability methods for use in geotechnical engineering. *Extract, Transform and Load* 1110-2-547 (1995).
11. Phoon, K.K. & F. H. Kulhamy. On quantifying inherent soil variability. *American Society of Civil Engineers (ASCE), Geotechnical Special Publication* 58: 326-340 (1996).
12. Lacasse, S. & F. Nadim. Uncertainties in characterizing soil properties. *American Society of Civil Engineers (ASCE), Geotechnical Special Publication* 58: 49-75 (1996).
13. Kulhamy, F. & C.H. Trautman. Estimation of in-situ test uncertainty. *American Society of Civil Engineers (ASCE), Geotechnical Special Publication* 58:269-286 (1996).
14. Griffiths, D.V. Influence of soil strength spatial variability on the stability of an undrained clay slope by finite elements. In: *Slope Stability 2000,* Griffiths, D.V. & G.A. Fenton. (Eds.) American Society of Civil Engineers, Reston, VA, USA, p. 184–193 (2000).
15. Griffiths, D.V. Probabilistic slope stability analysis by finite elements. *ASCE - Journal of Geotechnical and Geo-environmental Engineering* 130(5): 507–518 (2004).

16. Rubio, E., J.W. Hall & M.J. Anderson. Uncertainty analysis in a slope hydrology and stability model using robabilistic and imprecise information. *Computational Geotechnique* 31: 529–536 (2004).
17. Khan, A. H. *Failure of anchor pile foundation in Lahore – A case study*. Proceedings of 2nd British Geotechnical Association Conference, University of Dundee, Scotland, UK. p. 705-716 (2008).
18. Khan, A. H. 2009. *Probabilistic analysis of deep excavation practices in Pakistan.* Proceedings of 4th Young Geotechnical Engineering Conference of International Society of Soil Mechanics and Geotechnical Engineering, Alexandria, Egypt, p. 297-300 (2009).

Proceedings of the Pakistan Academy of Sciences 48 (1): 13–17, 2011

ISSN: 0377 - 2969

Pakistan Academy of Sciences

Methylcyclohexane Dehydrogenation over Commercial 0.3 Wt% Pt/Al_2O_3 Catalyst

Muhammad R. Usman*

School of Chemical Engineering and Analytical Science,
The University of Manchester, U.K.

Abstract: Dehydrogenation of methylcyclohexane is studied over commercial 0.3 wt% Pt/Al_2O_3 catalyst. The effect of catalyst particle size, space velocity, temperature, and partial pressure of hydrogen was studied. It was observed that the dehydrogenation reaction is a strong function of the ratio of reactor internal diameter to catalyst particle size, temperature, and feed composition. The experimental data obtained was kinetically analyzed and first order power law model considering reversible reaction was found appropriate. The apparent activation energy of the catalyst was 100.6 kJ/mol.

INTRODUCTION

The three most important reasons for studying the dehydrogenation reaction are: a) exploiting methylcyclohexane (MCH) as a fuel; b) investigating the MCH dehydrogenation model reforming reaction; and c) the potential of MCH as a hydrogen energy storage material [1]. As a hydrogen storage energy material, MCH is exploited in the MTH (methylcyclohexane-toluene-hydrogen)-system [2-7]. The MTH-system is a safe and efficient means of storage and "on-board" hydrogen generation. The dehydrogenation reactor installed within the vehicle itself produces hydrogen (see Eq. 1), which can either be used in a spark-ignition engine or in a fuel cell stack. The products of dehydrogenation reaction are cooled and toluene is condensed and separated *in situ*. At the filling station, toluene is pumped out while methylcyclohexane is pumped into the vehicle. Toluene is transported to the hydrogenation plant where it is hydrogenated back to methylcyclohexane (Eq. 2). Hydrogen required for the hydrogenation is produced from a sustainable energy source, such as solar, wind, wave, or even nuclear power. The heart of the MTH-system is the dehydrogenation reaction. An efficient dehydrogenation catalyst is required that is highly active, highly selective towards toluene, and stable over an extended period of time. Established commercial catalyst is ideally suited and can be readily incorporated to obtain reaction data for design and development of practical reactors. This approach saves time, effort, and cost associated with the development of a new catalyst. In the literature, there is a massive controversy among researchers over the kinetics of the dehydrogenation reaction. A wide range of apparent activation energy values are reported, ranging from 17.6 kJ/mol [8] to 220.7 kJ/mol [9]. Therefore, it was thought worthwhile to test a commercial catalyst and to study the kinetics of the reaction. In this study, a commercial dehydrogenation catalyst was studied for methylcyclohexane dehydrogenation. The dehydrogenation reaction was studied for varying particle size and space times at different temperatures both with and without hydrogen addition in the feed. The data so obtained was analyzed numerically and a kinetic model is proposed for the catalytic reaction following the reaction sequence:

Forward Reaction:

$$\underset{MCH}{C_7H_{14}} \xrightarrow{+\text{ Heat}} \underset{Toluene}{C_7H_8} + 3\ H_2 \quad (+\Delta h^{\circ}_{rxn} = 205\ \text{kJ/mol}) \qquad (1)$$

Reverse Reaction:

$$\underset{Toluene}{C_7H_8} + 3\ H_2 \xrightarrow{-\text{ Heat}} \underset{MCH}{C_7H_{14}} \quad (-\Delta h^{\circ}_{rxn} = 205\ \text{kJ/mol}) \qquad (2)$$

MATERIALS AND METHODS

The experimental setup, shown in Fig. 1, mainly consisted of a 11.2 mm I.D. glass fixed bed tubular reactor, a three zone furnace to maintain uniform reactor wall temperature, cooler-condenser operated on glycol refrigeration

Received January 2011, Accepted March 2011
*Present address: Institute of Chemical Engineering and Technology, University of the Punjab, Lahore (54590), Pakistan E-mail: mrashidusn@gmail.com

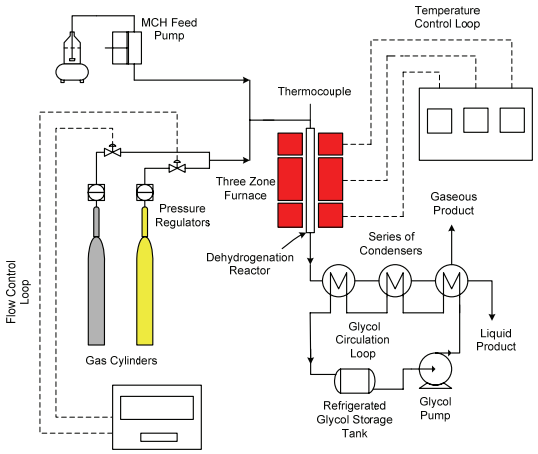

Fig. 1. Experimental setup for studying the dehydrogenation reaction of methylcyclohexane.

system, an HPLC feed pump and instruments to measure and control the required process variables. Specifications of the reactor assembly are given in Table 1. The catalyst employed was commercial 0.3 wt% Pt/Al_2O_3. This was the only information provided by the supplier and no further attempt was made to characterize the catalyst. However, visual inspection of the catalyst cross-section reveals that the catalyst is an "egg-shell" type. As received, the catalyst was spherical shaped 1.5 to 2.0 mm (1.75 mm average) diameter. The catalyst was used as supplied in a spherical form, catalyst was halved and cut to quarter portions of the original catalyst size. Experiments were performed for three different reactor internal diameters to catalyst particle ratios (24.0, 36.0, and 72.0). Internal diameter of the reactor is the equivalent diameter of the annular region between the reactor tube and thermowell, while catalyst particle size is the nominal particle size, d_{vs}, defined as the volume to surface diameter of the particle, which for spherical particle of 1.75 mm diameter, as received, was calculated as 0.30 mm, for halves as 0.20 mm, and for quarters as 0.10 mm.

Table 1. Specifications of the reactor assembly.

Description	Specification
Length of the reactor tube	600 mm
O.D. of the reactor tube	15.1 mm
I.D. of the reactor tube	11.2 mm
Length of the thermowell	550 mm
Thermowell external diameter	4 mm
Thermowell internal diameter	2 mm
Recommended operating temperature	550°C
Maximum working pressure	1.013 bar

For each run 2.0 g of the catalyst was used. Calcination and reduction of the catalyst were done *in situ*. Reduction step was performed for all three catalyst forms; however, calcination was performed only for the spherical form. The calcination was conducted at 500 °C under air flow of 100 ml/min for 5 h, while reduction was done under 100 ml/min hydrogen flow at 450 °C for 16 h. The reactor wall temperatures were maintained at 380 and 430 °C, H_2/MCH ratios were 0 and 8.4 and molal space velocity was in the range of 3.09×10^4 to 2.46×10^5 s·g-cat/mol MCH. All experiments were performed under atmospheric pressure. MCH was obtained from Sigma-Aldrich with purity of 99.0 wt%. Hydrogen gas was taken from BOC with purity greater than 99.995 mol%. Reaction products were analyzed by GC-FID system containing non-polar capillary column (BP-5: 5% phenyl and 95% dimethylpolysiloxane).

RESULTS AND DISCUSSION

Catalytic Experiments

Fig. 2 shows the effect of the ratio of the reactor internal diameter to nominal catalyst particle size on the conversion of methylcyclohexane. The nominal particle size as defined earlier is the volume to surface diameter of the particle. It is shown that under all three ratios, conversion increases with an increase in W/F_{A0}. The conversion of MCH increases dramatically when the catalyst is halved. For example, the

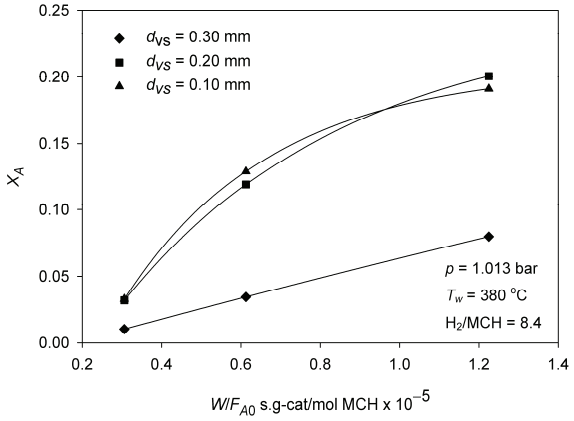

Fig. 2. Effect of particle size on methylcyclohexane conversion.

conversion increases more than two folds from 8.0% to 19.1% for the highest W/F_{A0} at 380 °C wall temperature and 8.4 H_2 to MCH ratio. However, decreasing the catalyst particle from half (d_{vs} = 0.20 mm) to quarter (d_{vs} = 0.10 mm) gives virtually no difference. Overall methylcyclohexane was only fairly dehydrogenated at the wall temperature of 380 °C in the presence of hydrogen using H_2/MCH molar ratio of 8.4. The maximum conversion was only 20.1% even at the highest W/F_{A0} ratio used which was 1.24×10^5 s.g-cat/mol MCH in the present case. An enhanced methylcyclohexane conversion with decrease in catalyst particle size may be explained on the basis of channeling phenomenon. With large particles, the bed voidage was too large especially near the wall of the reactor. This caused poor contact of gaseous MCH and the catalyst particles. A decrease in the particle size, however, improved the contact and hence the conversion. It is important to mention here that diffusion was not the reason because the catalyst was an egg-shell type. As further decrease in the size beyond d_{vs} = 0.20 mm had virtually no beneficial effects; therefore, the remaining experiments were performed on the halved particles (d_{vs} = 0.20 mm). This might be because voidage beyond this value was not appreciably influencing the flow patterns.

Fig. 3 compares the results with and without hydrogen in the feed. It is observed that methylcyclohexane conversion is a strong function of hydrogen addition and decreases strongly when hydrogen is in the feed. Hydrogen is a reaction product; therefore, the presence of hydrogen in feed was expected to decrease the dehydrogenation rates. Moreover, in the catalytic reaction, hydrogen may compete for the active sites and can provide product inhibition. Again at highest W/F_{A0}, conversion increases more than twice when there is no hydrogen in the feed. It was observed that the conversion could reach up to 21.4% and 49.0%, respectively, for the lowest and highest values of W/F_{A0} used.

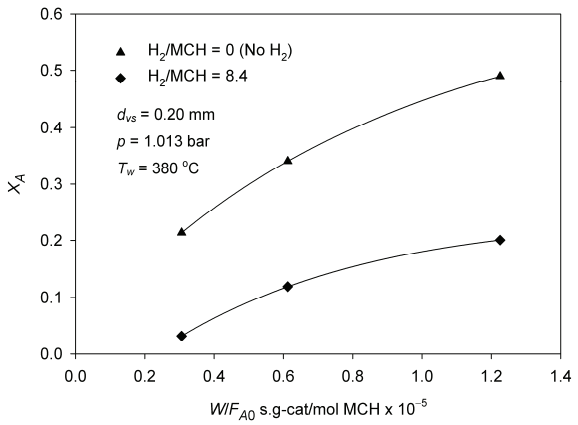

Fig. 3. Effect of hydrogen presence in the feed (feed composition) on methylcyclohexane.

Fig. 4 shows the effect of reactor wall temperature on MCH conversion without hydrogen in the feed. At the wall temperature of 430°C, substantial improvement in conversion is observed as expected. At that temperature, 97.5% methylcyclohexane was dehydrogenated at 2.46×10^5 s·g-cat/mol MCH. Under all conditions of temperatures, with and without hydrogen, the catalyst proved to be very selective towards toluene and no appreciable byproducts were observed.

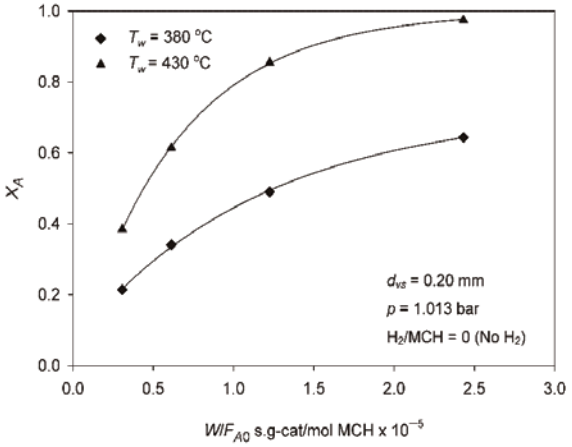

Fig. 4. Effect of reactor wall temperature on methylcyclohexane conversion.

Kinetic Modeling

The experimental data obtained over 0.30 wt% Pt/Al_2O_3 catalyst was subjected to kinetic analysis. The fixed bed reactor was assumed to follow one dimensional plug flow reactor and the following expression was used to model the reaction kinetics.

$$\frac{W}{F_{A0}} = \int_0^{X_A} \frac{dX_A}{(-r_A)} \tag{3}$$

The rate of reaction, $(-r_A)$, is expressed in terms of the partial pressures of reacting species via the first order power law kinetics:

$$(-r_A) = k \cdot \left(p_A - \frac{p_B \cdot p_C^3}{K} \right) \tag{4}$$

where, K is equilibrium constant for methylcyclohexane dehydrogenation and is given by [10]:

$$K = 3600 \cdot \exp\left(\frac{-217650}{R}\left(\frac{1}{T} - \frac{1}{650}\right)\right) \quad (5)$$

with K in bar^3, R in J·mol^{-1}·K^{-1}, and T in K.

The rate constant k is assumed to follow the Arrhenius temperature dependency and may be written as:

$$k = k_0 \cdot \exp\left(\frac{-E}{R \cdot T}\right) \quad (6)$$

Eq. 6 is reparameterized, as follows, in terms of k_r (k at the reference temperature, T_r), to reduce the correlation among the parameters and to converge the solution more rapidly.

$$k = k_r \cdot \exp\left(B \cdot \left(1 - \frac{T_r}{T}\right)\right) \quad (7)$$

where, B is dimensionless activation energy and is given by:

$$B = \frac{E}{R \cdot T_r} \quad (8)$$

and T_r is the reference temperature which is taken as 661.8 K.

The regression of the kinetic data was carried out using FORTRAN routine based on Marquardt algorithm; and sum of squares of the errors (objective function) was minimized.

Details of the above equations and the regression analysis may be found in Usman [7].

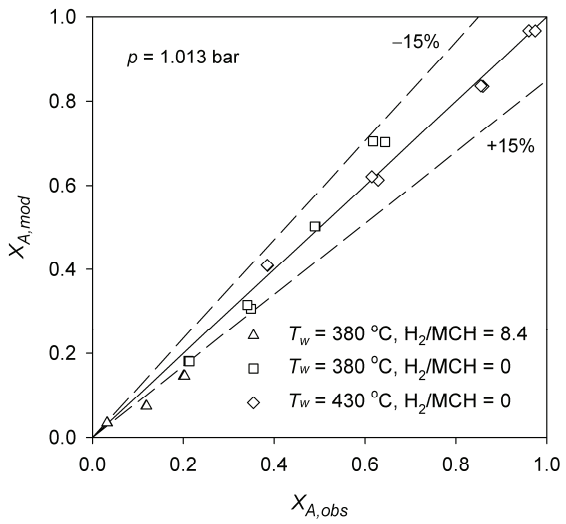

Fig. 5. Scatter diagram between observed conversion and model or calculated conversion.

Fig. 5 is the scatter diagram relating observed conversion and model conversion. Most of the data were observed to be fitted within ±15% error and showed an overall good fit to the first order reversible kinetics. Apparent activation energy was calculated as 100.6 kJ/mol and k_r as 1.65 × 10^{-5} mol·s^{-1}·g-cat^{-1}·Pa^{-1}.Touzani et al. [11], Van Trimpont et al. [12], Rimensberger [13] and Manser Sonderer [14] by studying the dehydrogenation reaction over Pt containing alumina catalysts also found values close to the above activation value.

CONCLUSIONS

The dehydrogenation reaction was strongly affected by catalyst particle size, temperature and feed composition. MCH conversion reached 97.5% in the absence of hydrogen at 430 °C wall temperature and a space velocity of 2.46×10^5 s·g-cat/mol MCH. First order reversible kinetics was found appropriate to fit the experimental data. Apparent activation energy was 100.6 kJ/mol.

NOMENCLATURE

B	dimensionless activation energy
d_{vs}	volume to surface diameter, m
F_{A0}	initial molar flowrate of methylcyclohexane (MCH), mol/s
Δh°_{rxn}	standard heat of reaction, J/mol
k	rate or velocity constant, mol·s^{-1}·kg-cat^{-1}·Pa^{-1}
k_r	rate constant at reference temperature, mol·s^{-1}·kg-cat^{-1}·Pa^{-1}
k_0	frequency factor, mol·s^{-1}·kg-cat^{-1}·Pa^{-1}
K	dehydrogenation reaction equilibrium constant, Pa^3
p_A	partial pressure of methylcyclohexane, Pa
p_B	partial pressure of toluene, Pa
p_C	partial pressure of hydrogen, Pa
$(-r_A)$	rate of the dehydrogenation reaction, mol·s^{-1}·kg-cat^{-1}
R	universal gas constant, m^3·Pa·K^{-1}·mol^{-1}
T	average temperature, K
T_r	reference temperature, K

W	weight of the catalyst, kg
X_A	fractional conversion of methylcyclohexane to toluene
$X_{A,obs}$	observed fractional conversion
$X_{A,mod}$	model or calculated fractional conversion

ACKNOWLEDGMENT

The author acknowledges the Higher Education Commission of Pakistan for funding the study.

REFERENCES

1. Schildhauer, T.H. *Untercuchungen zur Verbesserung des Wärmeübergangs in Katalytischen Festbettreaktoren für Energiespeicheranwendungen.* PhD Thesis. ETH No. 14301. Eidgenössischen Technischen Hochschule. Zürich (2001).
2. Bustamante, G.V.S.C., Y. Swesi, I. Pitault, V. Meille & F. Heurtaux. *A Hydrogen Storage and Transportation Mean.* Proc. Int. Hydrogen Energy Cong. Exh. IHEC, Istanbul (2005).
3. Cresswell, D.L. & I.S. Metcalfe. Energy Integration Strategies for Solid Oxide Fuel Cell Systems. *Solid State Ionics* 177: 1905–1910 (2006).
4. Tsakiris, D.E. Catalytic Production of Hydrogen from Liquid Organic Hydride. Ph.D. Thesis. The University of Manchester, Manchester (2007).
5. Yolcular, S. & Ö. Olgun. Hydrogen Storage in the Form of Methylcyclohexane. *Energy Sources* 30: 149–156 (2008).
6. Alhumaidan, F.S. *Hydrogen Storage in Liquid Organic Hydrides: Producing Hydrogen Catalytically from Methylcyclohexane.* PhD Thesis. The University of Manchester, Manchester (2008).
7. Usman, M.R. *Kinetics of Methylcyclohexane Dehydrogenation and Reactor Simulation for "On-board" Hydrogen Storage. PhD Thesis. The University of Manchester,* Manchester (2010).
8. El-Sawi, M., F.A. Infortuna, P.G. Lignola, A. Parmaliana, F. Frusteri, & N. Giordano. Parameter Estimation in the Kinetic Model of Methylcyclohexane Dehydrogenation on a Pt-Al_2O_3 Catalyst by Sequential Experiment Design. *Chem. Eng. J.* 42: 137–144 (1989).
9. Maria, G., A. Marin, C. Wyss, S. Müller & E. Newson. Modelling and Scalup of the Kinetics with Deactivation of Methylcyclohexane Dehydrogenation for Hydrogen Energy Storage. *Chem. Eng. Sci.* 51: 2891–2896 (1996).
10. Schildhauer, T.H., E. Newson & S. Müller. The Equilibrium Constant for Methylcyclohexane-Toluene System. *J. Catal.* 198: 355–358 (2001).
11. Touzani, A., D. Klvana & G. Bélanger. Dehydrogenation of Methylcyclohexane on the Industrial Catalyst: Kinetic Study. *Stud. Surf. Sci. Catal.* 19: 357–364 (1984).
12. Van Trimpont, P.A., G.B. Marin & G.F. Froment. Kinetics of Methylcyclohexane Dehydrogenation on Sulfided Commercial Platinum/ Alumina and Platinum-Rhenium/Alumina Catalysts. *Ind. Eng. Chem. Fundam.* 25: 544–553 (1986).
13. Rimensberger, T.K. *Kinetische Untersuchungen der dehydrierung von methylcyclohexan zu toluol im mikropulsreaktor, im kontinuierlichen mikroreaktor und im laborfestbettreaktor.* PhD Thesis. No. 8278. Swiss Federal Institute of Technology, Zürich (1987).
14. Manser Sonderer, R.H. *Methylcyclohexane Dehydrogenation Kinetics, Reactor Design and Simulation for a Hydrogen Powered Vehicle.* PhD Thesis. ETH No. 9996. Swiss Federal Institute of Technology, Zürich (1992).

Proceedings of the Pakistan Academy of Sciences 48 (1): 19–32, 2011

ISSN: 0377 - 2969


Pakistan Academy of Sciences

Satellite-Based Snowcover Distribution and Associated Snowmelt Runoff Modeling in Swat River Basin of Pakistan

Zakir H. Dahri[1*], Bashir Ahmad[1], Joseph H. Leach[2] and Shakil Ahmad[3]

[1] Pakistan Agricultural Research Council, Islamabad, Pakistan
[2] Department of Geomantic, The University of Melbourne, Australia
[3] National University of Science and Technology, Islamabad, Pakistan

Abstract: The snowcover and glaciers of Hindu Kush–Himalayan (HKH) region are one of the largest repositories of inland cryosphere outside Polar Regions and obviously the lifeline for the people of sub-continent. However, reliable estimates of the snow area extent and snowmelt runoff have been lacking in this largely inaccessible and data sparse region. This is particularly important in view of the climate change impacts on hydrological resources of the region. Present study utilized GIS, RS and hydrological modeling techniques to estimate spatial and temporal distribution of snowcover; quantified snowmelt and rainfall runoff components; and developed prediction models for snowmelt and river discharges. The results revealed that Swat River Basin of Pakistan is predominantly snow-fed, as the annual snowmelt runoff contribution to the total runoff may range 65–75 %. A significant effect of snowcover variation was observed on river discharge and snowmelt runoff. Snowcover and associated snowmelt runoff remain highly variable throughout the calendar year. Snowfall usually starts abruptly in September and October months but the following four main winter months (i.e., November–February) generally bring in most of the snowfall. Snowcover increases from less than 2 % of the Basin area in August, only at higher altitudes, to about 64 % by the end of January or early February. Snowmelt generally continues throughout the year but contribution of winter snowmelt runoff is generally very low. Unlike snowfall, snowmelt runoff usually progresses gradually and smoothly and is more predictable. The summer snowmelt normally gets momentum in March and increases from around 30–60 m^3/sec to 400-760 m^3/sec in late June or early July. Thereafter, it declines gradually, reducing to 30-50 m^3/sec in December. The December–February runoff normally remains the same.

Keywords: Snowcover, snowmelt, runoff, hydrological modeling, GIS, RS

INTRODUCTION

Snow and glaciers are the frozen reservoirs of fresh water and cover a significant part of many mountain chains on the globe. In Pakistan about 5218 glaciers covering an area of 15,040 sq km were identified in the ten sub-basins of Indus River System [1]. These glaciers constitute 11.7 % of the total area of these basins and are an important source of fresh water in Pakistan as 50 – 85 % of the country's total flows come from melting snows and glaciers of the this region [1, 2, 3]. The major tributaries of the Indus River originate from the Hindu Kush-Himalayan (HKH) region and have their upper catchments in the high mountain snow covered areas and flow through steep mountainous slopes. The planning of new projects on HKH rivers in Pakistan emphasizes the need for reliable estimates of the snow extent and glacier runoff because it provides a more dependable and perennial flow. Despite their well recognized importance and potential, little attempts have been made to assess in detail the contributions of snowmelt runoff in these rivers.

No detailed investigation of snow and ice processes or their relevance to climate has taken place in most areas of the Himalayan and other high ranges. Baseline studies are lacking for most areas, particularly for those higher than 4,000 masl, and there has been little long-term

Received June 2010, Accepted March 2011
*Corresponding author: Zakir H. Dahri; E-mail: zakirdahri@yahoo.com

monitoring of climatic variables, perennial snow and ice, runoff and hydrology in the extremely heterogeneity of mountain topography [4]. In the areas where bulk of the water originates, above 3000 meters or so, there are no permanent observation stations. The main need is for the investigation of water resources at elevations between 3000 to 7000 meters. There is a dire need for cryosphere database development and to study the impact of climate change on the cryosphere. Remote sensing techniques are the only way to analyze glaciers in remote mountains and they are certainly the only way to monitor a large number of glaciers simultaneously.

Recent advances in GIS, remote sensing and hydrological modeling techniques allow their powerful integration. In the field of snowmelt runoff modeling, such integration provides valuable basis for better understanding of snow accumulation and snowmelt runoff processes within the catchments, as well as for incorporating the spatial variability of hydrological and geographical variables and their impacts on catchment responses [5].

Rango et al. [6] employed snow-covered area data obtained from meteorological satellites over remote regions of Pakistan and concluded that it can be scientifically related to seasonal stream flow in regression analysis for the Indus River above Besham and Kabul River above Nowshera in Pakistan [6]. Combining the remote sensing derived snow and ice cover maps with a hydrologic runoff model the daily runoff can be calculated [7, 8]. Snow and icemelt are important contributors to the total yearly runoff volume in high alpine basins. Schaper and Seidel [9] carried out runoff simulations for snow and icemelt for the basins of Rhine-Felsberg, Rhône-Sion and Ticino-Bellinzona. This study provides a method to calculate runoff from snow- and icemelt using meteorological data and remote sensing derived snow and ice cover maps.

The Snowmelt Runoff Model (SRM) is one of a very few models in the world today that requires remote sensing derived snow cover as model input. Owing to its simple data requirements and use of remote sensing to provide snow cover information, SRM is ideal for use in data sparse regions, particularly in remote and inaccessible high mountain watersheds [10].

Runoff computations by SRM appear to be relatively easily understood. To date the model has been applied by various agencies, institutes and universities in over 100 basins, situated in 29 different countries. More than 80% of these applications have been performed by independent users, as is evident from 80 references to pertinent publications. SRM also successfully underwent tests by the World Meteorological Organization with regard to runoff simulations [11] and to partially simulated conditions of real time runoff forecasts [12].

Seidel et al. [13] successfully simulated the runoff in the large Himalayan Basin, e.g. Ganges and Brahmaputra basins, by applying SRM [13]. SRM performs well in the Gongnaisi River basin and results also show that SRM can be a suitable snowmelt runoff model capable of being applied in the western Tianshan Mountains [10]. Emre et al. [14] applied SRM in upper Euphrates River using MODIS-8 daily snow cover products for 2002-04. The initial results of their modeling process show that MODIS snow-covered area product can be used for simulation and also for forecasting of snowmelt runoff in basins of Turkey. The SRM application in Kuban river basin using MOD10A2 eight-day composite snow cover data enabled the investigator to conclude that the model can be used for short-term runoff forecasts in the mountain and foothill areas of the Krasnodar reservoir basin [15].

Climate change is likely to affect basin's water resources so there is a need to monitor and estimate the fresh water resource base (snowcover) and assess the impacts of its variation on net water availability. Present study has been conducted in Swat River Basin which is snowfed and source of fresh water especially in summer season. The specific objectives of this research study are:

- Estimation of spatial and temporal distribution of snowcover through satellite remote sensing;
- Estimation and quantification of snowmelt and rainfall runoff components through hydrological modeling; and
- Development of snowmelt runoff prediction models.

Characteristics of the Study Area

The study was undertaken in the catchment area of Swat River upstream of Chakdara gauge. The study area is located between the latitude and longitude range of 34.57 to 35.9 and 71.9 to 72.8 decimal degrees respectively covering an area of 5713.4 km^2. Its northern part has high mountainous of rugged terrain with elevation range of 2000–5808 m a.s.l., whereas the southern part is relatively flat with elevation range of 686–2000 m a.s.l. having some crop fields on either side of the river as shown in Fig. 1.

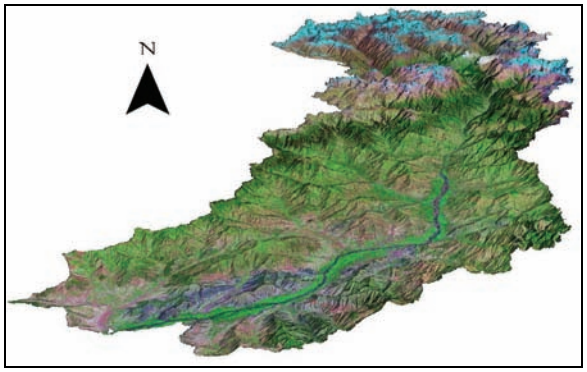

Fig. 1. True color LANDSAT image of the study area .

Based on the historic as well as prevailing climatic conditions, the study area can be divided into two parts. The upper north-eastern part – Kalam and surrounding areas – comprises very rugged mountain topography and may reach a maximum temperature of 37 °C in June at Kalam to as low as –18.2 °C in January at Shandur. The lower south-eastern part near Saidu Sharif and Chakdara is relatively flat, having considerably higher temperatures ranging from -2 °C in January to as high as 45 °C in June. Similarly, the precipitation pattern in the lower south-western part is influenced by the summer monsoon rainfall. The upper north-eastern part on the other hand is dominated by the winter rainfall mainly received from the Western Disturbances, which come from the Mediterranean Sea after passing through Iran and Afghanistan enter Pakistan in December and continue till early April. The northern highlands receive most of winter precipitation in the form of snow 1 km at nadir. The 1st two bands were imaged at a nominal resolution of 250 m at nadir, next five bands at 500 m, and the remaining 29 bands at 1 km. The MODIS snow products use only the 1st seven and last two bands between 0.405 and 14.385 µm for different uses. Its spatial resolution varies with spectral band, and ranges from 250 m to instrument acquires images in 36 spectral.

METHODOLOGY

The methodology employed to accomplish this study is summarized in the flow chart shown in Fig. 2. The important steps are described in the following paragraphs.

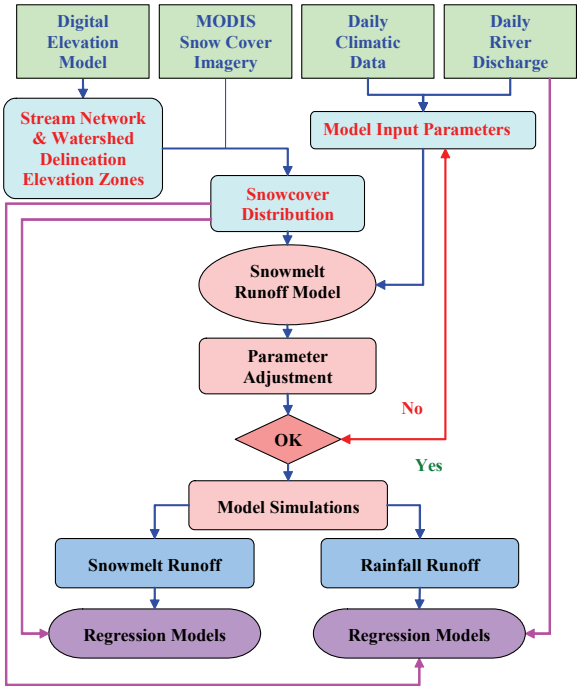

Fig. 2. Flow diagram of the methodological approach.

Snowcover Estimation

The snowcover was estimated using the Snowcover products of MODIS (Moderate Resolution Imaging Spectroradiometer) instrument onboard the Terra spacecraft launched on December 18, 1999 and the Aqua spacecraft, launched on May 4, 2002. Terra's orbit around the Earth is timed so that it passes from north to south across the equator in the morning, while Aqua passes south to north over the equator in the afternoon.

The development of the MODIS snow mapping algorithm (snowmap) is chronicled in detail by [16–21]. The basic techniques used in

the snowmap algorithm are grouped-criteria incorporating the normalized difference between bands, threshold-based criteria tests, and decision rules [18]. The first test of snow detection uses the Normalized Difference Snow Index (NDSI) approach, which is an effective way to distinguish snow from many other Generally, snow is characterized by higher NDSI values than other surface types and pixels. A pixel is mapped as snow if the NDSI value is ≥ 0.4 and the reflectance in MODIS band 2 is greater than 0.11. However, if the reflectance in MODIS band 4 is less than 0.10 then the pixel will not be mapped as snow even if the other criteria are met [18, 19]. This minimum reflectance test screens low reflectance surfaces, e.g. water that may have a high NDSI value from being erroneously detected as snow. However, in forest areas snow-covered pixels may have considerably lower NDSI values and to correctly classify these pixels as snow covered, NDSI and NDVI are used together to the pixels that have an NDSI value in the range of 0.1 to 0.4. The NDVI is calculated as:

$$NDVI = \frac{Band2 - Band1}{Band2 + Band1}$$

Snow cover tends to lower the NDVI therefore pixels with NDVI value of ≈ 0.1 may be mapped as snow even if the NDSI < 0.4 [17]. Moreover, pixels with an absolute reflectance greater than 0.11 in MODIS band 2 & greater than 0.10 in MODIS band 1 are labeled as snow.

Because of higher reflectance of clouds in near-infrared wavelengths the NDSI generally separates snow from most obscuring cumulus clouds, but it cannot always discriminate optically-thin cirrus clouds from snow. Instead, cloud discrimination is accomplished by using the MODIS cloud mask product, MOD35L2, [22, 23], which employs a series of visible and infrared threshold and consistency tests to specify confidence that an unobstructed view of the Earth's surface is observed. An indication of shadows affecting the scene is also provided.

Land and inland waters are masked with the 1 km resolution land/water mask, contained in the MODIS geolocation product (MOD03). Thermal mask is used to improve the snow mapping accuracy and to eliminate the spurious snow especially in warm climates. Using MODIS infrared bands 31 (10.78–11.28 μm) and 32 (11.77–12.27 μm), a split window technique [24] is used to estimate ground temperature [19]. surface features taking advantage of strong visible reflectance and strong short-wave IR absorbing characteristics of the snow pack. The NDSI is defined as:

$$NDSI = \frac{Band4 - Band6}{Band4 + Band6}$$

If the temperature of a pixel is greater than 283 ^{0}K then the pixel will not be mapped as snow [21].

Fractional snow cover is calculated using the regression equation of Salomonson and Appel [25], which is based on a statistical-linear relationship developed between the NDSI from MODIS and the true sub-pixel fraction of snow cover as determined using Landsat scenes from Alaska, Canada and Russia. The data inputs to the MODIS snowmap algorithm are summarized in Table 1.

Table 1. MODIS data product inputs to the MODIS snowmap algorithm.

Earth Science Data Type (ESDT)	Long Name	Data Used
MOD02HKM	MODIS Level 1B Calibrated Geolocated Radiances	Reflectance for MODIS bands: 1 (0.645 μm) 2 (0.865 μm) 4 (0.555 μm) 6 (1.640 μm)
MOD021KM	MODIS Level 1B Calibrated & Geolocated Radiances	31 (11.28 μm) 32 (12.27 μm)
MOD03	MODIS Geolocation	Land/Water Mask Solar Zenith Angles Sensor Zenith Angles Latitude Longitude
MOD35L2	MODIS Cloud Mask	Cloud Mask Flag Unobstructed Field of View Flag Day/Night Flag

Source: After [21]

The accuracy of snowmap has been tested over a variety of surface covers relative to other derived snow cover maps. Under ideal conditions of illumination, clear skies and several centimeters of snow on a smooth surface

the snow algorithm is about 93-100% accurate at mapping snow [20]. Lower accuracy is found in forested areas and complex terrain and when snow is thin and ephemeral. Very high accuracy, over 99%, may be found in croplands and agricultural areas.

Snow Melt Runoff Model

The snowmelt runoff model (SRM), also known as "Martinec-Rungo Model" [26] is a semi-distributed, deterministic and degree-day hydrological model especially designed to simulate and forecast daily stream flow inmountain basins where snowmelt is major runoff factor [27]. The model utilizes ambient air temperature values combined with a degree-day coefficient in order to estimate the ablation factor of the snow cover and takes input of snow covered area and its variation along meteorological data. The basin area is divided in to a suitable number of elevation zones (not exceeding 16) and various input parameters including basin characteristics, climatic variables, snow covered area, runoff co-efficients, recession coefficients, etc are specified for each elevation zone. The model manages a physical database of both input and output for a given basin. Each simulation in the model is a unique entity operating on a 2– 366 days. Different simulations can be sequenced for greater time periods. The SRM computes daily water produced from snowmelt and rainfall, superimposes it on the calculated recession flow and transforms it into daily discharge from the basin according to the following equation.

$$Q_{n+1} = \left[c_{Sn} a_n (T_n + \Delta T_n) S_n + c_{Rn} P_n\right] \frac{A.10000}{86400} (1 - k_{n+1}) + Q_n k_{n+1}$$

Where:

Q = average daily discharge [$m^3 s^{-1}$]

c = runoff coefficient expressing the losses as a ratio (runoff/precipitation), with c_S referring to snowmelt and c_R to rain

a = degree-day factor [cm $^oC^{-1}$ d^{-1}] indicating the snowmelt depth resulting from 1 degree-day

T = number of degree-days [^oC d]

ΔT = the temperature lapse rate correction factor [^oC d]

S = ratio of the snow covered area to the total area

P = precipitation contributing to runoff [cm]. A pre-selected threshold temperature, T_{CRIT}, determines whether this contribution is rainfall (immediate) or snow (delayed).

A = area of the basin or zone [km^2]

k = recession coefficient indicating the decline of discharge in a period without snowmelt or rainfall. K = Q_{m+1}/Q_m (m, m + 1 are the sequence of days during a true recession flow period).

n = sequence of days during the discharge computation period. Equation (1) is written for a time lag between the daily temperature cycle and the resulting discharge cycle of 18 hours. In this case, the number of degree-days measured on the n^{th} day corresponds to the discharge on the n + 1 day. Various lag times can be introduced by a subroutine.

10000/86400 = conversion from cm·km^2 d^{-1} to m^3 s^{-1}

Derivation of Model Input Parameters

The input data requirements of the SRM are categorized into three categories i.e. basin characteristics, variables and parameters. The basin characteristics are usually computed from the digital elevation model of the area. The variables include temperature, precipitation and snowcover. The actual/observed records of temperature and precipitation are available while snowcover is estimated from MODIS satellite imagery. The parameters are temperature lapse rate, critical temperature, degree day factor, time lag, runoff coefficient, rainfall contributing area, and recession coefficient. These parameters can be computed from field measurements, derived from the variables or determined through physical laws. In cases where actual data are not available, adjustment and refinement of certain parameters within permissible limits during model verification is usually done.

Basin Characteristics

The watershed and river network has been delineated from the SRTM DEM data of the Swat basin using ArcHydro extension of ArcGIS software. Since, the SRM represents a semi-distributed approach, considering each catchment section with similar hydrological characteristics as a single unit (hydrological response unit, HRU), the basin has been divided

into five elevation zones (Zone-A to Zone-E) keeping in view the available elevation range of 686 m–5808 m as shown in Fig. 3. The total area of the basin is 5713.38 sq. km with a mean hypsometric elevation of 2727.2 m. The mean hypsometric elevations for each elevation zone are 1133.42, 1956.63, 3014.76, 4007.57, 4726.55 m respectively.

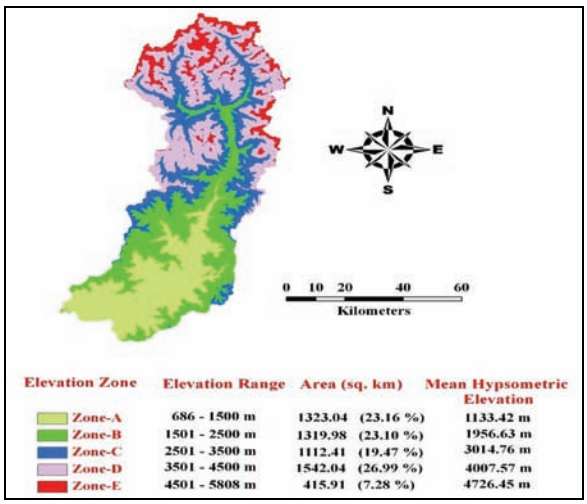

Fig. 3. Elevation zones, their areas & mean hypsometric elevation.

Variables

The daily meteorological data for a number of met stations in the vicinity of study basin has been acquired from Pakistan Meteorological Department (PMD) and Surface Water Hydrology Project of WAPDA. The study utilizes temperature data of Kalam observatory for each elevation zone. For precipitation, data of Saidu Sharif (961 m amsl) is used for Zone A, Kalam (2103 m amsl) for Zones B, C, and D and Shandur (3719 m amsl) for Zone E. Snowcover extent in the watershed and in each elevation zone has been determined from the eight daily MOD10A2 MODIS snowcover product. A total of 138 satellite images spread over a period of three years (1st January 2002 to 31st December 2004) are processed through ERDAS Imagine and ArcGIS softwares.

Temperature lapse rate: The temperature lapse rate due to elevation difference is estimated by plotting the temperature records of a number of met stations located in the vicinity of study basin. The computed temperature lapse rates for January to December months are 0.68, 0.69, 0.69, 0.67, 0.70, 0.73, 0.62, 0.61, 0.64, 0.68, 0.66, and 0.65 ^{0}C / 100 m respectively.

Degree day factor: Since, the average temperatures always refer to a 24 hour period starting at 6.00 hrs; they become degree-days, T (^{0}C.d). The degree-day factor (a) can be determined by comparing degree-day values (temperature values above a certain base temperature) with the daily decrease of snow water equivalent (SWE). However, the data on variation of SWE is rarely available. In the absence of any detailed data, the degree day factor can be calculated from the following empirical relation [27]:

$$a = 1.1.\frac{\rho_s}{\rho_w}$$

Where: a is the degree day factor (cm/^{0}C/d), and ρ_s & ρ_w are densities of snow and water respectively. Density of snow usually varies from 0.3 to 0.55 gm/cc resulting in value of degree-day factor in the range of 0.35 – 0.61, with lower value recommended for fresh snow and snow under forest canopy. However, slightly higher values have also been reported in the snow melt runoff modeling studies [27]. The degree-day factor converts the number of degree-days T [^{0}C·d] into the daily snowmelt depth M [cm] by the following relation:

$$M = a.T$$

Critical temperature: Critical temperature determines whether the precipitation is in the form of rain or snowfall. Usual values ranging from +3^{0}C in April to 0.75^{0}C in July are reported [26] with higher values in snow accumulation periods. A similar trend with a narrower range +1.5^{0}C to 0^{0}C is reported by US Army Corps of Engineers [29]. It is very difficult to differentiate exactly between rain and snow because the temperature used is the daily average while precipitation may occur at any time during the day and that particular moment may be warmer or colder than the assigned temperature value. SRM needs the critical temperature only in the snowmelt season in order to decide whether precipitation immediately contributes to runoff, or, if T < TCRIT, whether snowfall took place. This parameter is more important for year round simulations which model both snow accumulation and snow ablation periods.

Rainfall contributing area: Snow pack is usually dry before and during early snowmelt season and most of the rain falling on snow pack is normally retained by it. Only snow free area contributes to rainfall runoff during that period. However, at

some later stage the snow pack becomes wet and the rain falling afterwards can flow as runoff. The user has to decide which time periods snow pack in a particular area and height will be dry and assign that input to the model accordingly. The melting effect of rain however is neglected because the additional heat supplied by the liquid precipitation is considered to be very small [30].

Runoff coefficient: The runoff coefficient takes care of the losses from the basin's available water resources (rain + snow) during its conveyance to the outlet. The average value of runoff coefficient for a particular basin is given by the ratio of annual runoff to annual precipitation. The comparison of historical precipitation and runoff ratios provide starting point for estimation of runoff coefficient. However, more often it varies throughout the year as a result of changing temperature, vegetation and soil moisture conditions. Moreover, very high uncertainty involved in the measurement of true representative precipitation poses serious difficulties in its correct estimation. For this reason, among SRM parameters, the runoff coefficient is the primary candidate for adjustment during model calibration [27]. Runoff coefficient is usually higher for snow melt than for rainfall due to effect of cold water soil hydraulic conductivity.

Recession coefficient: Stream flow recession represents withdrawal of water from the storage with no or little inflow. River discharge data of Chakdara gauge station, which is located at the exit point of the basin, was collected from Surface Water Hydrology Project (SWHP) of Water and Power Development Authority (WAPDA), Pakistan. The discharge on a given day (Q_n) is plotted on the logarithmic scale against the value of discharge on the following day (Q_{n+1}) as shown in the Fig. 4. An envelop is drawn to enclose most of the points and the lower envelop line of all points is considered to indicate the k-values.

For $Q_{n+1} = 700$ and $Q_n = 900$, the value of k is derived from relation $k = Q_{n+1} / Q_n$, or $k = 700/900 = 0.777$. Similarly, the value of k_2 can be derived from the other corresponding values of Q_{n+1} and Q_n. It is observed that the value of k increases with decreasing Q, by solving the equation $k_{n+1} = x.Q_n^{-y}$, the values of constants x and y are computed for two corresponding Q and k values.

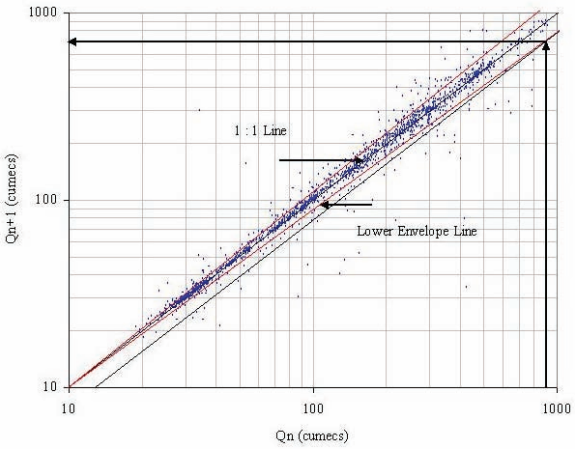

Fig. 4. Recession flow plot Q_n vs Q_{n+1} for the Swat River Basin of Pakistan.

Time lag: For large basins with multiple elevation zones, the time lag changes during the snowmelt season as a result of changing spatial distribution of snow cover with respect to the basin outlet. Generally the time lag in a basin increases as the snow line retreats. If there is uncertainty, the time lag can be adjusted in order to improve the synchronization of the measured and simulated peaks of average daily flows.

Model Calibration and Verification

The mountain hydrology is mainly the function of topography and meteorology however the knowledge about interaction of these components of mountain hydrology is generally limited and qualitative in nature [31]. Therefore, there is more reliance on river flow data of the mountain areas which largely represent the hydrological responses of all the existing topographical factors and meteorological events taking place in the mountain regions [32, 33].

The SRM normally does not require calibration as its input parameters are generally derived from the field data and historical records through physical laws and empirical relationships. However, gathering of all the required data is only a dream for a highly rugged mountain terrain in a country like Pakistan, where inaccessibility and lack of resources generally limit collection of such data. Hence, calibration of the model and some rational adjustment of few input parameters are unavoidable and in fact the user gains more confident over the simulation results. Therefore, some of the parameters were adjusted during calibration and verification against the daily

river inflows of year 2002 to 2004. Besides visual inspection, the accuracy of calibration was judged from the two well established accuracy criteria [27], the coefficient of determination (R^2) and the deviation of runoff volumes (Dv).

RESULTS AND DISCUSSION

Spatial and Temporal Distribution of Snowcover

Determining contribution of snowmelt runoff to river discharges has great practical significance as snowmelt runoff is more dependable source of fresh water. Unfortunately, the highly rugged ground control to accurately monitor metrological data and snowcover information on a continuous basis. In such circumstances satellite remote sensing has great value and seems to be the only viable alternative, as it can provide repetitive data on snow area extent at different, regular time intervals. The study utilized MODIS snowcover products to estimate snow area extent in the Swat River Basin of Pakistan. The MODIS 8-daily (level 3, version 5) maximum snow extent composite snowcover product (MOD10A2) was processed in a RS and GIS environment to estimate spatial and temporal variation of snow cover in the basin. In all 140 images distributed over three years period (Jan. 2002 to Dec. 2004), were processed and analyzed. Fig. 5 presents temporal (on daily basis) variation of snowcover at various elevation zones for the three years period, while Fig. 6 shows spatial distribution of snowcover through the sequence of selected time series GIS processed snowcover maps of the basin for the same period.

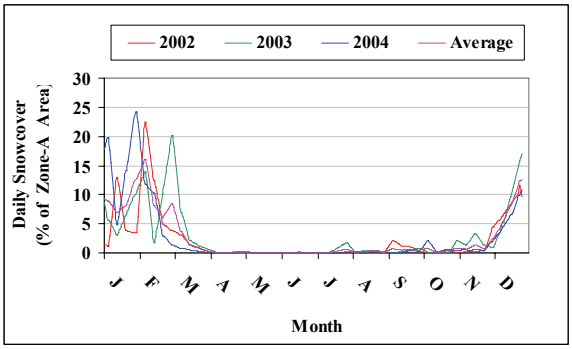

a. Snowcover distribution in Zone-A

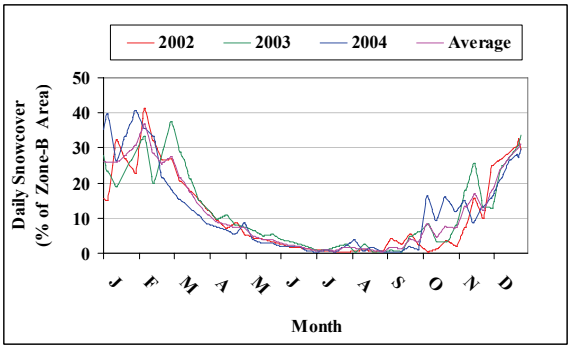

b. Snowcover distribution in Zone-B

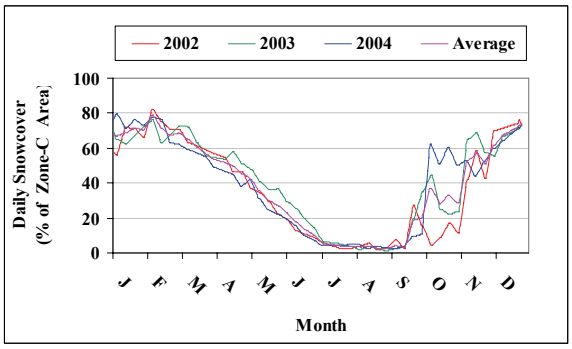

c. Snowcover distribution in Zone-C

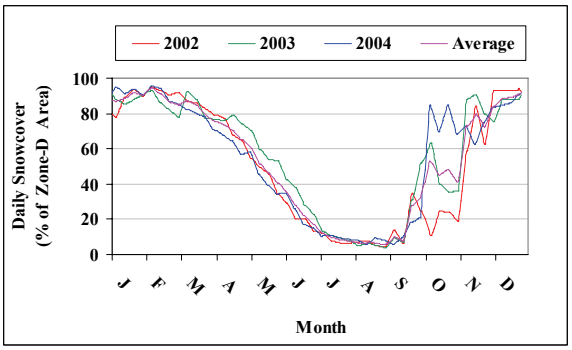

d. Snowcover distribution in Zone-D

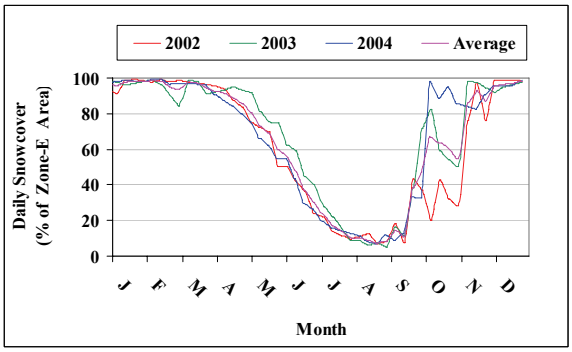

e. Snowcover distribution in Zone-E

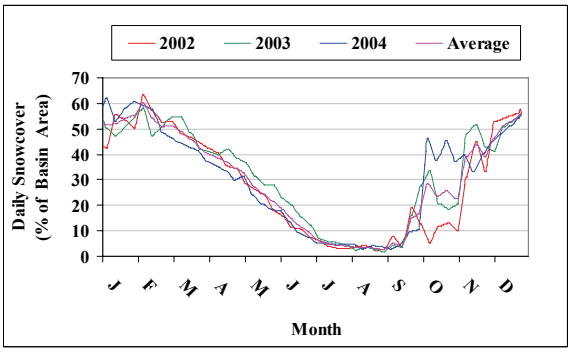

f. Snowcover distribution in Zone-F

Fig. 5. Temporal variation of snowcover at various elevation zones for the three years period.

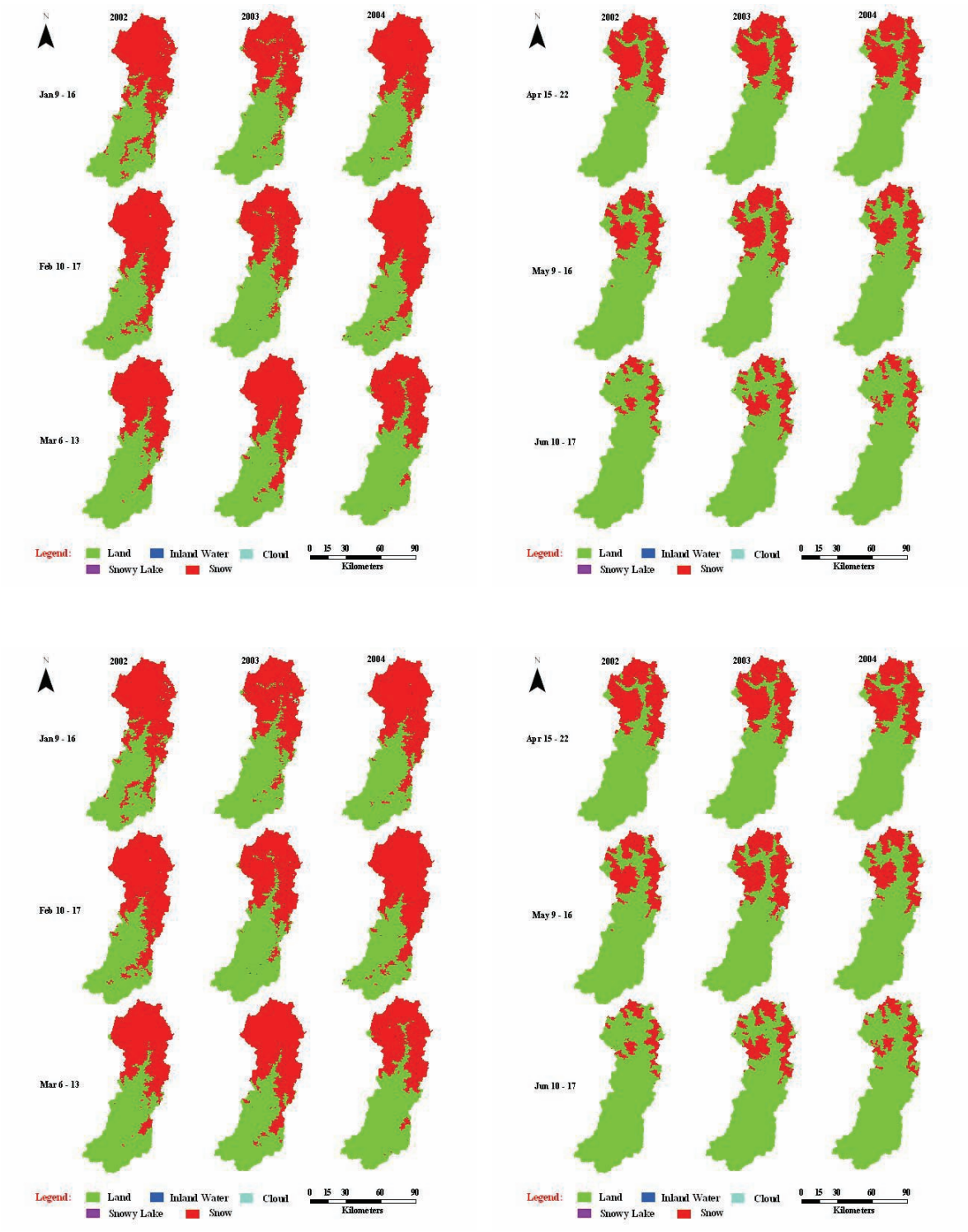

Fig. 6. Snowcover variation during Jan – Mar, Apr – Jun, Jul – Aug, and Sep – Dec.

The analysis and visual observation of the generated snowcover maps and developed graphs reveal that snowfall and subsequent snowmelt in the Swat river basin is highly variable in terms of altitude, space and time. The snowfall usually starts by the mid to late September initially at higher elevations and snow area may be increased abruptly from less than 2% in August to about 10–20 % of the total basin area. Occasional and unpredictable rainstorms in September and October months most often bring immediate, abrupt and significant increase in snowcover area and snowcover may cover about 45% of the total basin area by the end of October. However, the following few weeks are unable to maintain that

tempo due to temperature variation and consequently some decline in snowcover is usually observed in many cases due to subsequent and immediate melting of that fresh and temporary snowcover. The main winter months (Nov–Feb) generally bring in most of the snowfall and snowcover keeps accumulating reaching its peak area by the end of January or early February covering about 58 – 64 % of the basin area. Significant snowfall at lower elevations is also witnessed during these main winter months as the snowcover gets extended down to valleys in southern parts and snowline may reach at elevations less than 1500 m. At higher elevations above 3500 m a.s.l. snow may continue to fall even in March and April months (Fig. 5d, 5e) when snow area in 2003 increased during these months.

Snowmelt generally continues throughout the year but contribution of winter snowmelt runoff is often insignificant. Flow during the winter season is usually augmented from surface flow due to seasonal rains, sub-surface flow, and ground-water contribution and is termed as the base flow. Unlike snowfall, snowmelt usually progresses gradually and smoothly and is more easily predictable. The summer snowmelt normally gets momentum in the month of March which may also bring in some new snows at times of cold waves accompanied with precipitation particularly at higher elevations. The net outcome however is towards snowmelt. At first the snow starts disappearing rapidly from valleys at southern parts of the basin and from elevations less than 2500 m in early March, which gradually widens and the snowline retreats upward as the summer season progresses and temperature is increased. At elevations greater than 4500 snowmelt starts in late April and continues till mid September. During July to mid September temperatures are usually sufficient enough to melt the snow and snowmelt is mainly the function of available snow, which is mostly concentrated at highest elevations and is about to finish. Minimum snowcover is usually observed in the late August until the new snowfall season starts in September. During the monsoon season, the peak snowmelt runoff is augmented by monsoon rains to produce higher discharges and occasional peak floods sometimes destroy the infrastructure.

The three-year snowcover monitoring with remote sensing shows that under conducive climatic conditions, the maximum snow area extent may cover about 64 % of the total area of the basin during January-February to as low as 1.7 % in late August during the snowmelt season. However, spatial analysis of the three years snowcover maps as shown in Fig. 7 suggests that not always the same area receives snowfall. Table 2 further depicts that about 79.14 % of the area received snowfall at any time during 2002 – 2004. This area can be termed as area which generally accommodates temporary and seasonal snowfall. A handful of 20.72 % never received snowfall during that period; while only in 0.14 % (8.187 sq. km) of the basin area, snow cover remained in tact and could not be melted during that three years period. This area can be termed as permanent snow or glaciated area. It means that the entire basin predominantly accommodates temporary and seasonal snowcover, which is an important element of the hydrological cycle of the basin and major contributor to the basin's fresh water resources.

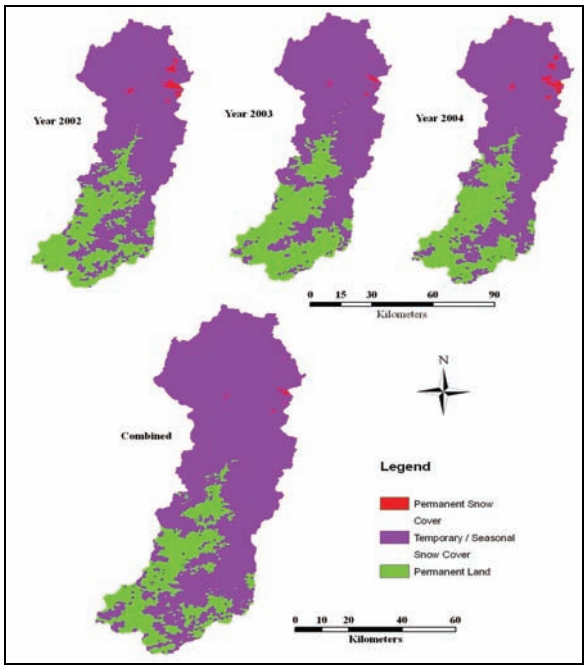

Fig. 7. Spatial analysis of permanent and temporary snow cover.

Table 2. Area under permanent and temporary snow covers for three study years.

Year	Permanent Land (sq km)	Temporary Snow (sq km)	Permanent Snow (sq km)
2002	1617.960 (28.32)	4043.269 (70.77)	52.150 (0.91)
2003	1809.644 (31.67)	3888.715 (68.06)	15.021 (0.26)
2004	1675.184 (29.32)	3981.328 (69.68)	56.867 (1.00)
2002–2004	1183.646 (20.72)	4521.546 (79.14)	8.187 (0.14)

Runoff Simulation Results

After estimation and derivation of all the model input parameters, the SRM was calibrated against the actually observed river flows during 2003. Some parameters were slightly adjusted and the calibrated model was verified for 2002 and 2004 river flows. Fig. 8 compares the simulated and actually observed river flows for years 2002, 2003 and 2004 while Table 3 assesses the accuracy of the simulation results by means of two statistical measures, i.e., coefficient of determination (R^2) and deviation of runoff volumes (D_v). The coefficient of determination is 0.796, 0.824 and 0.802 and the volume difference – 2.815%, - 4.077 %, and 3.202 % for 2002, 2003 and 2004 respectively. The calibration and verification results can be termed good and well within acceptable limits as SRM has been applied for over 112 basins in the past with 42% and -7.5 to +29.9% values of both these criteria, respectively [27]. Hence the calibrated and verified model can be used for simulation of any scenario.

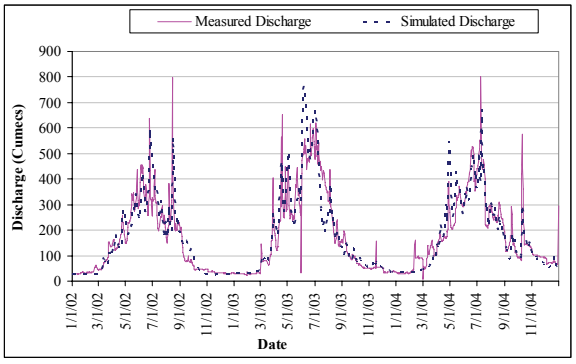

Fig. 8. Simulated and measured river flows.

Three scenarios have been developed in the present study. The first scenario runs the model with each year's own data and computes the daily runoff. The second scenario runs the model for each year's data but with no rainfall to calculate the respective share of snowmelt runoff into river discharge from the input of snowcover. The third scenario runs the model for each year with no rainfall and with normalized (putting historical average temperature values rather than each year's own temperature data) temperature. This scenario is developed to normalize the effect of temperature. It means whatever the effect of temperature is, it remains the same for each year and only the effect of snowcover change on snowmelt runoff is simulated.

Table 3. Year round simulation statistics for different study years.

Simulation Year	Measured Runoff Volume 10^6 m^3)	(Simulated Runoff Volume (10^6 m^3)	Volume Difference (%)	Coefficient of Determination (R^2)
2002	4465.18	4590.86	- 2.82	0.796
2003	5742.86	5977.02	- 4.08	0.824
2004	5874.32	5686.18	3.20	0.801

Simulated snowmelt and rainfall contribution components to runoff, computed through the SRM, are presented in Fig. 9. The figure clearly indicates the dominancy of snowmelt runoff as the basin is predominantly a snow-fed. However, there is also significant contribution of rainfall to runoff particularly in the summer monsoon moths of July and August. Snowmelt runoff contribution to the total runoff may ranges from 65–75 %. The results further suggest that about 30–60% of the total rain fall runoff occurs in monsoon season (July–September) and about 25–50 % in March to May period. The average contribution of snowmelt runoff to the total monthly runoff is 98.5, 91.2, 61.3, 61.6, 70.8, 83.0, 67.6, 53.3, 61.5, 73.1, 82.5, and 86.7 % for January–December months respectively.

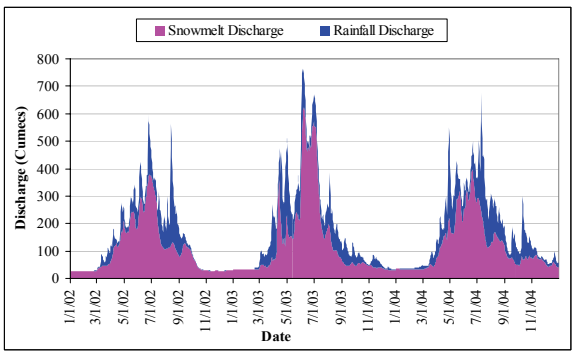

Fig. 9. Computed snowmelt and rainfall runoff components.

The study employed daily record of snowcover which show that snowfall can take place during eight months (September–April) and even minute amounts can be observed during the four main summer months. Therefore, relating winter snowcover with total summer runoff volume may give reasonable estimates for only the four main summer months (May–August). Instead this study not only relates the daily river discharges with the daily snow area extent but also develops prediction model for the total runoff volume of the four main summer months. The study also relates the simulated snowmelt runoff (excluding rainfall runoff component) with the snow area extent.

Fig. 10 clearly indicates a definite response of observed river discharges and simulated snowmelt runoff to seasonal snow cover changes, i.e. an increasing discharge associated with a decrease of snow area extent during the early summer (March-June), and decrease in discharge with decreasing snowcover in the late summer, monsoon season (July–August). Accordingly, two prediction models, described below, are developed to relate snowcover with river and snowmelt discharge.

Fig. 10(a) relates snow cover with river and snowmelt discharges for the early summer snowmelt season (March-June). This relationship can be described by the negative linear regression model as the river discharge increases with decrease in corresponding snowcover. Its relationship with the daily simulated snowmelt runoff is also negative but slightly different and is best explained by the third order polynomial function. This difference between the two regression models is due to variation of rainfall runoff component in the river discharges. Moreover, this inverse relationship is only true for the first part of the snowmelt season during which availability of snowcover is generally not a limiting factor and snowmelt runoff is largely the function of available temperature. But as the melting season progresses, the available snowcover gets depleted and it starts limiting the snowmelt runoff more than the temperature. Relationship between snowcover, snowmelt runoff and river discharge during the second part of the snowmelt season (July–August) as in Fig. 10(b) is completely different from that of the first part. During this summer monsoon period, most of seasonal snowcover at lower to medium elevations is melted and snowmelt runoff mainly comes from snowcover at high altitudes and permanent snow and glaciers of higher elevations. Unlike the previous model, this regression model shows positive relationship of average daily snowcover with the two runoffs. Also, there is exchange in type of regression model between the two relationships. The average daily snowcover now relates the simulated snowmelt runoff linearly, whereas its relationship with the average daily observed river discharge can be simplified by the second order polynomial function. The river discharge during the early July month tends to remain constant but greater river discharges in mid or late July than the early July month are due to greater contribution of rainfall runoff component during that period, otherwise snowmelt runoff decreases linearly during the following period.

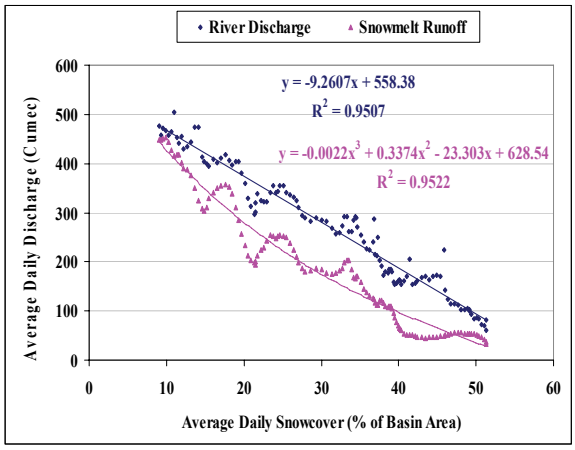

Fig. 10 (a) Relationship of daily snowcover with simulated snowmelt runoff and observed runoff for March–June months.

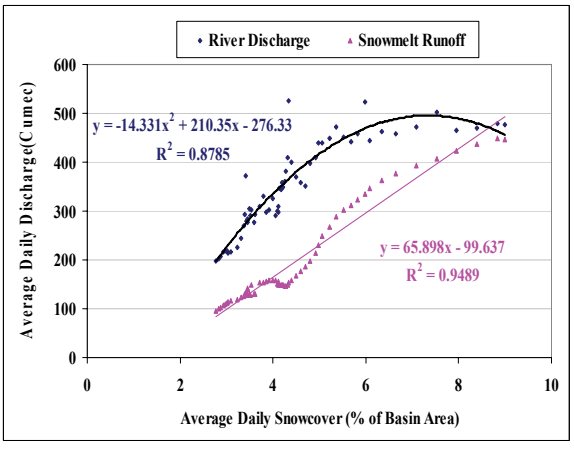

Fig. 10 (b) Relationship of daily snowcover with simulated snowmelt runoff and observed runoff for July–August months.

CONCLUSIONS

The altitudinal, spatial and temporal distribution of snowcover in the Swat River Basin of Pakistan was successfully evaluated using remotely sensed satellite imagery of the MODIS, GIS techniques and snowmelt runoff modeling. Increase in snowcover is observed in October and snow area extent sometimes may cover about 45 % of the basin area. The main winter months (i.e., November–February) generally bring in most of the snowfall and snowcover accumulates about 64 % from end of January or early February. The snowmelt normally starts in late February from lower elevation and increases gradually from around 30–60 m^3/sec to more than 400 m^3/sec to as high as 760 m^3/sec in late June or early July. The July–early September runoff is believed to be coming mainly from the melting of permanent snow and glacier melt at the highest elevations after most of the snowcover at lower to medium elevations disappears. On the basis of three-year simulation results, the study basin is found predominantly a snow-fed as annual snowmelt runoff contribution to the river flow may ranges 65–75 %. About 66 % of the total runoff (46 % snowmelt and 20 % rainfall) is generated during four main summer months (i.e., May–August).

REFERENCES

1. PARC & ICIMOD. *Inventory of glaciers, glacial lakes and glacial lake outburst floods (GLOFs) in the mountains of Himalayan Region*. International Centre for Mountain Development (ICIMOD) and Pakistan Agricultural Research Council (PARC), Islamabad **(**2005).
2. Tarar, R.N. Water resources investigation in Pakistan with the help of Landsat imagery — snow surveys 1975-1978. Hydrological Aspects of Alpine and High Mountain Areas, *Proceedings of the Exeter Symposium.* IAHS Pub. No. 138 (1982).
3. Hewitt, K. Snow and ice hydrology in remote, high mountain regions: the Himalayan sources of the river Indus. *Snow and Ice Hydrology Project, Working Paper. No. 1*, Wilfred Laurier University, Waterloo, Ontario, Canada (1985).
4. Liu, X. & B. Chen. Climate warming in the Tibetan Plateau during recent decades. *International Journal of Climatology* 20**:** 1729-1742 (2000).
5. Ahmad, B. *Development of a distributed hydrological model coupled with satellite data for snowy basins.* PhD thesis, University of Tokyo, Japan (2005).
6. Rango, A., V.V. Salomonson & J.L. Foster Seasonal stream flow estimation in the Himalayan region employing meteorological satellites snowcover observations. *Water Resources Research* 13(1): 109-112 (1977).
7. Ehrer, C., K. Seidel & J. Martinec. *Advanced analysis of snow cover based on satellite remote sensing for the assessment of water resources.* Proceedings of the IAHS Symposium: Remote Sensing and Geographic Information Systems for Design and Operation of Water Resources Systems, Rabat, Morocco, *IAHS Pub*. 242: 93–101 (1997).
8. Martinec, J. Snowmelt-runoff model for streamflow forecasts. *Nordic Hydrology* 6: 145 – 154 (1975).
9. Schaper, J. & K. Seide. *Modeling daily runoff from snow and glacier melt using remote sensing data.* Proceedings of EARSeL-SIG-Workshop Land Ice and Snow, Dresden/FRG (2000)
10. Hong, M. & C. Guodong. A test of Snowmelt Runoff Model (SRM) for the Gongnaisi River basin in the western Tianshan Mountains, China *Chinese Science Bulletin* 48 (20): 2253-2259 (2003).
11. WMO. *Inter-comparison of models of snowmelt runoff. Operational Hydrology Report 23,* World Meteorological Organization (WMO), Geneva, Switzerland. WMO -No. 646 (1986).
12. WMO. *Simulated real-time inter-comparison of hydrological models. Operational Hydrol.* Report 38, *WMO*, Geneva, Switzerland (1992).
13. Seidel K., J. Martinec & M.F. Baumgartner. Modeling runoff and impact of climate change in large Himalayan Basins. *Integrated Water Resources for Sustainable Development* 2: 1020-1028 (2000).
14. Emre, T., A. Zuhal, S. Arda, Ş Aynur & Ş. Ünal. Using MODIS snow cover maps in modeling snowmelt runoff process in the eastern part of Turkey. *Remote Sensing of Environment* 97(2): 216-230 (2005).
15. Georgievsky, M.V. Application of the Snowmelt Runoff model in the Kuban river basin using MODIS satellite images. *Environ. Res. Lett. 4*. doi:10.1088/1748-9326/4/4/045017 (2009).
16. Hall, D.K., G.A. Riggs, & V.V. Salomonson. Development of methods for mapping global snow cover using moderate resolution imaging spectroradiometer data. *Remote Sensing of Environment* 54: 127-140 (1995).
17. Klein, A.G., D.K. Hall & G.A Riggs. Improving snow cover mapping in forests through the use of a canopy reflectance model. *Hydrological Processes* 12: 1723-1744 (1998).
18. Hall D.K., R.A. Riggs & V.V. Salomonson. Algorithm theoretical basis Document (ATBD) for MODIS snow & sea ice-mapping algorithms. http://modis.gsfc.nasa.gov/data/atbd/atbd_mod10.pdf. (2001).

19. Hall, D.K., G.A. Riggs, V.V. Salomonson, E.D. Nicolo & J.B. Klaus. MODIS snow-cover products, *Remote Sensing of Environment* 83: 181-194. doi:modis-snow-ice.gsfc.nasa.gov/ap_ snowcover02.pdf (2002).
20. Hall, D.K. & G.A. Riggs. Accuracy assessment of the MODIS snow products. *Hydrological Processes* 21: 1534 – 1547 (2007).
21. Riggs, G.A., D.K. Hall & V.V. Salomonson. MODIS snow products user guide to collection 5. doi:modis-snow-ice.gsfc.nasa.gov/sug_c5.pdf (2007).
22. Ackerman, S. A., KI.Strabala, P.W.P. Menzel, R.A. Frey, C.C. Moeller, & L.E. Gumley. Discriminating clear sky from clouds with MODIS. *Journal of Geophysical Research* 103: 32141– 32157 (1998).
23. Platnick S, M.D. King, S.A. Ackerman, W.P. Menzel, B.A. Baum, J.C. Ri´edi, R.A. Frei. The MODIS cloud products: algorithms and examples from Terra. *IEEE Transactions on Geoscience and Remote Sensing* 4: 459–473 (2003).
24. Key, J. R., J.B. Collins, C. Fowler, & R.S. Stone. High-latitude surface temperature estimates from thermal satellite data. *Remote Sensing of Environment* 61: 302– 309 (1997).
25. Salomonson, V.V. & I. Apppel. Estimating fractional snowcover from MODIS using the normalized difference snow index. *Remote Sensing of Environment* 89: 351-360 (2004).
26. Martinec, J. Snowmelt runoff model for stream flow forecasts. *Nordic Hydrology* 6: 145–154 (1975).
27. Martinec, J., A. Rango & R. Roberts. Snowmelt Runoff Model (SRM) User's Manual, Updated Edition for Windows, WinSRM Version 1.11 (2007).
28. Martinec, J. The degree-day factor for snowmelt runoff forecasting. IUGG General Assembly of Helsinki, IAHS Commission of Surface Waters, IAHS Publication No. 51, 468-477 (1960).
29. US Army Corps of Engineers. *Snow Hydrology, North Pacific Division.* Corps of Engineers, US Army, Portland, Oregon (1956).
30. Wilson, W. T. An outline of the thermodynamics of snow-melt. Trans. *Am. Geophys. Union,* Part 1, 182-195 (1941).
31. Ahmad, S. & M.F. Joya. *Northern Areas Strategy for Sustainable Development – Background Paper: Water.* IUCN Pakistan, Northern Areas Progamme, Gilgit, Pakistan (2003).
32. Singh, P., S. K. Jain, and N. Kumar, Estimation of snow and glacier-melt contribution to the Chenab River, Western Himalaya. *Mountain Research and Development* 17: 49-56. doi:links.jstor.org/sici?sici=0276-4741%28199702%2917%3A1%3C49%3AEOSAGC%3E2.0.CO%3B2-9 (1997).
33. K.M. Siddiqui, S. Ahmad, A.R. Khan, A. Bari, M.M. Sheikh & A.H. Khan. *Global change impact assessment for the Himalayan mountain regions of Pakistan, country case studies of Siran and Hunza Valleys.* Report-2002, APN Project # 2002-03 (2003).

Proceedings of the Pakistan Academy of Sciences 48 (1): 33–38, 2011

ISSN: 0377 - 2969

Pakistan Academy of Sciences

Identification of a New Brown Alga, *Spatoglossum qaiserabbasii,* from the Karachi Coast of North Arabian Sea

Alia Abbas[1] and Mustafa Shameel[2*]

[1]Department of Botany, Federal Urdu University of Arts, Science and Technology, Gulshan-e-Iqbal, Karachi-75300, Pakistan
[2]Department of Botany, University of Karachi, Karachi -75270, Pakistan

Abstract: A new alga, *Spatoglossum qaiserabbasii* Abbas *et* Shameel, *sp. nov.* (Dictyotales, Phaeophycota) was collected from the coast of Karachi, Pakistan during March 2009 and investigated for its taxonomy, anatomy and reproductive structures. It is characterised by very rough surface of the thallus, small proliferations all over the surface and highly undulate margins. Anatomically there are variable shapes of the peripheral cells, *i.e.,* cubical or rectangular, triangular or polygonal. The sporangial sori are scattered on both surfaces embeded in peripheral layers, and two types of cortical cells in the basal portion of thallus which have a peculiar arrangement.

***Keywords*:** Marine algae, Karachi coast, Phaeophycota, *Spatoglossum,* morphology, anatomy

INTRODUCTION

Spatoglossum Kützing 1843: 339 is a commonly occurring genus of brown seaweeds at the coast of Pakistan. Initially, its growth was observed in 1930s at the coast of Karachi [1, 2], and gradually its five species, *i.e., S. asperum* J. Agardh 1894: 36, *S. australasicum* Kützing 1859: 20, *S. schroederi* Kützing 1859: 21, *S. shameelii* Abbas 2010: 34 and *S. variabile* Figari *et* De Notaris 1853: 158 were reported to occur at Karachi [3-8] and other coastal areas of Pakistan [9-11]. *S. chaudhrianum* P. Anand *in* Salim 1965: 196 is *nom. inval.,* because no taxonomic description and no diagram of this species are available anywhere. It was simply mentioned in a list as "*Spathoglossum chaudhriana"* [2], which is not an appropriate name [12]. During a large collection survey of Karachi Coast, some specimens were found different from all the existing species. On the basis of their characteristics these are being described here as a new species.

MATERIALS AND METHODS

The specimens were collected during March 2009 from Buleji, a coastal area near Karachi, Pakistan. Material was brought to the laboratory, washed thoroughly and preserved in 4 % formalin–seawater solution for further investigations. Some material was preserved in the form of herbarium sheets and kept in the Herbarium, Department of Botany, Federal Urdu University (FUU-SWH-14). Cross sections (C.S.) of the material were obtained by free hands with the help of shaving blades, which were then stained with iodine, mounted in glycerine and sealed with the help of nail-polish. Prepared slides were examined under Nikon PFX microscope, and photographs were taken with F 601 camera.

RESULTS

The general observation and microscopic investigation of the collected specimens indicated the following characters:

Spatoglossum qaiserabbasii Abbas et Shameel, sp. nov.

Diagnosis

Pagina scaber, apice late obtusus, margine laviter undulatus, superficebus ambabus cum parvulus prolificatio, peripheriae cellulare variabilis, pagina cum sporangium sori

Received September 2010, Accepted March 2011
*Corresponding author: Mustafa Shameel; Email: abbasalia@gmail.com

dispersus, thallus basilis cum bimorphis corticalis cellulae.

Morphological characters

Thalli erect, flat, foliaceous, greenish brown in colour, surface rough; sub-dichotomously or irregularly branched; apex broadly obtuse, margins slightly undulated; proliferations do not arise from margins, small outgrowths or proliferations present all over the surface on both sides; thalli 25 cm long, 2 – 5 mm broad at the apex, 2 – 4 cm broad at the middle and 2 – 3 cm broad at the base; from basal portion few small branches or proliferations arise; attached with the help of a small compact holdfast (Fig. 1).

Anatomical features

In surface view: peripheral cells variable in shape *i.e.* cubical or rectangular or triangular or polygonal; small, rounded oil globules arranged near the cell-wall; cells thin-walled, arranged in irregular manner; 20.0 – 55.5 µm in length and 15 – 47.5 µm in breadth; sporangial sori scattered all over the surface, dark brown, variable in shape, rounded to irregular (Fig. 2).

In the apical portion: thalli consist of 4 (-5) layers *i.e.* upper and lower peripheral layers enclosing 2 (-3) cortical layers; peripheral cells large, palisade-like, thin-walled, with dense phaeoplasts, 25 – 50 µm in length and 20 – 30 µm in breadth; 2 – 3 layered cortex composed of large, polygonal or cubical cells, intercellular spaces present, poor in contents, thin-walled, arranged irregularly, 20 – 75 µm in length and 17.5 – 32.5 µm in breadth (Fig. 3).

In the middle part: thalli 5 layered *i.e.* upper and lower peripheral layers and 3 cortical layers; peripheral cells palisade like, large, thin-walled with dense phaeoplasts, 25.0 – 47.5 µm in length and 20.0 – 37.5 µm in breadth; cortical cells vertically elongated, large and thin-walled, intercellular spaces absent, poor in contents, some cells cubical and small but other cells very large, 50.0 – 112.5 µm in length and 25.0 – 37.5 µm in breadth (Fig. 4).

In the basal portion: thalli consist of 5 – 6 (-7) layers *i.e.* upper and lower peripheral layers enclosing 4 – 5 central layers; peripheral cells large, broad and thin-walled, cubical with dense phaeoplasts, edges of cells slightly rounded, 25.0 – 62.5 µm in length and 25 – 60 µm in breadth; central portion divided into two types of cells: in the center 2 layers composed of large, polygonal or cubical, thick-walled cells, cell-wall thickness 7.5 – 10.0 µm, poor in contents, intercellular spaces absent, 25 – 75 µm in length and 25.0 – 37.5 µm in breadth; on both sides of these large cells 1 – 2 layers are present, which consist of small, vertically elongated cells, in some places only one but usually two layers, intercellular spaces present, cells thin-walled, 25 – 50 µm in length and 17.5 – 30.0 µm in breath (Fig. 5).

Margin composed of 4 – 5 cells, arranged in regular tiers, thin-walled, dark-coloured, 20 – 50 µm in length and 22.5 – 30.0 µm in breadth (Fig. 6); phaeophycotean hairs arise from hair cavities, present on the peripheral layer; hairs multicellular, dark brown, found in groups, 25 – 75 µm in length and 10.0 – 17.5 µm in breadth (Fig. 7).

Reproductive structures

Sporangia present in the form of sori, scattered on both surfaces of the thallus (Fig. 2); sporangia dark brown, cubical or rounded or squarish, embeded in peripheral layers (Fig. 8).

Type locality

Buleji, Karachi, Pakistan (FUU-SWH-14).

Habitat

Collected as drift material at Goth Haji Ali, Buleji (*Leg*. Alia Abbas 31-3-2009).

DISCUSSION

Spatoglossum is a genus of brown algae (family Dictyotaceae, order Dictyotales, class Dictyophyceae, phylum Phaeophycota; *fide* [13, 14], which is represented by four species in the Indian Ocean [12], while *S. chaudhrianum* does not exist being a misidentification. The present species resembles the five species described from the coast of Karachi *i.e. S. asperum, S. australasicum, S. schroederi, S. shameelii,* and *S. variabile* in the general appearance such as foliaceous thalli with sub-dichotomous or irregular branching. It is smaller in height than *S. asperum* and *S. variabile* but longer than other three species [3-8]. The basal part of thallus of the present species contains 5-7 layers, in this way it resembles *S. asperum* and *S. schroederi* but differs from *S. australasicum* which contains only 4 layers and the other two species contain 9-20 layers (Table 1).

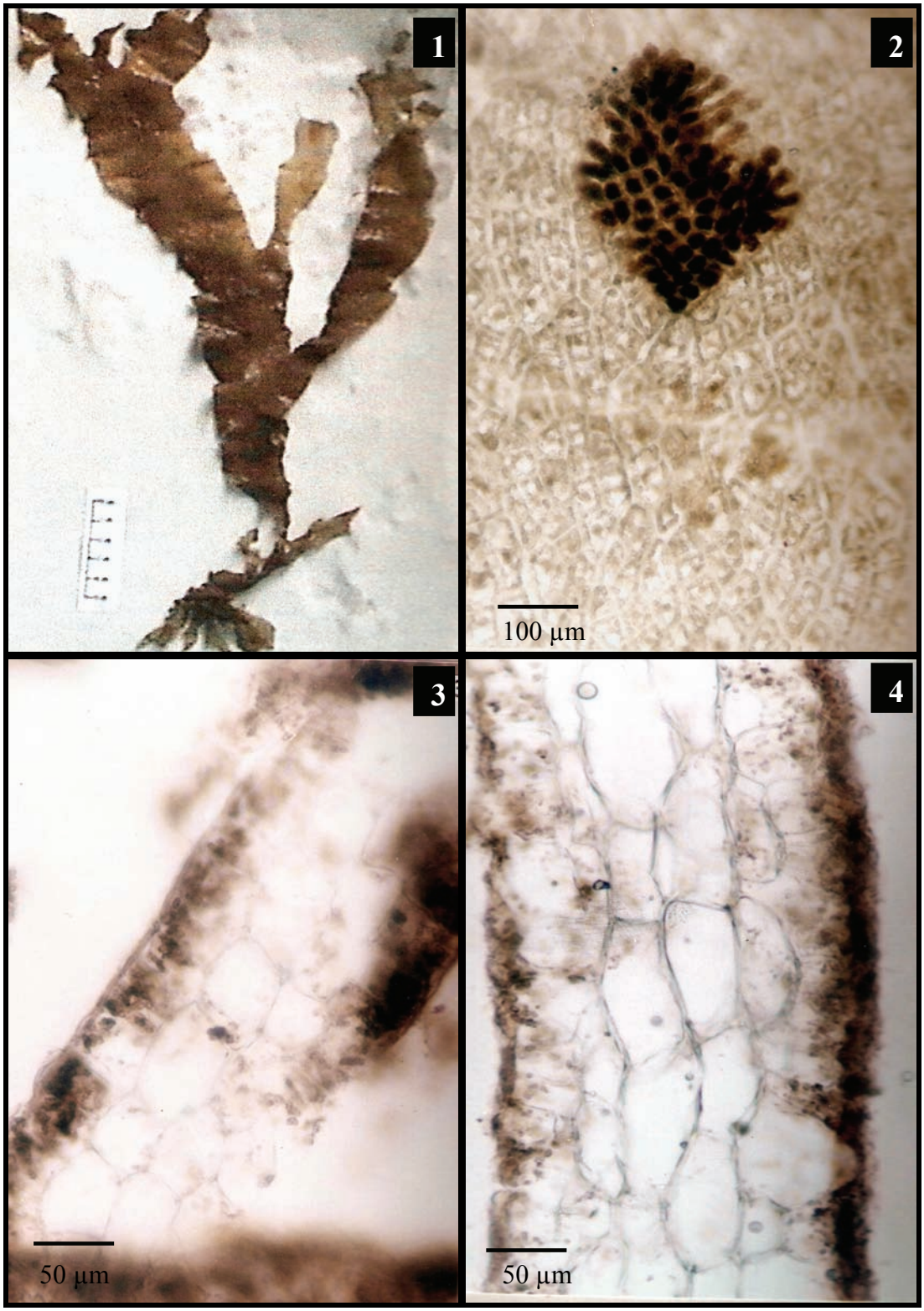

Fig. 1-4. *Spatoglossum qaiserabbasii*: **1.** Habit of the thallus, **2.** Surface view of thallus with sporangial sori, **3.** C.S. of apical portion, **4.** C.S. of middle part.

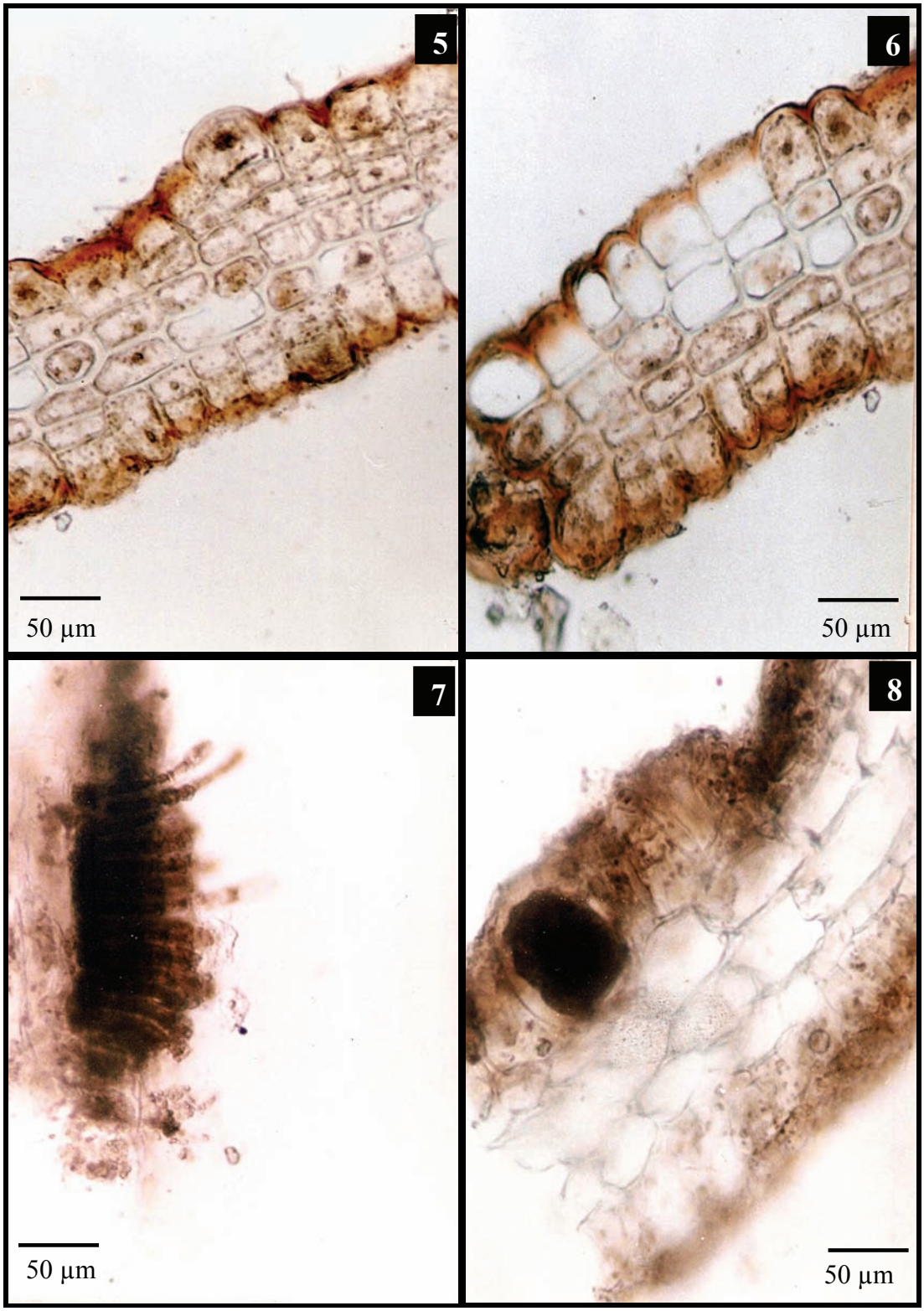

Fig. 5-8. *Spatoglossum qaiserabbasii*: **5. C.**S. of basal portion of the thallus, **6.** C.S. of basal part with margin, **7.** C.S. of thallus showing phaeophycotean hairs, **8.** C.S. of thallus with sporangium.

Table 1. Comparative account of the species of *Spatoglossum* growing at the coast of Karachi with *S. qaiserabbasii.*

Characters	*S. asperum*	*S. australasicum*	*S. schroederi*	*S. shameelii*	*S. variabile*	*S. qaiserabbasii*
Thallus colour	Olive brown	Olive green	Golden brown	Dark green	Dark brown	**Greenish brown**
Surface	Smooth	Rough	Smooth	Smooth	Rough	**Rough**
Margin	Entire	Slightly undulate	Very few dentations	Dentate	Entire-crenate	**Slightly undulate**
Tip	Palmate	Broadly obtuse	Palmate	Slightly pointed	Oblong	**Broadly obtuse**
Proliferations	From margin	From surface	Rarely proliferated	From margins	From margins	**From surface**
Height (cm)	5-40	7-20	10-14	18	10-35	**25**
Breadth (cm)						
upper	2-5	1.5-5.0	2-4	k0.2-0.8	0.2-1.5	**0.2-0.5**
middle	2-12	2.0-4.5	3-4	2.0-3.5	2-5	**2-4**
lower	1-7	0.3-1.0	1-2	0.5-1.0	1-2	**2-3**
Basal part (layers)	6	4	5-7	20	9-12	**5-7**

The present species is characterised by variable shape of peripheral cells *i.e.* cubical or rectangular or triangular or polygonal. Presence of sporangial sori on the surface, very rough surface of the thallus, small proliferations all over the surface, highly undulate margins, two types of cortical cells in the basal portion of thallus and their peculiar arrangement are those characters in which it differs from all other species of *Spatoglossum* described so far [15-26]. Therefore, it has been considered as a new species and is named after Prof. Dr. Syed Qaiser Abbas for his valuable contributions in the field of marine mycology.

ACKNOWLEDGEMENT

We are grateful to Dr. Sultanul Abedin, Senior Taxonomist, Herbarium, Department of Botany, University of Karachi for his kind help in translating the diagnosis in latin.

REFERENCES

1. Børgesen, F. Some marine algae from the northern part of the Arabian Sea with remarks on their geographical distribution. *Kong. Dansk. Vidensk. Selsk., Biol. Meddel.* 11: 1-72 (1934).
2. Salim, K. M. The distribution of marine algae along Karachi Coast. *Bot. Mar.* 8: 183-198 (1965).
3. Nizamuddin, M. & S. Perveen. Taxonomic studies on some members of Dictyotales (Phaeophyta) from the coast of Pakistan. *Pak. J. Bot.* 18:123– 135 (1986).
4. Begum, M. & N. Khatoon. Distribution of and some ecological notes of Phaeophyta from the coast of Karachi. *Pak. J. Bot.* 20: 291-304 (1988).
5. Begum, M. & N. Khatoon. Addition to the species of *Dilophus* J. Agardh and S*patoglossum* Kuetzing (Phaeophyta – Dictyotales) from the coast of Karachi, Pakistan. *Pak. J. Bot.* 25: 93 – 97 (1993).
6. Shaikh, W. & M. Shameel. Taxonomic study of brown algae commonly growing on the coast of Karachi, Pakistan. *Pak. J. Mar. Sci.* 4: 9-38 (1995).
7. Begum, A. Taxonomic study of Phaeophycota from Karachi Coast. *Kar. Univ. Seaweed Biol. & Phycochem. Thesis* 12: 1-375 (2010).
8. Abbas, A. Studies on a new brown alga, *Spatoglossum shameelii* from the coast of Karachi. *Int. J. Phycol. Phycochem.* 6: 33-40 (2010).
9. Shameel, M. & J. Tanaka. A preliminary check-list of marine algae from the coast and inshore waters of Pakistan. In: *Cryptogamic Flora of Pakistan.* Vol.1. Nakaike, T. & S. Malik. p. 1 – 64. Nat. Sci. Mus., Tokyo (1992).

10. Shameel, M. Biodiversity of the seaweeds growing along Balochistan Coast of the northern Arabian Sea. In: *Proceedings of National O.N.R. Symposium in Arabian Sea as a Resource of Biological Diversity.* Ed. Ahmad, V. U. pp. 45 – 64. H.E.J. Res. Inst. Chem., Kar. Univ., Karachi (2000).
11. Shameel, M., S.H. Khan, & S. Afaq-Husain. Biodiversity of marine benthic algae along the coast of Balochistan, Pakistan. *Pak. J. Mar. Biol.* 6: 69-100 (2000).
12. Silva, P.C., P.W. Basson, & R. L. Moe. *Catalogue of the Benthic Marine Algae of the Indian Ocean.* Univ. Calif. Press, Berkeley (1996).
13. Shameel, M. An approach to the classification of algae in the new millennium. *Pak. J. Mar. Biol.* 7: 233-250 (2001).
14. Shameel, M. Change of divisional nomenclature in the Shameelian Classification of algae. *Int. J. Phycol. Phycochem.* 4: 225 – 232 (2008).
15. Taylor, W. R. *Marine Algae of the Northeastern Coast of North America.* Rev. Ed., Univ. Michigan Press, Ann Arbor (1957).
16. Taylor, W. R. *Marine Algae of the Eastern Tropical and Sub Tropical Coasts of the Americas.* Univ. Michigan Press, Ann Arbor (1960).
17. Duraitranam, M. Contribution to the study of the marine algae of Ceylon. *Fisher. Res. Stat. Ceylon Bull.* 10: 1-181 (1961).
18. Joly, A. B. Flora marinha do litoral morte de Estado de São Paulo e regiões circumvizinhas. *Bolet Facul Filos Ciên Let, Univ. São Paulo, Botânica* 21: 5- 393 (1965).
19. Misra, J. N. *Phaeophyceae in India*. Indian Council for Agricultural Research, New Delhi (1966).
20. Misra, J. N. 1967. The Phaeophyceae of the west coast of India. In: *Proceedings of the Seminar on Sea, Salt and Plants.* Ed. Krishnamurthy, V. p. 227 – 233. Bhavnagar, India (1966).
21. Earle, S. A. Phaeophyta of eastern Gulf of Mexico. *Phycologia* 7: 71-254 (1969).
22. Abbott, I. A. & , G. J. Hollenberg. *Marine Algae of California.* Stanf. Univ. Press, Stanford (1976).
23. Jaasund, E. *Intertidal Seaweeds in Tanzania.* Tromsø. Univ., Norway (1976).
24. Nizamuddin, M. Contribution to the marine algae of Libya: Dictyotales. *Biblith. Phycol.* 54: 1-122 (1981).
25. Womersley, H. B. S. *The Marine Benthic Flora of Southern Australia.* Part II. South Australian Government Printing Division, Adelaide (1987).
26. Wysor, B. and De Clerck, O. An updated and annovated list of marine brown algae (Phaeophyceae) of the Carribbean Coast of Republic of Panama. *Bot. Mar.* 46: 151-160 (2003).

Proceedings of the Pakistan Academy of Sciences 48 (1): 39–43, 2011

ISSN: 0377 - 2969

Pakistan Academy of Sciences

Distribution of ABO and Rh Blood Group Alleles in Sahiwal district of the Punjab, Pakistan

Mohammad Anees[1*] and Aksa Jawad[2]

[1] Deparment of Biological Sciences, The University of Gujrat, Gujrat, Pakistan
[2] Department of Zoology, University of the Punjab, Lahore, Pakistan

Abstract: A study was carried out to determine blood groups of a random population sample from urban and rural areas of Sahiwal district, Punjab province, Pakistan. Blood samples were collected from the patients visiting to the DHQ Hospital Sahiwal. A total of 20,010 subjects, comprising 3,901 (19.5%) female and 16,109 (80.5%) males, were screened for blood grouping. The objective of this study was to determine the frequency of different blood groups in this District, which would helpful in blood transfusion, organ transplantation, erythroblastosis fetalis, glaucoma and certain other diseases. The distribution of phenotypic frequencies for ABO group in the total sample were 22.0%, 36.9%, 9.9% and 31.3% for groups A, B, AB and O, respectively, while 87.1% of the subjects were Rh-positive. The calculated allelic frequencies were 0.182, 0.276 and 0.541, for group A, B and O, respectively, and 0.357 for d allele. From these studies it is concluded that phenotypically B group was dominant in both genders of the Sahiwal District with high allelic frequency of O group. These studies revealed that the gene frequencies in Sahiwal district are: O>B>A>AB.

Keywords: Alleles, gene frequency, blood groups, Rh factor, transfusion, Sahiwal district, Pakistan

INTRODUCTION

Since 1901, more than 20 distinct blood group systems have been characterized but the ABO and Rh blood groups remain the most important clinically [1]. The distribution of these 2 blood groups has been repeatedly investigated in various populations all over the world during the last half-century. The frequencies exhibit considerable variation in different geographic locations, reflecting the underlying genetic and ethnic diversity of human populations [2]. The relatively new science of DNA research applied to full-blooded, indigenous populations from around the world has led to the discovery and documentation of genetic markers that are unique to populations, forensic pathology, ethnicity and deep ancestral migration patterns [3]. The markers having very specific modes of inheritance, which are relatively unique to specific populations, are used, among other things, to assess ancestral and kinship probabilities [2, 4].

The blood groups may have some association with diseases like duodenal ulcer, diabetes mellitus, urinary tract infection, Rh and ABO incompatibility of newborn and all types of glaucomas [5-8]. All human populations share the same blood group systems; although they differ in the frequencies of specific types. The incidence of ABO and Rh groups varies very markedly in different part of the world and in different races. Even in Pakistan, there are some variations in different areas reflecting racial differences, evolution, their relation to disease and environment is being increasingly sought in modern medicine [9-10]. It is therefore, worth while to document the frequency of ABO and Rh blood groups in the different regions of Pakistan [11].

The gene symbols i or IO, IA and IB, are often used to denote these alleles. Two alleles, R and r are responsible for the inheritance of rhesus blood groups, with R denoting Rh+ve, and r being Rh–ve blood group allele. Gene frequency takes into consideration the numbers of various genotypes in the population, and the relative allele frequencies are determined by application of the Hardy-Weinberg Law [12].

The present study was carried out to record genotypic frequency of various alleles in blood

Received December 2010, Accepted March 2011
*Corresponding author: Mohammad Anees**;** E-mail**:** anees.50@hotmail.com

groups in a population of Sahiwal district of Punjab, Pakistan, and to compare our results with other studies conducted in Pakistan and elsewhere in the world [13-16] and its future utility for the health sector planners.

MATERIALS AND METHODS

Subjects

A total of 20,010 subjects, belonged to both rural and urban areas of Sahiwal District of Punjab, Pakistan. Blood grouping was carried out over a period of 12 months from January 2009 to December 2009. These were categorized according to ABO/Rh system and allele frequency was computed according to Hardy-Weinberg law [12].

Collection of blood samples

A 2.0 ml sample of blood was drawn from the antecubital vein of each subject in a disposable syringe, and transferred immediately to a tube containing ethylene diamine tetra acetic acid (EDTA).

Determination of blood groups

Blood grouping (ABO and Rh) was done by the antigen-antibody agglutination test. The antisera used were obtained from Plasmatic (Kent, UK). Plasmatic ABO monoclonal reagents are *in vitro* culture supernatants of hybridized immunoglobulin secreting mouse cell-line. For determination of Rh factor, plasmatic anti D (1.0 g) Lo-Du and LO-Du2 monoclonal reagents, prepared from different antibody producing human B-lymphocyte cell lines, were used.

RESULTS

Phenotypic and allelic frequencies of ABO blood groups in the studied population, with gender distribution, are given in Table 1. The distribution of phenotypes in the total sample was 22.0%. 36.9%, 9.9% 29.3% and 31.3% for groups A, B, AB and O, respectively, and the distribution of the alleles were 0.182, 0.276 and 0.541, for A, B and O, respectively, revealing that in district Sahiwal the phenotypically B group was dominant with high allelic frequency of O group. The distribution of phenotypes and allelic frequencies of various Rh blood group antigens in the studied populatio is presented in Table 2. Distribution of phenotypes in the total population sample was 87.1% Rh-positive and 12.9% Rh-negative and distribution of alleles for Rh-positive antigen was 0.643 and 0.357 Rh-negative antigen.

The distribution of allele frequencies of blood group ABO antigens in the sampled population of Sahiwal district with earlier studies on different populations, suggesting the dominance of O group is given in Table 3. Table 4 compares the distribution of allele frequencies of Rh factor antigens in the Sahiwal district population with earlier studies on different populations, suggesting the dominance of Rh positive group.

Table 1. Distribution of phenotypic and allelic frequencies of various ABO blood group system in the studied population of district Sahiwal.

Sex	Phenotypes					Allelic frequency		
	A	B	AB	O	Total	p	q	r
Male	3515 (21.8 %)	5835 (36.2%)	1480 (9.2%)	5279 (32.8%)	16109	0.169± 0.006	0.261± 0.007	0.572± 0.008
Female	888 (22.8%)	1539 (36.6%)	489 (12.5%)	985 (27.8%)	3901	0.196± 0.005	0.298± 0.006	0.510± 0.007
Total	4403 (22.0%)	7374 (36.9%)	1969 (9.9%)	5864 (31.3%)	20010	0.182± 0.005	0.276± 0.004	0.541± 0.005

Table 2. Distribution of phenotypic and allelic frequencies of various Rh blood group in the studied population at district Sahiwal.

Sex	Phenotypes			Allelic frequency	
	Rh+	Rh	Total	D	d
Male	14520 (90.1 %)	1589 (9.9%)	16109	0.686± 0.010	0.314± 0.010
Female	3277 (84.0%)	624 (16.0%)	3901	0.600± 0.012	0.400± 0.012
Total	17797 (87.1%)	2213 (12.9%)	20010	0.643± 0.011	0.357± 0.011

Table 3. Compares the distribution of allele frequencies of ABO blood group antigens in the Sahiwal district population with earlier studies elsewhere.

	Frequency of blood groups (%)				
Population	**A**	**B**	**AB**	**O**	**Reference**
Kuwait	0.2900	0.2300	0.1400	0.3500	[17]
Britain	0.4170	0.0860	0.0300	0.4670	[18]
Kenya	0.2620	0.2200	0.0440	0.4748	[19]
Nigeria	0.2443	0.2388	0.0275	0.4894	[20]
Hungary	0.2766	0.1218	0.0423	0.5553	[21]
Ukraine	0.2360	0.2250	0.0704	0.5760	[22]
Aborigines	0.3900	0.0000	0.000	0.6100	[03]
Turky	0.1220	0.1213	0.0085	0.7398	[23]
American Indian	0.0390	0.0110	0.000	0.9500	[24]
Bororo	0.0000	0.0000	0.000	0.1000	[3]
Rawalpindi (Pakistan)	0.2701	0.3350	0.0893	0.3031	[25]
Peshawar (Pakistan)	0.2800	0.3400	0.0700	0.3100	[26]
Swabi (Pakistan)	0.2760	0.3040	0.0880	0.3220	[27]
India	0.2470	0.3750	0.0530	0.3250	[18]
Hazara (Pakistan)	0.2400	0.3200	0.1100	0.3300	[28]
Bahawalpur(Pakistan)	0.2100	0.3600	0.0600	0.3700	[29]
Wah Cant (Pakistan)	0.1813	0.2450	0.0517	0.5400	[30]
Mandi Bauddin (Pakistan)	0.1583	0.2832	0.0448	0.5522	[14]
Gujrat (Pakistan)	0.1740	0.2229	0.0435	0.5596	[13]
Sahiwal (Pakistan)	**0.1744**	**0.2837**	**0.0494**	**0.5419**	Present study

Table 4. Frequency of Rh antigens in different populations.

	Allele Frequency		
Population	**Rh+**	**Rh-**	**Reference**
China	1.0000	0.0000	[31]
Germany	0.9500	0.0500	[32]
Nigeria	0.9430	0.0570	[20]
Mandi Bauddin (Pakistan)	0.9140	0.0860	[14]
Azad Jammu and Kashmir	0.8480	0.1520	[33]
Kenya	0.8030	0.1970	[19]
Gujrat (Pakistan)	0.7958	0.2042	[8]
Peshawar (Pakistan)	0.7680	0.2320	[34]
Wah Cantt (Pakistan)	0.7390	0.2710	[30]
Islamabad (Pakistan)	0.7290	0.2710	[25]
Mirpur (Pakistan)	0.7010	0.2990	[35]
Bannu (Pakistan)	0.6720	0.3280	[36]
Sahiwal (Pakistan)	**0.643**	**0.357**	Present study

DISCUSSION

By comparing the data shown in Table 3 with the present study under discussion (O=0.541, A=0.182 and B=0.276), it has been observed that the population of Sahiwal region is very close to Hungry, Ukraine, Wah Cant., Gujrat and Mandi Bahauddin population, and is different from the population of Kuwait, Germany, Turkey, American India, Bannu, Rawalpindi, Peshawar, Swabi, India, Hazara, Bahawalpur and other Districts. This data is similar to the previous finding that there is an equal dominance of group O and B in the Indo-Pak subcontinent, in contrast to dominance of only O group in the British and African populations [18-20]. It also has been previously described that the type O group is the oldest blood and shows a connection to high animal protein consumption; individuals generally produced higher stomach acids and experience more incidence of gastric ulcer diseases than the other groups [13]. Inspite of these problems with O group population several significant implications are also observed.

Firstly, it provides information to blood banks regarding the higher need for blood group O for transfusion purpose particularly for obstetrics, surgical purposes and during disasters. Secondly, studies concerning possible association between ABO blood group and cardiovascular diseases have confirmed that persons of group A are affected more with coronary heart disease, ischemic heart disease, venous thrombosis and atherosclerosis, while its low in people with blood group O which stated to have protective effect against some diseases [8, 9, 36].

These studies suggest that the people of the District Sahiwal are seemed to be more close to the Hungry and Ukraine peoples and the heterogeneity in the Sahiwal district population is may be due to the different genetic and environmental factors, which helps the expression of blood groups alleles A and B among the Pakistani populations. However, this requires further investigation on Pakistani population.

In terms of presence of Rh antigens, the data from several studies on China, Germany, African and Pakistani populations are compared in Table 4, along with the allele frequency of R and r. The findings of the present study (R= 0.643, r= 0.357) are inconsistent with the results obtained in an earlier study carried out in the population of Mirpur, Bannu, Lahore and Islamabad, where the allele frequency of Rh-positive (R) has been found very close to the to the population of Sahiwal. However, the allele frequency of Rh positive was less than the population of Azad Jummu and Kashmir, Gujrat, Mandi Bauddin, China, Germany and Nigeria (Table 4). Indicating, the progressively reduction of Rh-positive and the dominance of Rh nagitive group in Sahiwal region of the Punjab, Province of the Pakistan.

Studies of associations between various diseases and the ABO blood groups have shown elevated relative risks for some categories of disease. The study provides in depth information of the relative distribution of various alleles in the population and promises help in planning for future health challenges, especially for blood transfusion services, cardiovascular diseases and different organ transplantation studies [8,9,37] in the Sahiwal district.

ACKNOWLEDGEMENTS

I express my gratitude to the Medical Superintendent, DHQ Hospital, Sahiwal for facilitating collection of blood group data. I am also grateful to Professor Gohire, Department of Statistics, The University of Gujrat for his help in compiling results of this study.

REFERENCES

1. Amin-ud-Din M, N. Fazeli, M. Rafiq & S. Malik. Serological study among the municipal employees of Tehran, Iran. Distribution of ABO and Rh blood groups. *Haematology* 7: 502–4 (2004).
2. Sigmon, J.M. Basic principles of the ABO and Rh blood group systems for hemapheresis practitioners. *Journal of Clinical Apheresis* 7(3): 158–62 (1992).
3. Cavalli-Sforza, L.L., P. Menozzi & A. Piazza. *The History and Geography of Human Genes*. Princeton, New Jersey (1994).
4. David. J. A. The relationship between blood groups and disease. *Blood* 115: 4635-4643 (2010).
5. Akhtar, M.N., A. Tayyib, T. Tasneem & A.R. Butt. ABO blood group in patients with peptic ulcer disease: Association with secretor status. *Annuals of King Edward Medical University* 9: 238-40 (2003).
6. Qureshi, M.A & R. Bhatti, Frequency of ABO blood groups among the diabetes mellitus type 2 patients. *Journal of College of Physician and Surgeons Pakistan* 13: 453-5 (2003).
7. Ziegler, T., N. Jacobsohn & R. Funfstuck, Correlation Between blood group phenotype and virulence properties of Escherichia coli in patients with chronic urinary tract infection. *International Journal of Antimicrobial Agents* 24: 70-5. 5 (2004).
8. Khan, M.I., S. Micheal, F. Akhtar, A. Naveed A. Ahmed & R. Qamar. Association of ABO blood groups with glaucoma in the Pakistani population. *Canadian Journal of Ophthalmology* 44: 582-586 (2009).
9. Alam M. ABO and Rhesus blood groups in potential blood donors at Skardu (Northern Areas). *Pakistan Journal of Pathology* 16: 94–97 (2005).
10. Khan, M.S., F. Subhan, F. Tahir, B.M. Kazi, A.S. Dil & S. Sultan. Prevalence of blood groups and Rh factor in Bannu region NWFP (Pakistan). Pak. J. Med. Res. 43: 8–10 (2004).
11. Khaliq, M.A., J.A. Khan, H. Shah, & S.P. Khan. Frequency of ABO and Rh (D) blood group in Hazara division (Abbottabad). Pak. J. Med. Res. 23: 102–103 (1984).

12. Mollison, P.L., C.P. Engelfriet & M. Conteras. Immunology of red cells. In: *Blood Transfusion in Clinical Medicine*, 9th ed. Blackwell Scientific Publication p. 87–88 (1993).
13. Anees, M & M. Shabir. Distribution of ABO and Rh blood groups in Gujrat region, Punjab, Pakistan. *Proc. Pakistan Acad. Sci.* 42: 233-238 (2005).
14. Anees, M., J. Aksa, & H. Iftikhar, Distribution of ABO and Rh blood groups in Mandi Bauddin region, Punjab, Pakistan. *Proc. Pakistan Acad. Sci.* 44: 289-294 (2007).
15. Khan, M.N., M.N. Khan, I. Khaliq, A. Bakhsh, M.S. Akhtar, & M. Amin-ud-Din. Distribution of ABO and Rh D blood groups in the population of Poonch district, Azad Jammu and Kashmir. *Eastern Mediterranean Health Journal* 15: 717-21 (2009).
16. Gaertner, H., J. Lyko & S. Lyko. The antigens ABO and Rh (D) in Nigeria population. *Hamdard Medicus* 37: 81-91 (1994).
17. Al-Bustan, S., S. Al-Bustan, M. El-Zawahri, D. Al-Azmi & A.A. Al-Bashir. Allele frequencies and molecular genotyping of the ABO blood group system in a Kuwaiti population. *International Journal Hematology* 75: 147-153 (2002).·
18. Talib, V.H. *Hand book of Medical Laboratory Technology,* 2nd ed. CBS Publishers, New Delhi, India. p. 205-210 (1991).
19. Lyko, J., H. Gaertner, J.N. Kaviti, M.W. Karithi & B. Akoto. The blood groups antigens ABO and Rh in Kenyans. *Hamdard Medicus* 35: 59-67 (1992).
20. Odokuma, E.I, A.C. Okolo & P.C. Aloamaka. Distribution of ABO and rhesus blood groups in Abraka, Delta State, Nigeria. *Nigerian Journal Physiological Sciences* 89-91 (2007).
21. Tuaszik, T. Heterogeneity in the distribution of ABO blood groups in Hungary. *Gene Geoger.* 9:169-176 (1995).
22. Mukhin, V.N. Gene frequencies and heterozygosity of the population of Donetsk Province, Ukraine by the alleles of the ABO and Rhesus systems. *Tsitol Genet.* 33: 10-30 (1999).
23. Akbas, F., M. Aydin. & A. Cenani. AB0 blood subgroup allele frequencies in the Turkish population. *Anthropologischer Anzeiger* 61(3):257-60 (2003.)
24. Mourant, A.E., A.C Kipec & K. Domenjewska. *The Distribution of Human Blood Groups*. Oxford Press, London. p. 10-19 (1976).
25. Khan, M. M., N. Farooq, N. Qamar, F. Tahir, F. Subhan, B.M. Kazi, M. Fiyaz & K.A. Karamat. Trend of blood groups and Rh factor in the twin cities of Rawalpindi and Islamabad. *Journal of Pakistan Medical Association* 56: 299-302 (2006).
26. PMRC. Some normal parameters of Pakistani in the Peshawar area 1976-1982. *Pakistan Medical Research Council*, KMC p. 21 (1982).
27. Khurshid, B., M. Naz, M. Hassan & S.F. Mabood. Frequency of ABO and Rh (D) blood groups in district Swabi N.W.F.P (Pakistan). *Journal of Science and Technology, University of Peshawar* 16:5-6 (1992).
28. Khaliq, M.A., J.A Khan, H. Shah, & S.P. Khan. Frequency of ABO and Rh (D) blood groups in Hazara Division (Abbottabad). *Pakistan Journal Medical Research* 23: 102-103 (1984).
29. Yousaf, M., N. Yousaf, & A. Zahid. Pattern of ABO and Rh (D) Blood groups distribution in Bahawalpur Division. *Pakistan Journal Medical Research* 27: 40-41 (1988).
30. Khan, I.M., G.A. Khan, & A. Akbar. *Gene frequency of ABO and Rh blood group system in Wah Cantonment.* Botany Department, Peshawar University, Pakistan (1982).
31. Min, S., Z.L. Hu, P.T. Dong, Y. L. Xiao, R..L. De & C.Z. Zhi. Relationship between ABO blood groups and carcinoma of esophagus and cardia in Chaoshan inhabitants of China. *World Journal Gastroenterology* 7: 657-661 (2001).
32. Wagner, F.F., D. Kasulke, M. Kerowgan, & W.A. Flegel. Frequencies of the bloods group ABO, Rhesus D category VI. Kell and of clinically relevant high frequency antigens in Southwestern Germany. *Infusions her Transfusions medicine* 22: 285-290 (1995).
33. Rashid, M. *Gene frequency of ABO blood groups in Azad Kashmir*. M.Sc. Thesis, Department of Botany, University of Peshawar, Peshawar, Pakistan (1983).
34. Parveen, N. *Incidence of ABO and Rh system in Lahore area*. M.Phil. Thesis, University of Peshawar, Peshawar, Pakistan (1983).
35. Khalid, M & M.A. Qureshi. Frequencies of the blood group antigens and corresponding alleles in the population of Mirpur, Azad Jummn Kashmir. *Journal of Animal and Plant Sciences.* 16: 96-97 (2006).
36. Khan, M.S., F. Subhan, F. Tahir, B.M. Kazi, A.S. Dil, S. Sultan, F. Deepa, F. Khan & M.A. Sheikh. Prevalence of blood groups and Rh factor in Bannu District (NWFP) Pakistan. *Pakistan Journal Medical Research* 43:8-10 (2004).
37. Kazunari, T., I. Hideki, O. Kazuya, S. Tomokazu & S. Hiroki. Antibody-mediated rejection: a single center experience at Tokyo Women's Medical University. *Clinical Transplant* 363-369 (2006).

Proceedings of the Pakistan Academy of Sciences 48 (1): 45–49, 2011
Pakistan Academy of Sciences

ISSN: 0377 - 2969

A Note on Laskerian Rings

Tariq Shah and Muhammad Saeed*

Department of Mathematics, Quaid-i-Azam University, Islamabad, Pakistan

Abstract: Let D be an integral domain with quotient field K and $\overline{D}$ is its integral closure. (1) If $\overline{D}$ is a one dimensional Laskerian ring such that each primary ideal of $\overline{D}$ is a valuation ideal, then each overring of D is Archimedean. (2) If D is not a field, then D is a Dedekind domain if and only if D is a Laskerian almost Dedekind domain. (3) $\overline{D}$ is one dimensional Laskerian and each primary ideal of $\overline{D}$ is a valuation ideal if and only if $\overline{D}$ is one dimensional Prufer and $\overline{D}$ has finite character. In this case D is Laskerian. (4) $\overline{D}$ is one dimensional Prufer (respectively almost Dedekind) if and only if every valuation ring of K lying over D is Laskerian (respectively strongly Laskerian). (5) The complete integral closure of a pseudo-valuation domain (D, M) is Laskerian of dimension at most one.

Keywords: Laskerian ring, overrings, complete integral closure, pseudo-valuation domain

1. INTRODUCTION

In 1905, Emanuel Lasker introduced the notion of primary ideal, which corresponds to an irreducible variety and plays a role similar to prime powers in the prime decomposition of an integer. He proved the primary decomposition theorem for an ideal of a polynomial ring in terms of primary ideals [1]. Emmy Noether, in her seminal paper [2], proved that in a commutative ring satisfying the ascending chain conditions on ideals, every ideal is the intersection of finite number of irreducible ideals (an irreducible ideal of a Noetherian ring is a primary ideal). She established several intersection decompositions. Among rings without the necessary ascending chain conditions, the rings in which such decomposition holds for all ideals are called Laskerian rings.

Throughout this note all rings are commutative with identity. The letter D denotes an integral domain with quotient field K. By an overring of D we mean a ring between D and K. We use $\overline{D}$ to denote integral closure of D in K, $\dim D$ to represent Krull dimension of D. By [3, Page 360], D is said to have valuative dimension n, represented as $\dim_v D = n$, if each valuation overring of D has dimension at most n and if there exists a valuation overring of D of dimension n. A commutative ring R with identity is Laskerian if each ideal of R admits a shortest primary representation; R is strongly Laskerian, if R is Laskerian and each primary ideal of R contains a power of its radical [3, Page 455]. It is equivalent to say that a commutative ring R with identity is Laskerian (respectively strongly Laskerian) if every ideal of R can be represented as a finite intersection of primary ideals (respectively strongly primary ideals), whereas an ideal Q of R is primary if each zero divisor of the ring R/Q is nilpotent and Q is strongly primary if Q is primary and satisfies $\left(\sqrt{Q}\right)^n \subset Q$ for some n. Following [4, Page 505], R is a zero divisor ring ($Z.D$ ring), if $Z_R(R/I)$, the set of zero divisors of R/I, is a finite union of prime ideals for all ideals I of R.

In general, *Artinian* $\Rightarrow$ *Noetherian* $\Rightarrow$ *Strongly Laskerian* $\Rightarrow$ *Laskerian* $\Rightarrow$ *Z.D ring,* But none of the above implication is reversible.

An integral domain D is said to be a Prufer domain if D_P is a valuation ring for every prime

Received July 2010, Accepted March 2011
* Corresponding author: Muhammad Saeed; Email: saeedharris@hotmail.com

ideal P of D. By [3, Page 434], a domain D is an almost Dedekind domain if D_M is a Noetherian valuation ring for each maximal ideal M of D and its dimension is at most one. If D is a Prufer domain, then D is Laskerian if and only if dim $D \leq 1$ and each nonzero element of D belongs to only a finitely many maximal ideals of D [3, Page 456].

In this note we discuss the overrings, integral closure and complete integral closure of an integral domain in Laskerian perspective. First we transformed ($\Rightarrow$) of : Integral closure $\overline{D}$ of an integral domain D is a Dedekind domain $\Leftrightarrow$ every overring of D satisfies $ACCP$ (or atomic) [5, Theorem 1], as: If integral closure $\overline{D}$ of an integral domain D is a one dimensional Laskerian ring such that each primary ideal of $\overline{D}$ is a valuation ideal, then each overring of D is Archimedean. In the second proposition we prove the necessary and sufficient condition for an almost Dedekind domain to be a Dedekind domain through the Laskerian property. We also show that $\overline{D}$ is a one dimensional Laskerian and each primary ideal of $\overline{D}$ is a valuation ideal if and only if $\overline{D}$ is a one dimensional Prufer and $\overline{D}$ has finite character. In this case D is Laskerian. With the inspiration; a valuation ring V is a Laskerian ring (respectively a strongly Laskerian ring) if and only if V has rank at most one (respectively V is discrete of rank at most one) (see [3,Page 456]), we establish that every valuation ring of K lying over D is Laskerian (respectively strongly Laskerian) if and only if $\overline{D}$ is a one dimensional Prufer domain (respectively an almost Dedekind domain). Further we observed that the complete integral closure D_0 of a pseudo-valuation domain (PVD) (D, M) (i.e. in D every prime ideal is strongly prime) is Laskerian of dimension ≤ 1 and its maximal ideal is contained in M .

2. MAIN RESULTS

Following [6], an integral domain D is Archimedean in case $\cap_{n\geq 1} Dr^n = 0$ for each nonunit $r \in D$. The most natural examples of Archimedean domains are completely integrally closed domains, one dimensional integral domains and Noetherian integral domains. An ideal A of a domain D is a valuation ideal if there exist a valuation ring $D_v \supset D$ and an ideal A_v of D_v such that $A_v \cap D = A$.

Lemma 2.1

Let D be an integral domain. If D is Laskerian, such that every primary ideal is a valuation ideal, then D is Prufer.

Proof: Since D is Laskerian, it is clear that each ideal of D has finitely many minimal prime divisors. Since a ring with later property has Noetherian spectrum if and only if ascending chain condition for prime ideals is satisfied in D, therefore by [7, Theorem 3.8] D is a Prufer domain.

Proposition 2.2

Let D be an integral domain such that its integral closure $\overline{D}$ is a one dimensional Laskerian ring and each primary ideal of $\overline{D}$ is a valuation ideal, then each overring of D is Archimedean.

Proof: If integral closure $\overline{D}$ of an integral domain D is a one dimensional Laskerian ring, such that each primary ideal of $\overline{D}$ is a valuation ideal, then by [3, Theorems 36.2 and 30.8] , $\dim_v D = \dim_v \overline{D} = \dim \overline{D} = \dim D \leq 1$. So by [8, Corollary 1.4], each overring of D is Archimedean.

Remark 2.3

Each overring of an integral domain D is Noetherian if and only if D is Noetherian and $\dim D \leq 1$ [3, Page 493, Exercise 16]. This cannot be generalized in Laskerian domains. Because, if D is a non Noetherian Laskerian integral domain such as a one dimensional valuation ring (the case when Archimedean and Laskerian behave alike), then overrings of D do not satisfy ACCP [9, Theorem 2.1].

It is easy to demonstrate that a Dedekind domain is a Laskerian domain. We prove in the next proposition that an almost Dedekind domain which is not Dedekind is not a Laskerian domain. This then demonstrates a clear difference between Dedekind domains and non Noetherian almost Dedekind domains. Here the concept of Laskerian domain is expanded to provide a way of measuring how close an almost

Dedekind domain which is not Dedekind is to being Dedekind.

Proposition 2.4

In an integral domain D with identity which is not a field, the following conditions are equivalent:

(1) D is a Dedekind domain.

(2) D is a Laskerian almost Dedekind domain.

Proof: (1) $\Rightarrow$ (2): D is Dedekind $\Rightarrow D$ is Noetherian. If M is maximal ideal of D, then D_M is a nontrivial Noetherian valuation ring. Therefore by [3, Theorem 17.5], D_M is rank one discrete and D is almost Dedekind.

(2) $\Rightarrow$ (1): If D is an almost Dedekind then $\dim(D)=1$. In a Prufer domain, the Laskerian property in D is equivalent to the condition that each nonzero element of D belongs to only finitely many maximal ideals of D [3, Page 456, Exercise 9]. Hence by [3, Theorem 37.2] D is a Dedekind domain.

Mori and Nagata have proved that if D is Noetherian and one or two dimensional, then $\overline{D}$ is Noetherian [10]. Hence if D is Noetherian and one dimensional, then $\overline{D}$ is a Dedekind domain. On the other hand if the integral closure $\overline{D}$ of D is Dedekind, it is not necessary that D is Noetherian. For example if $R = \mathrm{Q} + X\overline{\mathrm{Q}}[X] = \left\{a_0 + \sum a_i X^i \mid a_0 \in \mathrm{Q},\ a_i \in \overline{\mathrm{Q}}\right\}$, where Q is the field of rational and $\overline{\mathrm{Q}}$ is algebraic closure of Q, then $\overline{R} = \overline{\mathrm{Q}}[X]$ is a PID but R is not Noetherian. In [11, Lemma 2] it is proved that if integral closure $\overline{D}$ of an integral domain D is a Dedekind domain then D is Laskerian. In the next proposition we observe that D remains Laskerian if integral closure of D is one dimensional Prufer with finite character.

Proposition 2.5

Let $\overline{D}$ be integral closure of an integral domain D. $\overline{D}$ is one dimensional Laskerian and each primary ideal of $\overline{D}$ is a valuation ideal $\Leftrightarrow$ $\overline{D}$ is one dimensional Prufer and $\overline{D}$ has finite character. When this is the case, D is Laskerian.

Proof: By Lemma 2.1 $\overline{D}$ is Prufer. Since $\overline{D}$ is Laskerian (by [12, Theorem 4]) it has Noetherian spectrum which means that every non zero element of $\overline{D}$ belongs to finite number of maximal ideals of $\overline{D}$, that is, $\overline{D}$ has finite character.

($\Leftarrow$) Since $\overline{D}$ is one dimensional Prufer and has finite character, therefore, by [3, Page 456, Exercise 9], $\overline{D}$ is Laskerian and every primary ideal of $\overline{D}$ is a valuation ideal [7]. Next we show that D is Laskerian. By Proposition 2.2, $\dim(D) \le 1$. Proper prime ideals are maximal in D, then every ideal of D is equal to its kernel [13, Page 738]. Since every proper ideal in D has a finite number of prime divisors, every ideal in D is an intersection of a finite number of pair wise co-maximal primary ideals in D.

Lemma 2.7

Let V be a non trivial valuation ring on the field K. Then V is completely integrally closed $\Leftrightarrow$ V is one dimensional $\Leftrightarrow$ V is Laskerian $\Leftrightarrow$ V is Archimedean.

Proof: A valuation ring V is completely integrally closed if and only if V is one dimensional (cf. [3, Theorem 17.5]). By [3, Page 456], a valuation ring V is Laskerian if and only if V has rank at most one. Since all valuation rings are GCD domains, by (cf. [14, Theorem 3.1]), V is Archimedean if and only if V is completely integrally closed.

Remark 2.8

A rank 2 valuation ring is not Laskerian (according to [3, Page 456]). However any valuation ring is a $Z.D$ ring [4, Page 507].

Theorem 2.9

Let D be an integral domain with quotient field K. Then the integral closure $\overline{D}$ of D is a one dimensional Prufer domain $\Leftrightarrow$ every valuation ring of K lying over D is Laskerian.

Proof: Let $\overline{D}$ be a one dimensional Prufer domain and let D_v be a valuation overring of D. So $\overline{D} \subset D_v \subset K$. Let P_v be the centre of D_v in $\overline{D}$. Since $\overline{D}$ is a one dimensional Prufer domain, therefore $\overline{D}_{P_v}$ is a rank one valuation

ring (and hence a maximal ring in K) and hence $\overline{D}_{P_v} = D_v$. Since every valuation ring lying over D is of rank one, it is Laskerian.

Conversely, suppose that every valuation ring V of K lying over D is Laskerian, therefore by Lemma 2.7, V is one dimensional. Hence by [11, Theorem 1] $\overline{D}$ is a Prufer domain.

Theorem 2.10

Every valuation ring of K lying over an integral domain D is strongly Laskerian $\Leftrightarrow$ $\overline{D}$ is an almost Dedekind domain.

Proof: Suppose every valuation ring V of K lying over D is strongly Laskerian, therefore V is discrete rank one (see [3, Page 456]). By [3, Theorem 36.2], $\overline{D}$ is an almost Dedekind domain.

Conversely, suppose $\overline{D}$ is an almost Dedekind domain (hence one dimensional) and let D_v be a valuation overring of D (ring between D and K). Then $\overline{D} \subset D_v \subset K$. If P is the centre of D_v in $\overline{D}$, then $\overline{D}_P \subset D_v$; since $\overline{D}_P$ is discrete rank one, it follows that $\overline{D}_P = D_v$. Therefore every valuation ring of K lying over D is strongly Laskerian (see [3, Page 456]).

Remark 2.11

Theorems 2.9 and 2.10 respectively generalize [5, Theorem 1] as follows: Let D be an integral domain. Then the integral closure of D is a Dedekind domain (respectively Prufer 1-dimensional domain, respectively, an almost Dedekind domain) if and only if every overring of D satisfies ACCP (respectively every valuation overring of D is Laskerian, respectively every valuation overring of D is strongly Laskerian).

By [15], an integral domain D with quotient field K, is said to be pseudo-valuation domain (PVD), if whenever P is a prime ideal in D and $xy \in P$, where $x, y \in K$, then $x \in P$ or $y \in P$ (i.e. in a PVD every prime ideal is strongly prime). An integral domain D with quotient field K, is said to be PVD if for every nonzero $x \in K$, either $x \in D$ or $ax^{-1} \in D$ for every nonunit $a \in D$. A valuation domain is a PVD but the converse is not true necessarily, for example the non- integrally closed PVD $\mathrm{R} + X\mathrm{C}[[X]]$, is not a valuation domain.

Theorem 2.12

Let (D, M) be a PVD. The complete integral closure D_0 of D is quasilocal Laskerian ring of dim≤1.

Proof: If (D, M) is a PVD with quotient field K, then there is a valuation overring V of D such that $Spec(D) = Spec(V)$ [15, Theorem 2.7 and Theorem 2.10], and hence D_0 is the integral closure of V. Thus (i) $D_0 = V_p$ if V has a height-one prime ideal P or (ii) $D_0 = K$ if V does not have a height one prime ideal. In both cases D_0 is a Laskerian ring.

In the following we restate theorem [16, Theorem 4] by replacing Archimedean valuation domain with Laskerian valuation domain.

Theorem 2.13

Suppose D is an integral domain with quotient field K and let L be an extension field of K. If the complete integral closure of D is an intersection of Laskerian valuation domains on K, then the complete integral closure of D in L is an intersection of Laskerian valuation domains on L.

ACKNOWLEDGEMENT

The authors wish to thank the referees for their priceless suggestions.

REFERENCES

1. Lasker, E. Zur Theorie der Moduln und Ideal. Math. Ann. 60: 20-116 (1905).
2. Noether, E. Idealtheorie in Ringbereichen. Math. Ann. 83: 24-66 (1921).
3. Gilmer, R. *Multiplicative Ideal Theory.* Marcel Dekker, New York (1972).
4. Evans, Jr., E.G. Zero divisors in Noetherian-like rings. Trans. Amer. Math. Soc. 155: 505-512 (1971).
5. Dumitrescu, T., T. Shah & M. Zafrullah. Domains whose overrings satisfy ACCP. Commun. in Algebra 28(9): 4403-4409 (2000).

6. Sheldon, P. How changing D[[X]] Changes its quotient field. *Trans. Amer. Math. Soc.* 159: 223-244 (1971).
7. Gilmer, R. & J. Ohm. Primary ideals and valuation ideals. *Trans. Amer. Math. Soc.* 117: 237-250 (1965).
8. Ohm, J. Some counter examples related to integral closure in D . *Trans. Amer. Math. Soc*. 122: 321-333 (1966).
9. Beauregard, R.A. & D. E. Dobbs. On a class of Archimedean integral domains. Can. J. Math. 28(2): 365-375 (1976).
10. Nagata, M. On the derived normal ring of Noetherian integral domains. *Mem. Coll. Sci.* Uni. Kyoto 29: 293-303 (1955).
11. Butts, H. S. & W. W. Smith. On the integral closure of a domain. *J. Sci. Hiroshima Univ*. 30: 117-122 (1966).
12. Gilmer, R. & W. Heinzer. The Laskerian Property, Power series rings and Noetherian Spectra. *Proc. Amer. Math. Soc.* 79: 13-16 (1980).
13. Krull, W. Ideal theorie in Ringen Ohne Endlichkeit. *Math. Annalen*. 101: 729-744 (1929).
14. Bourbaki, N. Algebre commutative. Actualities Sci. Indust. no. 1293, Hermann, Paris (1961).
15. Hedstrom, J. R. & E. G. Houston. Pseudo - valuation domains. *Pacific J. Mathematics* 75(1): 137-147 (1978).
16. Gilmer, R. On complete integral closure and Archimedean valuation domains. *J. Austral. Math. Soc.* 61: 377-380 (1996).

.

Proceedings of the Pakistan Academy of Sciences 48 (1): 51–55, 2011

ISSN: 0377 - 2969

Pakistan Academy of Sciences

Variability of Solar Flare Duration and Its Effects on Ozone Concentration at Pakistan Air Space

[1]Saifuddin Ahmad Jilani* and [2]M. Ayub Khan YousufZai

[1]Department of Physics, Institute of Space & Planetary Astrophysics, University of Karachi, Karachi, Pakistan
[2]Department of Applied Physics, Solar-Terrestrial & Atmospheric Research Wing and Institute of Space & Planetary Astrophysics, University of Karachi, Karachi, Pakistan

Abstract: In this communication we have presented the existence of solar flares and their variability along with the correlation structure of ozone concentration. This can be accomplished by analyzing the data of solar flare duration and ozone content. The supremacy of gradual flares in depletion of ozone was recognized. Exploratory Data Analysis approach has been utilized to find the contribution of solar flares in ozone layer depletion.

Keywords: Exploratory data analysis (EDA), gradual flares, impulsive flares, mixed flares, ozone layer depletion (OLD)

INTRODUCTION

Ozone is formed primarily by chemical process involving the dissociation of O_2 by solar UV radiation. Thus there is a need for observational and theoretical study of the relationship of O_3 concentration to variations in solar activity [1]. Albeit the anthropogenic factors are the major contributors of the ozone layer depletion (OLD), it is important to study the natural events as well. Solar flares are the most important in this respect. They occur when strong magnetic fields extending high into the sun's atmosphere, suddenly collapse and then recombine into simpler structures [2]. The electrically charged particles emitted by some flares represent a potential hazard to man during space flights to the moon and the planet. These particles are greatly increased following the appearance of some large flares [3]. Most of the destruction (~ 70 %) of ozone rate is due to catalytic cycle involving N_2O, which is most likely to produce at the time of major flares [4 - 5].

Satellite measurements in the stratosphere and mesosphere indicate a possible correlation of ozone with 27-day variations in solar activity [6].

The opening of magnetic field lines initiates by an eruptive flare is connected with ejection of material called coronal mass ejection (CME). It has been known that the real agent that causes geomagnetic storms is CME, which can also originate in quiet parts of the sun. But it is misleading to jump to a conclusion that flares are not important any more in solar terrestrial relations. Flares are excellent indicators of coronal storms and the largest geomagnetic storms are caused by fast CME which usually are associated with flares, while moderate or small storms mostly have no association with flares [7]. Nearly 40 % of CME are accompanied by solar flares that occur about the same time and place [8]. A large solar flare also called solar proton event (SPE), can destroy 20 % of the earth's ozone in a matter of few days as was in August 1972 [9 -10].

MATERIALS AND METHODS

Exploratory data analysis is one of the statistical techniques adopted in analyzing the behavior of solar flare on ozone, for the period of 1972-2006. Solar flare activities at ionosphere have been recorded by Digisonde which is installed at SUPARCO HQ, Karachi. Another remote sensing device is Dobson Spectrophotometer, which is monitoring ozone contents at stratosphere in Dobson unit and being working at GC, Quetta. These data screening convey the fundamental properties about the nature of the data and the physical process following them

Received January 2010, Accepted March 2011
* Corresponding author: Saifuddin Ahmad Jilani; Email: saifjilani@yahoo.com

which is easy to communicate and helpful in further investigation.

According to duration solar flares are separated as impulsive and gradual modes i.e. less than and greater than 1 hour respectively. As in nature both of them exist arbitrarily, therefore we term a third category of flares called mixed flares. It is important to study their behavior in solar terrestrial relationship separately.

RESULTS AND DISCUSSION

Test of Normality

A small departure from normality is found in all three data series of SFD as shown in Fig 1-3. This is also supported by their KS-values in Table1. Their P-values confirm it with 90 % confidence interval. However Fig.4 of these measures supported with KS value is in favor to recognize ozone series as normally distributed. The P-value defines this with 95 % confidence interval [13 -14].

The role of central limit theorem is emphasizing in assessing the normality of data. It assures us that regardless the shape of the population distribution as the sample size increased the distribution approaches a normal distribution very rapidly. A large sample approaches infinity but in practice, is generally taken as a sample size of 30 or more [15, 18].

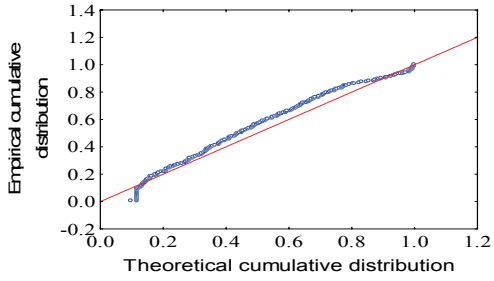

Fig. 1. Probability plot specify nature of data series for mixed flares.

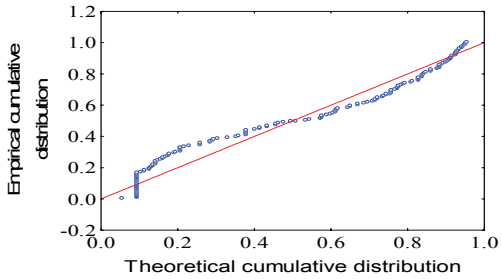

Fig. 2. Probability plot specify nature of data series for impulsive flares.

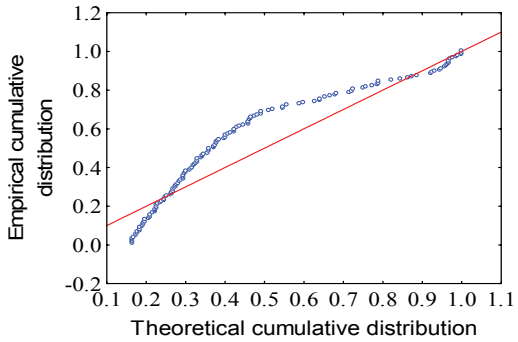

Fig. 3. Probability plot specify nature of data series for gradual flares.

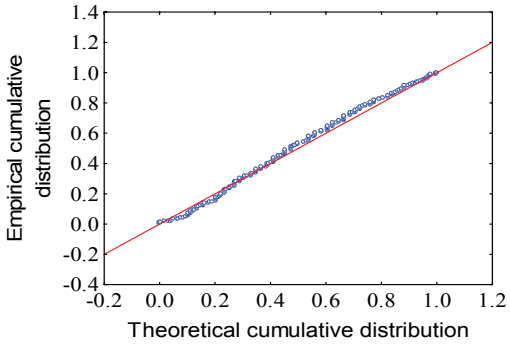

Fig..4. Probability plot specify nature of data series for ozone contents.

Pearson Index

The Pearson Index, specify that whether the distribution being analyzed is significantly skewed or consider as normally distributed.

$$PI = \frac{3(\bar{x} - median)}{s} \quad \text{---------- (1)}$$

where $\bar{x}$ is the sample mean and s the sample standard deviation.

If PI is not greater then +1 or less than −1, the distribution may not be significantly skewed. [11] The PI values for all of the four data samples in Table 1 are within this range.

Table 1. Test statistics.

	PI	KS	P-value
Mix - flares	0.43	0.09	< 0.010
Imp- flares	− 0.16	0.12	< 0.010
Grad- flares	0.98	0.19	< 0.010
Ozone	0.18	0.04	= 0.053

PI: Pearson's Index of skewness
KS: Kolmogorove-Smirnov test

Outlier Identification

An outlier may be an observation for which the value has been incorrectly recorded and so it should be removed. On the other hand, an outlier may also be an unusual item that has been correctly recorded and does belong in the data set and therefore should not necessarily be excluded [12, 15].

The Box Plot of Fig. 5 shows ten possible outliers found in the data series of solar flare duration (SFD) and six possible outliers in the data series of ozone. They are flagged with an asterisk so that these points can be checked [16].

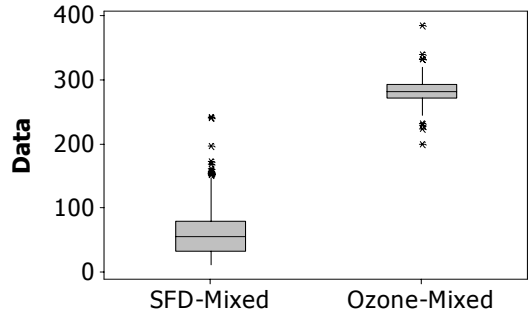

Fig. 5. Box plot identify possible outliers in the data series of SFD and ozone content.

Observations that are 2 or 3 times the IQR above the third quartile or below the first quartile are considered as outliers. [12]

Outliers $= Q_3 + 2\,(IQR)$ ---------- (2)

$= Q_1 - 2\,(IQR)$ ---------- (3)

The above measures identify three outliers in the data series of SFD and four outliers in the series of ozone content.

In the data series of ozone the outliers remains at the two extremes balance the data towards normality. On the other hand, all of the outliers of SFD exist in the right extreme makes the right tail slight heavy.

Estimation of Confidence Interval for the Population Mean of SFD

The interval estimates from the sample of solar flare duration (SFD), when the critical region is $\alpha = 0.1$ and the corresponding level of significance or the confidence interval at 90% respectively as followed.

$$\bar{x} - 1.64\frac{\sigma}{\sqrt{n}} < \mu < \bar{x} + 1.64\frac{\sigma}{\sqrt{n}}$$

$= 57.451 < \mu < 64.429$ ---------- (4)

$$\bar{x} \pm 1.64\frac{\sigma}{\sqrt{n}} = 60.94 \pm 3.49$$ --------- (5)

Testing Hypothesis

Testing the hypothesis is a procedure in which sample data are used to decide or not to reject a proposition made about the population parameter. Statistical hypothesis is a statement about a population whose validity is to be tested on the basis of a random sample drawn from the population. This statement may be an assertion about any population parameter [17].

(i) One sample test: SFD-mixed

For mixed category of flares, it would be hypothesize that gradual flares in future are more frequent then impulsive.

For sample size n = 325 with $\bar{x} = 60.94$

H_o: $\mu \geq 60$ (claim)

H_a: $\mu < 60$

Test Statistic:

$$Z = \frac{\overline{X} - \mu}{S/\sqrt{N}} = 0.44$$ ---------- (6)

Significance level = $\alpha = 0.10$; P = 0.671

Make the decision to accept the null hypothesis that the population mean of SFD either greater than or equal to 60 minutes which specify endanger of gradual flares.

(ii) Two samples test: ozone-imp Vs ozone-grad

This would be hypothesizes that ozone column on average would not remain identical during the two phases of impulsive and gradual flares. At $\alpha = 0.05$, the evidence to support the claim can be analyzed by using t-test. Therefore the series of SFD which designate as mixed flares have been separated into two series of impulsive and gradual flares according to their duration and ozone column corresponding to that period assigned as ozone-imp and ozone –grad. The two means are then compare as independent populations.

Table 2. Ozone statistics during two phases of solar flares.

	N	Mean	St.Dev	SE Mean
Ozone-Imp	178	281.57	25.16	1.89
Ozone-Grad	147	286.66	17.88	1.47

Ozone-Imp: Ozone during impulsive flares
Ozone-Grad: Ozone during gradual flares

H_o: $\mu_1 = \mu_2$
H_a: $\mu_1 \neq \mu_2$ (claim)
Test Statistic:

$$t = \frac{\overline{x}_1 - \overline{x}_2}{\sqrt{\frac{s_1^2}{n_1} + \frac{s_2^2}{n_2}}} = -2.06 \text{ ----------} \quad (7)$$

Significance level = α = 0.05; P = 0.040
95 % Confid. Interval = (−9.95, 0.22)

Make the decision to accept the alternate hypothesis that the two series of ozone column during impulsive and gradual phase of flares are not identical.

Linear Regression Approach

Regression analysis is the measure of the relationship between two or more variables in terms of the original units of the data [17].

Linear regression technique for each of the three data series of SFD with respective ozone content are represented in Fig 6-8. Their model equations are respectively as follows.

$$y = 278.57 + 0.074x \text{ ----------} \quad (8)$$

$$y = 275.14 + 0.185x \text{ ----------} \quad (9)$$

$$y = 290.57 - 0.042x \text{ ----------} \quad (10)$$

Table 3. Model validation parameters.

	F-value	P-value	R^2
Mix - flares	8.15	0.005	2.5 %
Imp- flares	2.15	0.145	1.2 %
Grad- flares	0.92	0.339	0.6 %

R^2: Coefficient of determination.

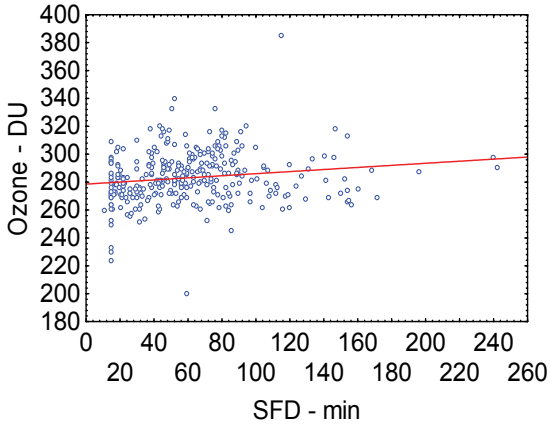

Fig. 6. Mixed flares show positive variation in ozone content.

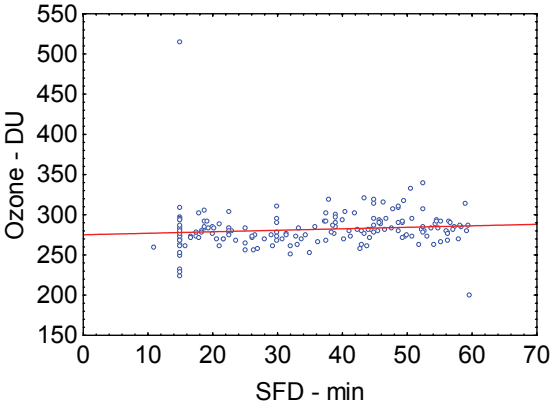

Fig. 7. Impulsive flares again show a minimal change in ozone content.

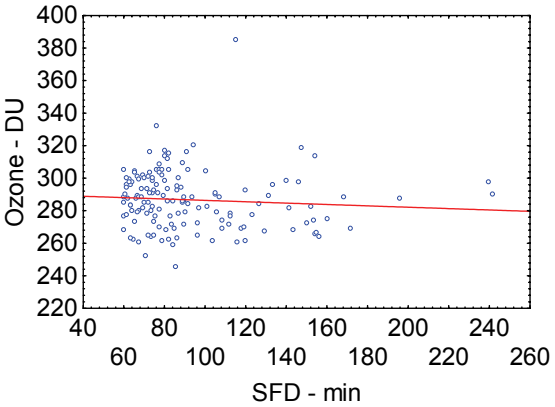

Fig. 8. Gradual flares shows decline in ozone content.

Among the three linear regression models it specifies that during gradual flares there is depletion in the ozone column. This trend is small but negative.

CONCLUSION

In this communication four samples are tested and found normally distributed. The least square estimate predicts ozone layer depletion (OLD) during gradual phase of solar flares. Mixed and impulsive categories of flares are found positively correlated with ozone concentration. Therefore Sun is responsible for both formation and annihilation of ozone. As the correlations are weak, the more improved results can be recorded using more sophisticated approach.

REFRENCES

1. Parker, E.N., C.F. Kennel & L.J. Lanzerotti. *Solar System Plasma Physics*, vol. I. North-Holland Publishing Company, Amsterdam, 30 pp. (1979).

2. Taylor, P.O. *Observing the Sun*. Cambridge University Press, UK, 108 pp. (1991).
3. Glasstone, S. *Sourcebook on the Space Science.* D. Van Nostrand Reinhold Company, Princeton, New Jersey, USA, 353 pp. (1965).
4. Walter, D., G.K. Hartmann & R. Leitinger. *The Upper Atmosphere: Data Analysis and Interpretation*. Springer-Verlag, Berlin, Germany (1996).
5. Herman, R.J., & R.A. Goldberg. *Sun, Weather and Climate*. Dover Publication, New York, USA, 170 pp. (1985).
6. Maran, S.P. & C. Sagan. *The Astronomy and Astrophysics Encyclopedia*. Cambridge University Press, Cambridge, 521 pp. (1992).
7. Dwivedi, B.N. & E.N. Parker. *Dynamic Sun*. Cambridge University Press, UK, 258 pp. (2003).
8. Lang, K.R. *The Cambridge Encyclopedia of the Sun*. Cambridge University Press, UK, 137 pp. (2001).
9. Bryant, E. *Climate Process and Change*. Cambridge University Press, U.K, 17 pp. (1993).
10. Whitten R.C. & S.S. Prasad. *Ozone in the Free Atmosphere*. Van Nostrand Reinhold Company, New York, 198 pp. (1985).
11. Bluman, A.G. *Elementary Statistics*, 5th ed., McGraw Hill, New York, USA, `293 pp. (2004).
12. Ruth M.M., O.J. Dunn. & V.A. Clark. *Applied Statistics: Analysis of Variance and Regression*. 3rd ed. Wiley-Interscience, John Wiley & Sons, Hoboken, New Jersey, USA, 8 pp. (2004).
13. Murphy, A.H. & R.W. Katz. *Probability Statistics and Decision Making in the Atmospheric Science.* West View Press, Boulder, CO, USA (1985).
14. Mathews, P.G. *Design of Experiments with MINITAB*. Pearson Education, Singapore Pte. Ltd., Indian Branch, Delhi, India (2005).
15. Fleming, M.C., & J.G. Nellis. *Principles of Applied Statistics*. Routledge, London, 144 pp. (1994).
16. Kathleen, M.M. & D.B. Wakefield. *An Introduction to Data Analysis*, Simon & Schuster Custom Publishing, San Jose, CA, USA (1997).
17. Yousuf Zai, M.A.K. *A Quantitative Study of Effects of Ozone Layer Depletion on Marine Organisms with Special Reference to Coastal Regions of Pakistan*. PhD thesis, University of Karachi, Karachi, Pakistan, 77 pp. (2003).
18. Fred, C. & H. Wright. *Success in Statistics*, John Murray Ltd., London, 220 pp. (1982).

Proceedings of the Pakistan Academy of Sciences 48 (1): 57–61, 2011

ISSN: 0377 - 2969

Pakistan Academy of Sciences

Citations of Elected Fellows

Prof. Dr. M. Asif Khan (2009)

Dr. M. Asif Khan has a Masters degree from the University of Peshawar and a DIC and PhD from the Imperial College London. He joined the National Centre of Excellence in Geology, University of Peshawar in 1981 and since then has progressed to the position of Tenure Track Professor and Director.

Dr. Khan won many international fellowships at pretigeous universities, including UT, Dallas (Fubright 1993-94), Penn State (NSF,1994), Oxford (Commonwealth, 1998-99), and Lehigh (NSF, 2004-05). On the national front, he was awarded Scientist of the Year award by National Book Council in 1990 and Gold Medal in Earth Sciences by Pakistan Academy of Sciences in 2002. President of Pakistan conferred on him the Civil Award of *Tamgha-i-Imtiaz* in 2000. Recently he was elected to the Honrary Fellowship of the Geological Society of London (2008).

In terms of research, over 82 research papers, two coloured geological maps, three books, one published by the Geological Society of London, reflect Dr. Khan's contributions. He has supervised over 25 research students for various degrees, of which over half were for PhD . He has conducted more than a dozen Research Projects at National and International level. He has presented invited talks and chaired sessions in over two dozens international conferences.

Besides research and institutional development, Dr. Khan is contributing to several projects of national interests. He is member of the Core Group of Pakistan Engineering Council that is overseeing the development of Building Codes of Pakistan. Besides, he is on the Board of Governors of Hydrocarbon Development Institute of Pakistan. He consulted for WAPDA on hydropower projects on Indus and Jhelum Rivers. Additionally, he advises multinational oil companies for structural prospection for oil and gas in Pakistan including Premier, Shell, Tullow and Marl Gas.

Lately, he has led the National Centre of Excellence in Geology, University of Peshawar in the capacity of Director. In four years of his leadership at the Centre, he has made significant contributions to academics, human resource development and laboratory infrastructure.

Prof. Dr. Raheel Qamar (2009)

After receiving his PhD in Biochemistry and Molecular Biology from the University of North Texas, USA in 1993, Prof. Qamar returned to Pakistan and worked at different research and teaching positions. Presently, he is working at the COMSATS Institute of Information Technology as Dean, Faculty of Sciences. Before this, from 2005-2008, he was Professor and Chairman of the Department of Biosciences.

While in Pakistan Prof. Qamar has worked extensively on identifying the genetic defects of Thalassaemia, Heart Diseases, Deafness & Eye Disorder patients and the Y-chromosomal & transplantation antigen (HLA) typing of different ethnic groups of Pakistan. His work on Thalassaernia, Hypercholesterolemia & Retinitis Pigmentosa is laying the foundation of the soon to be introduced gene therapy in Pakistan. In addition, in order to understand human genetic diversity, human migration patterns and disease susceptibility, Prof. Qamar has worked on the autosomal microsatellite analysis of different Pakistani and World populations. From 1998 to 2001 he worked at the University of Oxford, UK where he studied the Y-chromosomal polymorphisms of different ethnic groups of Pakistan.

Prof. Qamar has published numerous research articles in internationally recognised peer reviewed journals and national journals. In addition, he has written chapters in a number of text and reference books. At present he has an

Impact Factor of more than 130 and a citation index of more than 600. He has also delivered a number of invited lectures on current topics of research in addition to organizing a number of National and International Conferences to promote various new disciplines of Science. Recently, Prof. Qamar has been elected as the Pakistan National Node Manager of European Molecular Biology Network (EMBnet), where his role is to promote Bioinformatics in Pakistan. Prof. Qamar has been able to generate personal research funding of more than Rs. 30 Million as PI and Co-PI from various National and International agencies, such as the Higher Education Commission of Pakistan, the British Council, etc. He has already supervised 4 PhD students while 7 more are working towards their PhD under his guidance. In recognition of his services, Prof. Qamar was awarded the prestigious *Tamgha-i-Imtiaz* by the President of Pakistan.

Prof. Dr. Wasim Ahmad (2010)

Dr Wasim Ahmad, presently a Professor, Department of Biochemistry, Quaid-i-Azam University, Islamabad, obtained his PhD in 1990 from Trinity College Cambridge University, UK. Dr Ahmad has several years of Post-doctoral experience from PMRC, London; TIGEM, Italy; and Columbia University, New York, USA.

Over the past few years his laboratory has been mapping and identifying genes involved in human genetic disorders. Much of his work focuses on skin disorders including alopecia and ectodermal dysplasia, and hearing impairment, but also extends to other disorders like Neurological and Skeletal Dysplasias. These studies led to the discovery of a number of human genes and chromosomal loci for important genetic disorders. This includes mapping of 17 loci for hearing impairment genes, novel mutations in the hearing impairment genes, identification of four human hair loss genes and six novel loci, novel mutations in human hair loss genes, three novel Alopecia and Mental Retardation Loci, identification of genes responsible for hair and nail dysplasia and nail clubbing, identification of novel mutations in several genes involved in ectodermal dysplasias. These studies have been documented in some I10 papers published in high impact journals such as Science, Nature, Nature Genetics, Genomics, American Journal of Human Genetics, Journal of Medical Genetics, Human Genetics, Journal of Molecular Medicine and British Journal of Dermatology. Total impact factor and citations of Dr Ahmad papers is 505.549 and 1441, respectively. So far 18 students worked under his supervision, have been awarded PhD degree. In addition, 81 students have received MPhil degree.

Dr Ahmad's research programs are currently being funded by National Institute of Health (NIH), USA and Higher Education Commission (HEC), Islamabad, Pakistan.

Dr Ahmad's achievements have been recognized in the form of National Awards including *Sitara-e-Imtiaz* by Government of Pakistan in 2002, HEC Distinguished National Professor in 2005, Gold Medal by Pakistan Academy of Sciences in 2006 and appointment of Tenured Trech Professor in 2007 by Quaid-i-Azam University, Islamabad.

Prof. Dr. Khalid M. Khan (2010)

Prof. Dr. Khalid Mohammed Khan is among the most prominent young scientists of Pakistan. He has been Awarded Star Award 2003, Justice Qadeeruddin Gold Medal 2003, Pakistan Academy of Sciences Gold Medal 2004 and Star Award 2004. The President of Pakistan has awarded *Tamgha-i-Imtiaz* in recognition of his research work in the field of bioorganic and medicinal chemistry in the year 2004. He is an active member of organizing committees of a number of International Conferences/Workshops organized by HEJ Research Institute of Chemistry since 1987, which reflects his organizational capabilities. As Secretary, National Core Group in Chemistry (under Higher Education Commission, since 2002), Prof. Khan has rendered valuable services to the cause of education and research in the field of Chemical Sciences. He is also coordinating National Chemistry Talent Contest (NCTC) for young students; thus, playing a catalytic role in promoting chemical science awareness and interest in young generation. He is trainer leader and trainer of Four Bronze Medal Winner Pakistani Chemistry Olympiad Teams which participated in 39th and 41st International Chemistry Olympiad held in Russia and UK in 2007 and 2009, respectively. He is a member of various National Level Committees and NGOs

in recognition of his services for the promotion of Chemical Sciences in particular and science in general. He is elected Secretary General of the Chemical Society of Pakistan.

His contributions in the field of organic chemistry are numerous and noteworthy. These include establishment of one of the most productive laboratory working on the discovery of new enzyme inhibitors and training of young researchers in the important field of drug designing. The results of his scientific work have been published in journals of international repute. He was able to achieve this in a relatively short period of independent research (12 years) in an environment constrained with availability of chemicals and other research materials.

Prof. Khan got his early education in Nawab Shah (Sindh). He obtained his BSc. degree from the University of Sindh, Jamshoro and MSc from Quaid-i-Azam University, Islamabad. He earned his PhD in 1992 from the world famous H.E.J. Research Institute of Chemistry in synthetic organic chemistry. In 1992, he joined the Tübingen University (Germany) as a postdoctoral research fellow, with Prof. Dr. Wolfgang Voelter (Hilal-e-Pakistan, Sitara-e-Pakistan), where he carried out research on the development of synthetic methodologies based on carbohydrates and amino acids.

In September 1997, Prof. Khan joined the H.E.J. Research Institute of Chemistry as an Assistant Professor and currently is serving as Professor. He has authored or co-authored over 190 research papers published in journals of international repute having journal impact factor over 288 and Citation Index 1759. He is co-editor of two books, published by international publishers. He is also Recipient of Research Productivity Allowance (RPA) 2001, 2002, 2003, 2004, 2005, 2006 and 2007 from Pakistan Council for Science & Technology (PCST) in recognition of his high quality research.

Prof. Dr. Asghari Maqsood (2010)

Prof. Dr. Asghari Maqsood daughter of M. Ghulam Nabi, was born on 15th September 1947 in a small village of Jhang, Pakistan. There was no school for girls in her native village. She got early education in Abbottabad, Pakistan. Prof. Maqsood was an outstanding student and got a scholarship to study BSc (Hons) in Physics at Dhaka University (1966-1970). After the Dhaka fall, she returned to Pakistan, to join the University of the Punjab, Pakistan for her MSc degree in Physics. In 1972, she passed her MSc in 1st class with 1st position in the University and was awarded a Gold Medal by the University of the Punjab, on her excellent performance.

Prof, Maqsood started her professional career in 1973 at Department of Physics, Quaid-i-Azam University. In 1975, she won the British Council and Pakistan Overseas Scholarships for higher education. She opted for the British Council scholarship and joined Oxford University for MSc degree in Experimental Solid State Physics. She developed deep interest in the study of materials, especially the single crystal of $R_2Si_2O_7$ (R=Tm, Er, Ho, Dy). She was the first to grow single crystals of polymorphic $Er_2Si_2O_7$ with three phases, $Ho_2Si_2O_7$ with four phases, $Tm_2Si_2O_7$ and $Dy_2Si_2O_7$ with two phases. The ASTM cards 33-0531 ($Er_2Si_2O_7$), 33-0525 ($Dy_2Si_2O_7$), 33-0594 ($Ho_2Si_2O_7$) are based on her work. Important physical properties of these materials in the magnetic and thermal domain were undertaken by her. No other researcher has done the study of these materials up till now, except X-ray diffraction. After completion of her PhD from Gothenburg University, Sweden, she returned Quaid-i-Azam University, Islamabad in 1982 and established the Thermal Physics Laboratory in collaboration with Gothenburg and Uppsala Universities, Sweden. It was the first advanced research laboratory in the country headed by a women scientist. Prof. Maqsood is involved in the cutting edge research of advanced materials comprising rare-earth disilicates, high-Tc superconductors, ferrites, composites and semiconductor thin films for solar cells applications. The rare-earth disilicates have been prepared both in poly and single crystal forms and the physical properties of these materials have been measured successfully. High-Tc superconductors, both the 123 and Bi-based, were also developed in either single or poly crystal forms and studied by numerous techniques in her research laboratory. Preparation and thermophysical characterization of bulk as well as nano-sized particles of both hard and soft ferries are undertaken by her research group.

She has contributed significantly to the development of this important field in Pakistan not only by her own research but also by training other research scientists from various national

and international institutes. She has also developed the Transient Hot Strip (THS) and Transient Plane Source (TPS) techniques to measure thermal transport properties of insulators, conductors, high-Tc superconductors and liquids. The accuracy of the developed methods is so good that these might even be used for the measurement of specific heat capacity especially under difficult experimental conditions? A long standing limitation of THS technique - that this could be applied only to the insulating materials - was overcome in TPS technique. This technique can be used over a broad range of temperature (77-1000 K) and pressure using a specially designed sensor known as TPS element. These are the only experimental applications available in Pakistan for this purpose.

Dr. Asghari Maqsood was the first researcher to introduce the subject of Thin Film Technology at the University level in Pakistan. She supervised 15 MPhil and four PhD students and wrote outstanding papers in this field .The closed space sublimation apparatus for thin film deposition was designed and fabricated by her.

Prof. Maqsood's research laboratory has produced internationally recognized research, as evidenced by numerous leading archival of international repute journals, presentations in national and international conferences and their respective proceedings. Apart from her research she has contributed in the teaching at the MPhil and MSc levels along with the development of MSc laboratories at Quaid-Azam University, Pakistan. The number of PhD, MPhil and MS students supervised by her is around 100, which is the highest number in Pakistan, supervised in the field of Physics/ Materials Engineering. She has published most of her work in ISI INDEXED Journals.

Prof. Maqsood was a member of the selection committee of Rhodes Trust Scholarship for the Oxford University, UK. She was an Associate member of ICTP (1992-1997) and member of New York Academy of Sciences, America. She is a life member of Pakistan Institute of Physics (PIP) and Pakistan Physical Society. Recently, she was elected as a member of Thin Film Division of IUVSTA (July 2010).

Prof. Maqsood has published outstanding research papers in international journals; two papers appeared on the cover page of two journals, being published in USA: Journal of Material Science Letters and Applied Optics (OSA). She is a recipient of the coveted South Asia Publication Award "Star Woman 1994".

She was awarded Gold Medal and cash prize for "Physical Sciences 2000" by Pakistan Academy of Sciences, for her outstanding research work in the subject. She was honored by the Civil Award "President's Award for Pride of Performance 2002" in Science (Physics) by President of Pakistan and was awarded *Sitara-i-Imtiaz* on Pakistan Day 2010. She also got "The Best University Teacher Award 2002" from Higher Education Commission, Pakistan. On the World Teacher Day, she was awarded "Prime Minister's Gold Medal 2004" and was also honored by "President's Award: *Izaz-i-Fazeelat* for Academic Distinction 2005".

Prot Maqsood became Meritorious Professor of Physics in 2005, the first lady to achieve this prestigious position in Pakistan. She joined School of Chemical and Materials Engineering (SCME) in Jan-2008 at NUST, where she is involved in post graduate teaching and research Prof. Asghari has established Thermal Transport Laboratory at SCME, NUST.

Prof. Dr. Muhammad Sharif (2010)

Dr. M. Sharif did his MSc, MPhil and PhD in Mathematics from Quaid-i-Azam University, Islamabad. He completed his PhD under the supervision of Professor Asghar Qadir in the field of General Relativity. His work generalizes the concept of force in Relativity. This provides another way to define the well-known quantities energy and momentum. He has worked on a variety of research problems like black holes and some alternative theories of General Relativity.

He started his career as an Assistant Professor at Punjab University. Currently, he is working as a Professor at Department of Mathematics, Punjab University, Lahore. He has been associated, in particular, with MPhil/PhD programs of the Department in addition to some other programs. He has published 124 research papers in journals of international repute. He has delivered more than 45 seminars in different workshops, seminars and conferences at local and international level.

He got merit scholarship during his MSc, Dr. Raziuddin Siddiqui Research Fellowship during his MPhil and worked on a Pakistan Science

Foundation project during his PhD. He has completed a Research Project of Punjab University during 1998-1999. He has successfully completed Postdoctoral Fellowship twice, awarded once by Korea Science and Engineering Foundation during 2000 and second time by Ministry of Science & Technology during 2002 for UK. He has been regularly selected for Research Productivity Allowance since 2001 by Pakistan Council for Science and Technology. He was ranked top scientist by PCST and Punjab University during 2005. He has been awarded Dr. Raziuddin Siddiqui Prize and Gold Medal during 2002 and 2009 by Pakistan Academy of Sciences for his good quality research. He has been awarded a certificate for the citation of his paper in the top 1 % by THOMSON. He has been awarded *Izaz-i-Fazeelat* in 2007 and *Tamgha-i-Imtiaz* in 2008 by Government of Pakistan and Best University Teacher Award and Best Paper Award by HEC during 2008 and 2009, respectively.

He has been Research Fellow at ICTP Trieste-Italy during June-August, 1996 and Associate Member of Third World Academy of Sciences for Brazil during 1998-2000. He has been Visiting Professor at IMECC, University of Campinas, SP, Brazil during July-Oct., 1998 during June-August 2000. He has been Visiting Professor at Department of Mathematics, Canakkale Onsekiz Mart University, Turkey during June-July 2002. He has been supervising MPhil and Ph.D. students under the Indigenous Fellowship Program of HEC and has produced 28 MPhil and 4 PhD scholars. He has been acting as a referee of some reputed journals like *General Relativity & Gravitations, Modern Physics Letters A, Foundations of Physics, Astrophysics Space Science.*

He is an editor of *The Punjab University Journal of Mathematic*s and also an editor of *Proceedings of the Mini Workshop on Relativity, Astrophysics and Cosmology* held at Quaid-i-Azam University, Islamabad. He has been member of different societies like International Society on General Relativity. He has organized International Symposium on Relativity/ Conference/Lectures at Punjab University.

Proceedings of the Pakistan Academy of Sciences

Instructions for Authors

Purpose and Scope: Proceedings of the Pakistan Academy of Sciences (PPAS) is official journal of the Academy, published quarterly, in English. PPAS publishes original research papers in Engineering Sciences & Technology, Life Sciences, Medical Sciences**,** and Physical Sciences. State-of-the-art reviews (~ 20 pages, supported by recent references) summarizing R&D in a particular area of science, especially in the context of Pakistan, and suggesting further R&D are also considered for publication. All manuscripts under go double-blind review. Authors are not required to be Fellows or Members of the Pakistan Academy of Sciences or citizens of Pakistan.

Manuscript Format:
Manuscripts, typewritten in Times New Roman **Font Size 11**, double spaced; with one inch margins on all sides on A-4 size paper, should not exceed 20 pages including Tables, Figures and illustrations. Number manuscript pages throughout. *To conserve space, the Instructions are not double spaced and are in font size 10.*

The manuscripts may contain ***Abstract, INTRODUCTION, MATERIALS AND METHODS (or METHODOLOGY), RESULTS, DISCUSSION (or RESULTS AND DISCUSSION), CONCLUSIONS, ACKNOWLEDGEMENTS and REFERENCES*** *and any other information that the author(s) may consider necessary.*

Title Page: Should carry: (a) Concise **Title** of the article **(**in Initial Capital and then lower case letters for each main word; font size 16; **Bold**), ≤ 160 characters, depicting its contents. Do not use abbreviations or acronyms; (b) Author(s)' first name, middle initial and last name (font size 12, **Bold**), and professional affiliation(s) [i.e., each author's Department, Institution, Mailing address and Email address; but no position titles]; (e) Indicate the corresponding author with *****; (d) **Short running title** of ≤ 50 characters.

Second Page should start with the **Title** of the Article, followed by entire manuscript comprising **Abstract, Keywords, INTRODUCTION, MATERIALS AND METHODS, RESULTS, DISCUSSION, ACKNOWLEDGEMENTS, and REFERENCES**.

Headings and Subheadings: All flush left

LEVEL-1: **ALL CAPITAL LETTERS; Bold**
Level-2: **Initial Capital and then lower case letters for each main word; Bold**
Level-3: Initial Capital and then lower case letters for all words;Bold, italics
Level-4: *Run-in head*; *Italics*, in the normal paragraph position with only an Initial Capital and ending in a colon (i.e., **:**)

Abstract: Must be self-explanatory**,** of 200–250 words (in font size 10), stating rationale, objective(s), methodology, main results and conclusions of the study. Abbreviations, if used, must be defined on first mention in the Abstract as well as in the main text. ABSTRACT of review articles may have variable format, but must be of 200–250 words.

Keywords: Suggest three to eight keywords**,** depicting the article.

INTRODUCTION: Provide a clear and concise statement of the problem, citing relevant literature, and objectives of the investigation.

MATERIALS AND METHODS: Provide an adequate account of the procedures or experimental details, including statistical tests (if any), in a concise manner but sufficient enough to replicate the investigation.

RESULTS: Be clear and concise with the help of appropriate Tables, Figures and other illustrations. Data should not be repeated in Tables and Figures.

DISCUSSION: Provide interpretation of the Results in the light of previous relevant studies, citing published references.

ACKNOWLEDGEMENTS: In a brief statement, acknowledge financial support and other assistance.

REFERENCES: Cite references in the text **by number only** in **square brackets**, e.g. "Brown et al [2] reported ..." or ".. as previously described [3, 6-8]", and list them in REFERENCES section, in the order of citation in the text, Tables and Figures (not alphabetically). Only published (and accepted for publication) journal articles, books, and book chapters qualify for REFERENCES. List of REFERENCES may be prepared as under:

a. **Journal Articles** *(Name of the journal to be stated in full)*

1. Golding, I. Real time kinetics of gene activity in individual bacteria. *Cell,* 123**,** 1025–1036 (2005).
2. Bialek, W. & S. Setayeshgar. Cooperative sensitivity, and noise in biochemical signaling. *Physical Review Letters,* 100**,** 258–263 (2008).
3. Kay, R.R. & C.R.L. Thompson. Forming patterns in development without morphogen gradients: scattered differentiation and sorting out. *Cold Spring Harbor Perspectives in Biology,* 1, doi: 10.1101/cshperspect.a001503 (2009).

b. **Books**

4. Luellen, W.R. *Fine-Tuning Your Writing*. Wise Owl Publishing Company, Madison, WI (2001).
5. Alon, U. & D.N. Wegner (Eds.). *An Introduction to Systems Biology: Design Principles of Biological Circuits*. Chapman & Hall/CRC, Boca Raton, FL (2006).

c. **Book Chapters**

6. Sarnthein, M.S., & J.D. Stanford. Basal Sauropodomorpha: historical and recent phylogenetic developments. In: *The Northern North Atlantic: A Changing Environment*. Schafer, P.R. & W. Schluter (Eds.), Springer, Berlin, p. 365–410 (2000).
7. Smolen, J.E. & L.A. Boxer. Functions of Europhiles. In: *Hematology, 4th ed*. Williams, W.J., E. Butler, and M.A. Litchman (Eds.), McGraw Hill, New York, p. 103–101 (1991).

Tables, with concise but comprehensive headings, on separate sheets, must be numbered according to the order of citation (like **Table 1.**, **Table 2.**). If applicable, round off data to the nearest three significant digits. Provide essential explanatory footnotes, with superscript letters or symbols keyed to the data. Do not use vertical or horizontal lines, except for separating column heads from the data and at end of the **Table**.

Figures may be printed in two sizes: (i) column width of 8.0 cm; or (ii) entire page width of 16.5 cm. **Captions to Figures** may be typed on a separate page; number them as **Fig. 1.**, **Fig. 2.**, … in the order of citation in the text. Computer generated, laser printed, **line drawings** or original line drawings made with black ink on white drawing or tracing paper are acceptable. Do not use lettering smaller than 9 points or unnecessarily large. **Photographs**, as glossy prints, must be of high quality. If to form multiple panels on the journal page, they should be mounted and be separated from adjacent photographs by uniform spaces. A scale bar should be provided on all photomicrographs.

Declaration: Provide a declaration that the results are original; approval of all authors has been obtained to submit the manuscript; the same material is neither 'in press' nor under consideration elsewhere, and, in case the article is accepted for publication, its copyright will be assigned to *Pakistan Academy of Sciences*. Authors are responsible for obtaining permission to reproduce copyrighted material from other sources.

Reviewers: Authors must suggest three prospective reviewers, two local and one from a scientifically advanced country, who are expert in the paper's scientific area.

MORE DETAILED INFORMATION can be seen at **website** of Pakistan Academy of Sciences, i.e., www.paspk.org

Manuscript Submission: Soft copy of the manuscript in **Microsoft (MS) Word,** as e-mail attachment or on a CD, as well as its *one hard copy* **may be submitted to:**

Editor-in-Chief
Pakistan Academy of Sciences
3-Constitution Avenue, G-5/2, Islamabad, Pakistan
E-mail: pas.editor@gmail.com
Tel: 92-51-9207140
Website: www.paspk.org

Proceedings
OF THE PAKISTAN ACADEMY OF SCIENCES

CONTENTS

Volume 48, No. 1, March 2011 Page

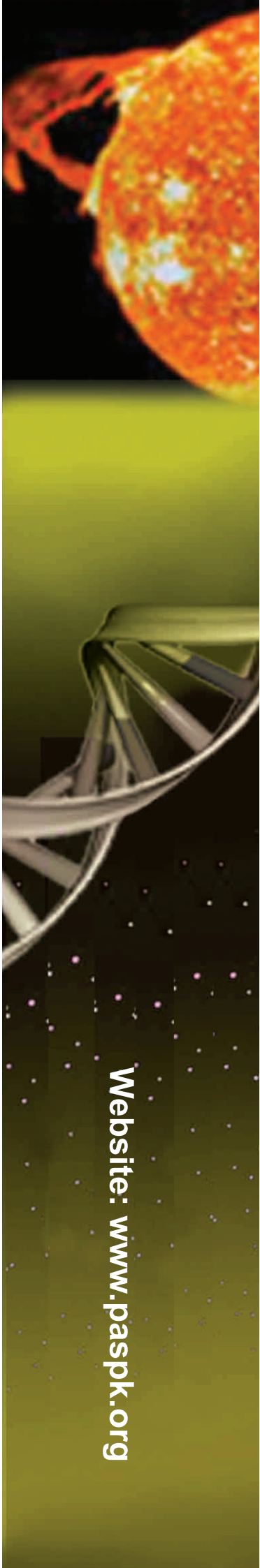

PAKISTAN ACADEMY OF SCIENCES, ISLAMABAD, PAKISTAN
HEC Recognised, Category X